2023

Evaluation and improvement of energy flexibility and performance of building heating, ventilation, and air-conditioning systems

Muhammad Bilal Awan

UNIVERSITY
OF WOLLONGONG
AUSTRALIA

Evaluation and improvement of energy flexibility and performance of building heating, ventilation, and air-conditioning systems

Muhammad Bilal Awan

B.Sc. Eng, M.Sc. Eng

Supervisors:

Prof. Zhenjun Ma

Dr. Wenye Lin

This thesis is presented as part of the requirement for the conferral of the degree:

Doctor of Philosophy

University of Wollongong

Faculty of Engineering and Information Sciences

Sustainable Buildings Research Centre

August 2023

Abstract

The foreseen reduction of available fossil fuels, the continued increase in global energy demand, and the irrefutable evidence of climate change, along with the implementation of a global commitment to achieve a net-zero emissions target, have greatly sharpened commercial interest in using renewable energy resources (RER). However, the high penetration of RER-based stochastic power generation systems has resulted in a significant requirement for increased flexibility on the demand side that can allow buildings to adapt to increasingly dynamic energy supply conditions to support power grid operation and optimization. Failure to adapt may carry serious electrical blackouts and can compromise the safety of the supply side.

The building sector accounts for a substantial amount of global energy usage and offers great opportunities for energy flexibility. Building energy flexibility is an important and emerging concept in the modern energy landscape, which can support the sustainable transition of the power sector. Building heating, ventilation, and air-conditioning (HVAC) systems are one of the leading energy consumers in buildings, which can be used as a key flexible source. The HVAC systems with integrated thermal energy storage (TES) can further enhance building energy flexibility.

This thesis contributes to the evolving field of demand flexibility and introduces methodologies to evaluate and improve energy flexibility and performance of building HVAC systems.

Firstly, a data-driven performance assessment strategy was developed to evaluate the performance of centralized chiller systems using multiple data analytics and advanced visualization techniques. The chiller performance was quantitatively and qualitatively analyzed using the Conditional inference tree (CIT) and Agglomerative hierarchical clustering (AHC), and Association rule mining (ARM), respectively. A new performance indicator of Coefficient of performance (COP) Destruction was introduced to represent the quality of the achieved COP. The performance of this strategy was evaluated using one-year operating data of a centralized chiller system installed in a commercial building. The findings of the analyses indicated that the developed strategy can be effectively used for the performance assessment of chiller

systems and can provide detailed insights for the performance improvement of these systems.

The flexibility potential and performance of buildings and building HVAC systems can be enhanced using TES systems. The performance of TES systems is greatly dependent on the type of storage materials used. Hence, a methodological approach was developed using a Weighted product method (WPM) based ranking strategy for near-optimal selection of phase change materials (PCMs) for thermal energy storage in building applications. The effect of better-ranked PCMs on the flexibility enhancement of an HVAC system was analyzed. Both the qualitative and quantitative attributes of PCMs were used to rank and determine near-optimal PCMs for given applications. Criteria to convert qualitative attributes into quantitative factors were introduced. A weight assignment process was also introduced to handle multiple characteristics of PCMs using priority-based clusters in the pair-wise matrix of the Analytic hierarchy process (AHP). The effectiveness of the strategy was evaluated by performing two case studies. Both case studies verified the effectiveness of the developed method.

Detailed evaluation of building energy flexibility is crucial to determining and selecting cost-effective energy flexible sources for increased energy flexibility. This can be typically accomplished using robust energy flexibility indicators (EFIs). Hence, a framework to formulate and aggregate EFIs was introduced. EFIs were developed using the important characteristics of building energy flexible sources, performance factors linked with flexibility services, and penalty factors based on the penalties introduced by the grid. A Multicriteria decision analysis (MCDA) method was then used to develop an Aggregated energy flexibility potential (AEFP) function that can consider the interactions between the power grid, buildings, and building energy systems to represent the building's overall energy flexibility potential with a single dimensionless value. The performance of the EFIs and AEFP developed was evaluated via a case study with two distinct scenarios through simulations. Both scenarios verified the effectiveness of the developed EFIs and the AEFP for evaluating building energy flexibility.

To fully utilize building energy flexibility, appropriate prediction of building energy flexibility potential and energy consumption is essential. An Extreme gradient

boosting (XGBoost) algorithm-based prediction model was developed to predict the energy flexibility and energy consumption of buildings and building energy systems. The performance of the model was evaluated through a case study to predict the energy flexibility potential and energy consumption of an HVAC system with integrated TES. The prediction was made using the data of outdoor air temperature and relative humidity, and indoor building sensible and latent thermal loads. The model demonstrated high prediction accuracy.

Overall, this thesis provided several new strategies to evaluate and improve energy flexibility and performance of building HVAC systems. The findings can be used to evaluate, predict, and improve the performance and energy flexibility of building energy systems under different operating conditions. Moreover, MCDA methods can be used to trace the best possible alternatives for energy storage materials in building applications and quantify the aggregated response of energy-flexible sources.

Acknowledgment

My deepest gratitude to my supervisor Prof. Zhenjun Ma for his continuous guidance and supervision with great support throughout my Ph.D candidature. He guided me to professionalize my skills related to report writing, critical and analytical thinking, and research fundamentals. I would also like to thank my co-supervisor *Dr. Wenye Lin.* Without his help, I would have faced several challenges in generating effective results from the simulation.

I would like to thank the staff and management of the University of Wollongong, Australia, and the Sustainable Buildings Research Centre (SBRC) for their constant support throughout my Ph.D. I am also very grateful to the Higher Education Commission (HEC), Pakistan, for providing me with the scholarship.

Finally, I am incredibly grateful for the support and encouragement I received from my Late-father, who supported me through thick and thin. He provided me with all resources I asked for, and was always standing firm beside me. He was the happiest person when I started my Ph.D. and would have been the happiest person upon completion of my Ph.D. I would also like to thank my amazing mother for her support, belief, and encouragement. Special thanks to my best friend, my wife, who has always supported me and made my life stress-free, exciting, and blessed. My special thanks to my siblings, having no interest in what I was doing but still kept asking the same question over the last three years about my Ph.D. completion date.

Overall, I had an amazing time in Australia and learned a lot from the local multicultural diverse society.

Certification

I, Muhammad Bilal Awan, declare that this thesis submitted in fulfilment of the requirements for the conferral of the degree: Doctor of Philosophy, from the University of Wollongong, is wholly my own work unless otherwise referenced or acknowledged. This document has not been submitted for qualifications at any other academic institution.

_____

Muhammad Bilal Awan

7 August 2023

List of publications

Journal papers published

M.B. Awan, K. Li, Z. Li, Z. Ma, 2021, 'A data driven performance assessment strategy for centralized chiller systems using data mining techniques and domain knowledge', Journal of Building Engineering, Volume 41, 102751. (Chapter 3 of this thesis was developed based on this publication).

M.B. Awan, Z. Ma, W. Lin, A.K. Pandey, V.V. Tyagi, 2023, 'A characteristic-oriented strategy for ranking and near-optimal selection of phase change materials for thermal energy storage in building applications', Journal of Energy Storage, Volume 57, 106301. (Chapter 4 of this thesis was developed based on this publication).

M.B. Awan, Y. Sun, W. Lin, Z. Ma, 2023, 'A framework to formulate and aggregate performance indicators to quantify building energy flexibility', Applied Energy, Volume 349, 121590. (Chapter 5 of this thesis was developed based on this publication)

Book chapters published

M.B. Awan, Z. Ma, 2023, 'Chapter 2 - Building energy flexibility: definitions, sources, indicators, and quantification methods', in Book: Building Energy Flexibility and Demand Management, Academic Press, Pages 17-40. (Part of Chapter 2 of this thesis was developed based on this publication).

E. Tunçbilek, Ç. Yıldız, M. Arıcı, Z. Ma, M.B. Awan, 2023, 'Chapter 5 - Thermal energy storage for enhanced building energy flexibility,' in Book: Building Energy Flexibility and Demand Management, Academic Press, Pages 89-119. (Part of Chapter 2 of this thesis was developed based on this publication).

Conference paper published

M.B. Awan, Z. Ma, W. Lin, 2021, 'Formulation of an inclusive demand-side energy flexibility quantification function for buildings with integrated thermal energy storage', Energy Proceedings, Vol. 20. (Part of Chapter 5 of this thesis was developed based on this publication).

Table of Contents

List of Figures

List of Tables

Nomenclature

e	evaporator
c	condenser
p	pump
in	inlet
o	outlet
$\dot{m}$	mass flow rate
T	temperature
ε	specified radius
$\dot{f}_{ij}$	scaled objective function
$\dot{V}_t$	length of the final vector
w	weight
$\prod$	multiplication
ϕ	phase transition stability
ɔ	chemical stability
rm	reversible freeze melt cycles
ϒ	recyclable
ς	corrosiveness
ŧ	toxicity
Ƒ	combustibility
ƨ	supercooling
Ǝ	explosiveness
R	rank
ρ	density
k	thermal conductivity
c_p	specific heat
Q_L	latent heat of fusion
C	cost
p	vapor pressure changes
V	volume changes at phase transition
T	melting temperature range
s	solid

l	liquid
W_{adj}	adjusted weight
CR	consistency ratio
CI	consistency index
γ	relative performance index
P_{flex}	power consumption with flexibility service
P_{inflex}	power consumption without flexibility service
t	time
E	energy
s	start
e	end
γ	energy autonomy
gen	self-generation
st	storage
con	consumption
exp	export
im	import
P_S	power demand reduction potential
$CO_{2\downarrow_{\%}}$	CO_2 reduction potential
F_P	flexibility potential in terms of peak demand reduction
t_e	effective flexible duration
F_C	flexibility potential in terms of cost reduction
C_S	cost reduction potential
rb	rebound
I_{rb}	intensity of rebound

Abbreviations

AEFP	aggregated energy flexibility potential
AHP	analytic hierarchy process
AHC	agglomerative hierarchical clustering
ARM	association rule mining
AHU	air handling unit

BG	building B ground floor
CIT	conditional inference tree
CPR	chiller power ratio
CHWP	chilled water pump
CWP	condenser water pump
CTF	cooling tower fan
COP	coefficient of performance
COPD	COP Destruction
COPRAS	complex proportional assessment
Cl.	cluster
CS	cooling storage
DoW	day of week
DBSCAN	density-based spatial clustering of applications with noise
EFI	energy flexibility indicator
ED	euclidean distance
E	east zone
Esc	building envelope application (space cooling)
ES_{ch}	building envelope application (space cooling or heating)
ES_{h}	building envelope application (space heating)
FAHP	fuzzy AHP
F	fitness centre
FCU	fan coil unit
HVAC	heating, ventilation, and air-conditioning
HS	heat storage
LHS	latent heat storage
MCDA	multi-criteria decision analysis
PCMs	phase change materials
PLR	part load ratio
PV	photovoltaic
R	reception
RMSE	root mean square error
TDE	water temperature difference across the evaporator
TDC	water temperature difference across the condenser

TES	thermal energy storage
TOPSIS	technique for order of preference by similarity to the ideal solution
WPM	weighted product method
W	west zone
XGBoost	extreme gradient boosting

Chapter 1 Introduction

1.1 Background and motivation

Climate change has evolved as one of the most challenging issues of the 21st century. Extreme climatic events have created a global recognition to conserve ecosystems. Ecosystems have been resilient to small environmental changes, but larger changes can cause catastrophic shifts in the ecosystems (Bastiaansen et al. 2020). Carbon emissions from fossil fuel burning are considered the root cause of drastic environmental changes. To reduce the environmental effects of energy generation resources, renewable energy resources (RER) penetration in the global energy mix is rising steadily that climbed up to 29% in 2020 (International Energy Agency & Timothy 2021), and it is expected that this number will continuously increase in the next several decades. The rising penetration of renewable energy resources will pose great challenges and uncertainty for the supply side, including power generation and distribution systems in planning and optimizing the power generation, transmission, and distribution, due to the intermittent nature of renewable energy generation. A tactical response to this challenge requires a strategic shift from generation on-demand to consumption on-demand (Jensen et al. 2017), and thus a bidirectional communication between end-users and power grids. For a smooth power supply, demand and supply sides must be flexible enough to adapt to sudden power shifts (Stinner et al. 2016). Energy flexibility options (e.g. heating, ventilation, and air-conditioning (HVAC) systems, electric vehicles, energy storage, and onsite generation) on the consumption side can help overcome the intermittency problem (Jabir et al. 2018). The building sector consumes over one-third of the total energy produced and emits around 38% of the total carbon emissions (Amasyali & El-Gohary 2018). Hence, flexible buildings can assist in boosting the penetration of RER by supporting the grid operation and reducing the building's operational costs and emissions.

Building energy flexibility is the ability of a building to manage its demand and generation according to user needs, energy network requirements, and local climate conditions. The major purpose of a building energy flexibility plan is to ensure that a building adapts to the power generation patterns without jeopardizing occupants' thermal comfort and other functional requirements while reducing building

operational costs and facilitating power grid optimization. The following factors make building energy flexibility plans attractive for different stakeholders.

Decarbonization: Environmental pollution has resulted in extreme weather conditions such as droughts, floods, heat waves, and heavy storms. It will also likely hit the world economy with a loss of 18% by the mid-century if no action is taken (Swiss Re 2021). The Paris Agreement set a target to keep the world temperature rise preferably below 1.5 ^{o}C and strictly below 2.0 ^{o}C by the mid-century compared to the pre-industrial level to mitigate the adverse effects of environmental changes (Horowitz 2016). Considering that a large share of global emissions is from the building sector, it is important to significantly reduce building emissions to help achieve this target (Laski & Burrows 2017). Research has shown that a building energy flexibility plan can greatly help mitigate building emissions without significant investments (H. Li et al. 2021).

Grid safety: Grid safety is critical to ensuring a continuous supply of electricity to consumers. The rising trend of solar systems has switched end-users from consumers to prosumers, i.e. consumers not only buy electricity from the grid but may also sell electricity to the grid (Marszal-Pomianowska et al. 2019). To stabilize the supply from the grid to buildings and from buildings to the grid, it is important to have a management plan that can effectively create a balance between supply and demand without affecting grid or building operations.

Cost savings: Rising utility prices pose economic pressure on consumers, and they can also have an impact on the economic development of a country (Fernández Álvarez & Gergely 2021; Jacobsen 2009). For instance, the Australian Energy Regulator recently announced that the benchmark electricity prices will increase by up to 18.3% for New South Wales (NSW) residential customers, largely due to a significant increase in wholesale electricity cost over the past year (‘Default market offer prices 2022–23 - Fact sheet’ 2022). Hence, the cost savings factor generates another exigency for the implementation of a building energy flexibility plan. Building operational costs can be greatly reduced using building energy flexibility via demand management strategies such as load shifting, load shedding, and load regulation.

Decentralization: Decentralized power plants are considered more resilient and environmentally friendly, less expensive because of the low infrastructure and operational costs, and more efficient because of low line losses, reliability, and flexibility (Karger & Hennings 2009). Moreover, decentralization of power generation systems can help avoid a complete nationwide blackout. To achieve decentralization, optimized management of building energy and storage systems is vital that can be effectively achieved using building energy flexibility.

Smart metering, smart management of building energy flexible sources, storage, onsite generation, and intelligent control systems have shown the capability to unlock flexibility in buildings (Jensen et al. 2017). HVAC systems have been identified as a key source of flexibility in buildings because of their ability to quickly increase, decrease or shift loads. The development of effective strategies that can be used to evaluate the performance and flexibility potential of HVAC systems, along with identifying opportunities for increased energy flexibility can further enhance the serviceability of these systems for enhanced energy flexibility. Detailed performance assessment of building HVAC systems is essential to tracing operational inefficiencies and changes in system performance under different environmental and operational conditions. Such assessment can lead to developing energy-flexible strategies for HVAC systems.

One of the technical solutions to increase the performance and energy flexibility of building HVAC systems is the use of thermal energy storage (TES) technologies that can help shift energy consumption of the HVAC systems from peak demand hours to off-peak demand hours, and thus support grid services and achieve cost reduction for building owners. A report by the International Renewable Energy Agency (IRENA) demonstrated that TES systems are more cost-effective than electrical storage systems (International Renewable Energy Agency 2020). Different types of TES technologies are available, including sensible storage, latent storage, and thermo-chemical storage. Among available storage technologies, latent heat storage (LHS) systems in the form of PCMs (i.e. paraffin and salt hydrates) have shown a high potential for coupling with HVAC systems (Souayfane et al. 2016). However, a unified model that can be used to select near-optimal PCMs for TES in building applications has not been reported yet.

Although different energy systems have shown high potential for enhancing building energy flexibility, one of the major challenges associated with flexibility implementation is the dearth of a standardized flexibility assessment procedure (Clauß et al. 2017). Addressing this challenge is critical to formulating metrics for the selection of optimized flexibility measures. Moreover, the requirement to formulate indicators that all stakeholders can easily understand worsens the complexity of this challenge. It can be handled by developing a framework that can formulate and aggregate energy flexibility indicators (EFIs) by considering the interactions between different stakeholders.

Building energy flexibility can also be enhanced by predicting the energy consumption and energy flexibility potential of buildings and building energy systems. Such prediction can also support the dynamic supply side and help aggregators to bid optimally in energy markets because of having prior information about energy consumption patterns. It can also increase the acceptability and useability of building energy flexibility among stakeholders.

1.2 Aim and objectives

To address the challenges mentioned above, this thesis aims to develop new strategies that can effectively evaluate and improve the energy flexibility and performance of building HVAC systems, and lead to increased sustainability of buildings powered by conventional and non-conventional energy resources.

The objectives of the thesis to achieve the desired aim strategically are as follows:

i) Develop a data-driven performance assessment strategy to evaluate the performance of chillers, commonly used in commercial office buildings, with distinctive insights into the operational performance of the system.

ii) Develop a strategy for near-optimal selection of PCMs for TES in building applications to increase the performance and energy flexibility of buildings and building energy systems.

iii) Develop a framework for the formulation and aggregation of energy flexibility indicators to evaluate the aggregated energy flexibility potential of buildings and building energy systems by providing distinctive insights into the energy flexibility improvement opportunities.

iv) Develop a prediction model for the prediction of the energy consumption patterns and energy flexibility offered by building energy systems to further enhance the value proposition of building energy flexibility in emerging energy markets.

1.3 Significance

This research seeks to contribute to the advancement of sustainable building practices by developing new strategies to evaluate and improve the energy flexibility and performance of building HVAC systems and proposing a new framework for energy flexibility quantification and energy consumption prediction. Through achieving the objectives outlined in this thesis, such as optimizing chillers' performance, selecting near-optimal thermal energy storage materials, and improving energy flexibility, this research strives to play a vital role in supporting decarbonization, grid safety, cost savings, and decentralization efforts. Ultimately, this thesis aims to enhance the value proposition of building energy flexibility in emerging energy markets and facilitate the transition to a more sustainable and resilient energy future.

1.4 Research methodology

The overall research methodology of the thesis is illustrated in Fig. 1.1. Since the purpose of the thesis was to develop effective strategies to evaluate and improve energy flexibility and performance of building HVAC systems. Hence literature review was initially performed based on the key objectives of the thesis, and relevant research gaps were then identified. The literature review was divided into five sub-sections, including HVAC performance assessment strategies, building energy flexibility fundamentals, TES for enhanced flexibility, building energy flexibility quantification methods, and prediction models.

Based on the identified research gaps and the aim of the thesis, the research tasks were then divided into two categories, in which the first category was focused on the performance assessment and flexibility improvement of building HVAC systems, and the second category was mainly focused on evaluation and prediction of the building energy flexibility. The first category covered the first two objectives, and the second category covered the last two objectives. For the first objective, real-time data from a commercial building was used. For all other objectives, a simulation system was

developed and used for data generation and verification of the developed strategies. Lastly, the key outcomes of the thesis were summarized, and future recommendations were made.

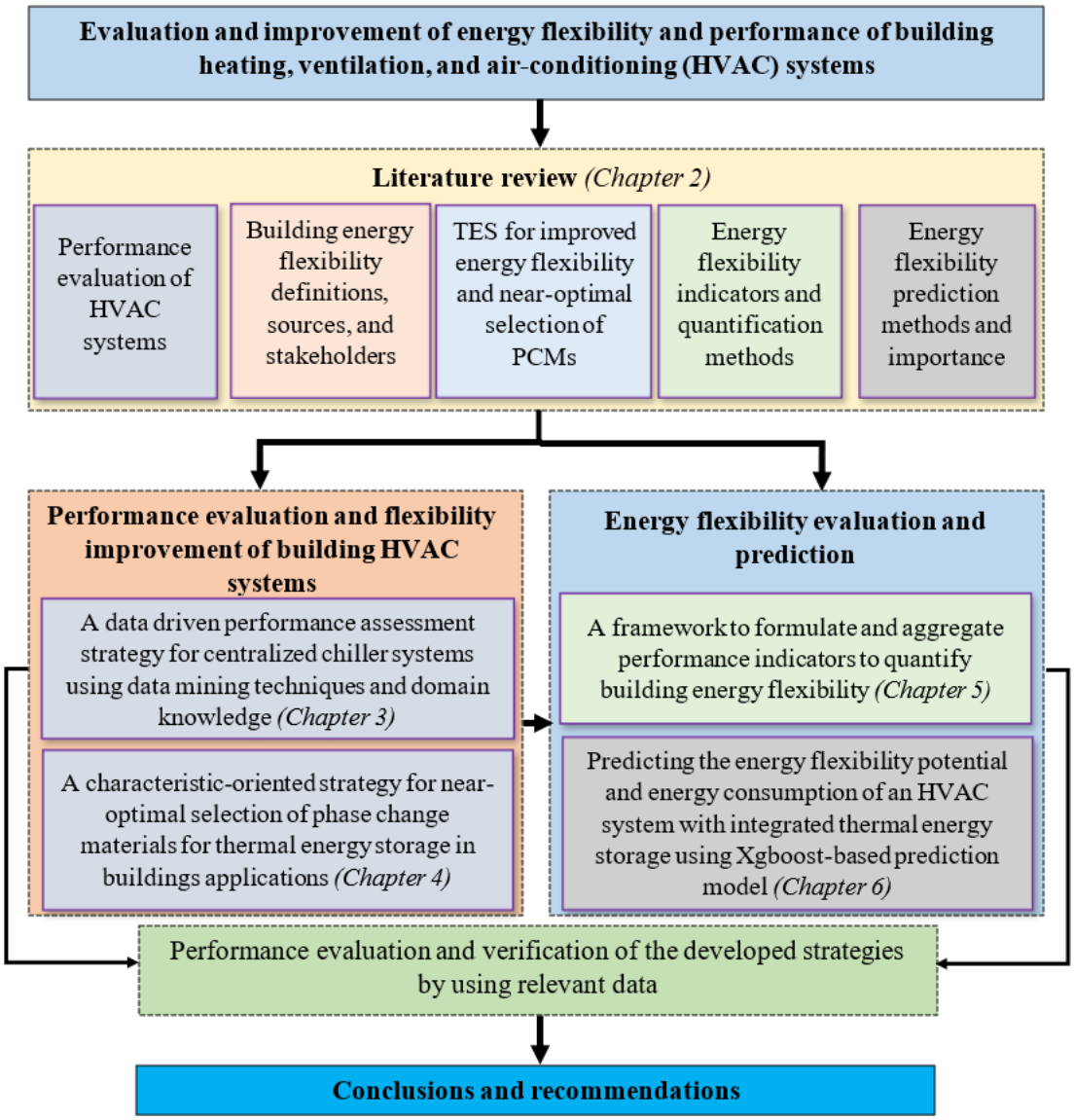

Fig. 1.1 Overall thesis methodology.

1.5 Thesis outline

The subsequent chapters of the thesis are structured as follows:

Chapter 2 reviews the data analytic techniques for HVAC performance assessment, building energy flexibility fundamentals, and applications of TES systems for enhanced performance and energy flexibility of buildings and building energy systems, along with the methods to select near-optimal TES materials for different

thermal energy storage applications. Methods for the quantification and prediction of building energy flexibility were also reviewed. Based on the literature review, several research gaps were then identified.

Chapter 3 introduces the development of a data-driven strategy to evaluate the performance of chiller systems using operational and performance factors. Detailed insights into the operational performance of the chiller system were provided along with the introduction of a new performance indicator, termed Coefficient of Performance (COP) Destruction. Data analytic techniques were used to evaluate the performance and provide unique visualization of the energy consumption patterns of the chiller system.

Chapter 4 presents the development of a strategy to select near-optimal PCMs for TES in building applications. A Multicriteria decision analysis method-based ranking strategy was developed by incorporating both the qualitative and quantitative characteristics of PCMs. Moreover, strategies to convert qualitative characteristics into quantitative factors and handle multiple characteristics of PCMs for weight assignment purposes were also developed. The performance of the strategy was tested and verified by performing two different case studies.

Chapter 5 introduces a framework to develop/select and aggregate EFIs. A novel all-inclusive energy flexibility quantification function that can consider the interactions between different stakeholders was developed. The developed indicators and the quantification function were tested to evaluate the flexibility potential of an HVAC system with integrated TES, and a building with integrated onsite generation system, respectively.

Chapter 6 introduces the development of an Extreme gradient boosting (XGBoost) based energy flexibility prediction model. The model was tested to predict the energy flexibility potential of an HVAC system with integrated TES under varying environmental and building thermal loading conditions. The energy consumption of the system was also predicted using the model.

Chapter 7 summarizes the key findings of this research along with a few recommendations for future research in this direction.

Chapter 2 Literature review

Building energy flexibility has evolved as an effective solution to support the transition towards a renewable energy future. Building heating, ventilation, and air-conditioning (HVAC) systems are an important part of modern society to provide thermal comfort to occupants. They can also be used as a key energy flexibility source due to their ability to rapidly modulate and shift loads. This chapter summarizes the strategies to assess the performance of building HVAC systems and provides a detailed review of building energy flexibility fundamentals. The role of thermal energy storage (TES) in enhancing building energy flexibility, and building energy flexibility quantification and prediction models is also reviewed. Limitations in the existing literature are highlighted as well.

2.1 Performance assessment of building HVAC systems

HVAC systems are responsible for controlling the temperature, air quality, and humidity levels within a building, which directly impacts the building's energy consumption. HVAC systems can also play a crucial role in enhancing building energy flexibility. By implementing energy-efficient HVAC systems, buildings can reduce their energy consumption and improve their energy flexibility. HVAC systems can also be integrated with energy storage technologies to further enhance their energy flexibility. Furthermore, implementing advanced HVAC controls, such as smart thermostats and demand-controlled ventilation, can enable buildings to adjust the operation of HVAC systems in response to changes in energy supply and demand conditions. This allows buildings to optimize their energy consumption and increase their energy flexibility. Energy consumption of HVAC systems is considered sensitive to operational, maintenance, environmental, and loading conditions (Bhawan & Puram 2006). Ji et al. (2017) reported that HVAC performance improvement is necessary for minimizing building energy consumption and operational costs, and a successful performance assessment using fault detection and diagnostics (FDD) can save up to 40% of the HVAC energy.

Performance assessment is the process of measuring, estimating, and verifying the performance and energy consumption of the HVAC systems at actual load and design conditions (Bhawan & Puram 2006). In current practice, the performance assessment

of building energy systems is often achieved through FDD and energy benchmarking (Ji et al. 2017). FDD methods can be classified into model-based, hardware-based, and history-based approaches and are used to discover the errors in physical systems while attempting to identify the source of the problem (Mouzakitis 2013). Benchmarking techniques are often used to identify and implement the best practices that lead to exceptional performance (Anand & Kodali 2008). The Coefficient of Performance (COP), Integrated part load value (IPLV), kW/ton, and Energy efficiency ratio (EER) or European seasonal energy efficiency ratio (ESEER) are often used as performance indicators. Yu et al. (2014) reviewed the standard performance indicators of chillers in nine countries, and it was found that IPLV and ESEER cannot truly reflect the part-load operation of chiller systems. It was recommended that HVAC performance standards should be further developed to allow operators and designers to analyze the performance under actual operating conditions with more transparency and details.

With the improvement in sensing and data collection technologies (H. Parveen & N. Showlat 2017), large sets of building energy usage data are now readily available. Data analytic techniques can extract useful information from this time-series data and provide additional insights into the performance improvement of HVAC systems. Data mining methods have been widely used for building energy profiling and benchmarking. Li et al. (2020), for instance, introduced a data-driven methodology to benchmark and evaluate the electricity consumption patterns of various buildings. A clustering technique was employed to group similar behaving buildings based on the yearly electricity consumption profiles. The Multivariate adaptive regression splines (MARS) model was employed to illustrate the complex non-linear relationships between the explanatory variables and building electricity consumption per square meter. Similarly, Panapakidis et al. (2014) developed a data-driven model to investigate the electricity consumption patterns of a building. The performance of various algorithms, including Fuzzy C-means, *k*-means ++, Self-organized map (SOM), and Minimum various criteria (MVM) with 8, 12, and 16 clusters, was evaluated. Other data-driven models such as Partitioning around medoids (PAM) (Ma et al. 2017), Symbolic aggregate approximation (SAX) (Ma et al. 2018), Agglomerative hierarchical clustering (AHC) (Li et al. 2019), and Gaussian mixture

model clustering (GMMC) (Li et al. 2018) have also been successfully used for the analysis of the building energy systems. Table 2.1 outlines some of the main data mining strategies that have been widely used for performance assessment and energy profiling of buildings and building energy systems.

Table 2.1 Main data mining strategies for performance assessment of buildings and building energy systems

Data mining technique	Description
Regression analysis (Li 2020)	Predicts a continuous dependent variable (e.g. energy consumption) based on one or more independent variables (e.g. weather, occupancy) using linear or non-linear regression models.
Decision trees (Li 2020)	Builds a tree-like model to make decisions based on multiple attributes and outcomes, suitable for classifying energy efficiency levels or identifying critical factors affecting building performance.
Random forest (Liu et al. 2021)	Ensemble learning methods, which combine multiple decision trees to improve accuracy and reduce overfitting, and often used for building energy consumption prediction and fault detection tasks.
Support vector machines (Wei et al. 2018)	It is a supervised learning algorithm that can be mainly used for classification and regression tasks. It is helpful for building energy load forecasting and identifying patterns in energy consumption data.
Clustering (Li 2020)	It is an unsupervised technique that is mainly used for grouping similar data points and is useful for segmenting buildings based on energy usage patterns, by identifying anomalies or classifying buildings into performance categories.
Neural networks (Wei et al. 2018)	Deep learning models with the capability of learning complex patterns from data, which can be applied to tasks like energy prediction, occupancy detection, or optimizing buildings and building energy systems control strategies for energy efficiency.
Principal component analysis (Du & Jin 2007)	Dimensionality reduction technique that can help identify the most significant features or variables in a dataset, and can be used for simplifying complex data structures and feature extraction for energy performance analysis.
Time series analysis (Zhou et al. 2013)	These techniques can be used for analyzing time-dependent data to discover patterns, trends, and seasonality in building energy consumption, supporting tasks like load forecasting, and identifying energy-saving opportunities.

Data mining technique	Description
Association rule mining (Fan et al. 2015)	Discovers relationships and dependencies between variables in large datasets. It is helpful for identifying correlations between building characteristics and energy performance metrics.
K-Nearest neighbors (Panapakidis et al. 2014)	A simple classification algorithm that classifies data points based on the majority class of its k-nearest neighbors, applicable to tasks like identifying similar buildings or predicting energy performance based on neighboring buildings.

Although data analytic techniques have been widely used for building energy profiling, the use of these techniques to evaluate the operational performance of building HVAC systems is still in its early stage. Li & Ju (2017) assessed the operating parameters of a chiller system using hierarchical clustering. The analysis was performed based on simulated datasets. It was concluded that the clustering technology offered a robust performance assessment of the chiller system. In a series of studies presented by Yu & Chan (2009, 2012d, 2012b, 2012c, 2012a, 2013), the performance of chiller systems was evaluated using various statistical and unsupervised learning technologies. In (Yu & Chan 2012d), the relationships between the chiller system COP and operating variables were established for each cluster using regression and Pearson correlation. However, the established relationships had a low R^2 value. In (Yu & Chan 2012b), energy conservation opportunities in the chiller system were identified using Data envelopment analysis (DEA) based benchmarking. It was concluded that the high performance of the chiller system can be achieved by fine-tuning the operating variables. Under perfect control conditions, the system COP can be enhanced from 3.87 to 4.56. In (Yu & Chan 2013), a correlation was built between the chiller system COP and the external (climate) variables using multivariate analysis. Part load ratio (PLR) and temperature differences across the evaporator and condenser were identified as the most significant variables. Three system effectiveness-based parameters, i.e. overall efficiency, scale efficiency and technical efficiency, were calculated. Scale efficiency was linked with the climate variables, whereas technical efficiency was independent of the climate variables. The results showed that fine tuning of the operating variables can achieve electricity savings of around 5.34%. In (Yu & Chan 2012a), cluster analysis was performed to evaluate the

performance of the chiller system and it was concluded that clustering is an efficient and rapid choice to assess chiller systems' performance.

These studies prove the effectiveness of data-driven methods for the performance assessment of HVAC systems. COP was mostly considered as the performance assessment indicator. However, COP alone may not be able to fully reflect the operational performance of chiller systems as it cannot determine how far the system performs from the respective ideal performance. Furthermore, these studies mainly focused on investigating the quantitative effect of the operating variables on the performance of the chiller system without developing a rational qualitative model. Also, they lacked the adaptability of advanced visualization techniques for identifying the distinctive energy usage patterns of the chiller systems that can aid in improving the energy flexibility and performance of building HVAC systems.

2.2 Building energy flexibility fundamentals

2.2.1 Building energy flexibility

The domain of building energy flexibility can be divided into eight categories, as shown in Fig. 2.1 (Marszal-Pomianowska et al. 2019). These categories include driving forces (i.e. why energy flexibility is needed or what benefits a building energy flexibility plan can offer), definitions (i.e. how building energy flexibility can be defined, and what characteristics can be considered to represent the interactions between systems and personals in defining building energy flexibility), methods (i.e. how to characterize and quantify building energy flexibility), energy demand, infrastructure (i.e. type of buildings and power systems), stakeholders, technologies (e.g. electric vehicles, building energy and storage systems, and power generation systems), and control (i.e. type of control schemes to modulate energy systems to achieve optimized flexibility).

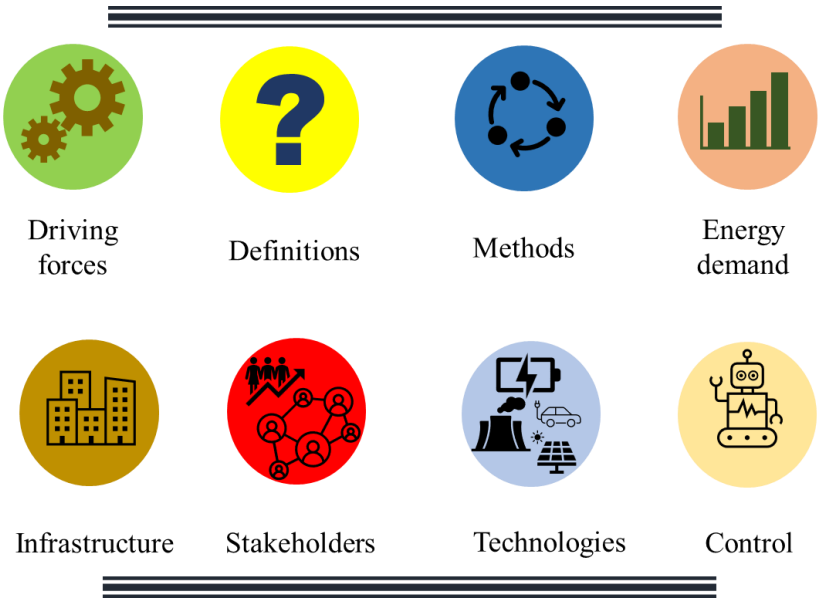

Fig. 2.1 Categorization of building energy flexibility domain.

Depending on the electricity generation and consumption profiles and the power grid operation requirement, different flexibility levels are required at different times and different time scales (duration). For instance, the Australian Energy Market Operator (AEMO) introduced Frequency Control Ancillary Services to maintain the frequency of the electrical power systems. It consists of different regulations and responses, such as fast response (6 seconds), slow response (60 seconds), and delayed response (5 minutes), to handle the drop or rise in frequency of the power generation system because of the change in generation and consumption ratio. Similarly, other ancillary services, such as Network Support and Control Ancillary Services and System Restart Ancillary Services, were also introduced to ensure the safety of the supply side (Operations 2010). Building energy systems, including self-generation, energy storage, and controllable loads, can help meet the targets set by the electricity providers according to different flexibility requirements, such as load covering, load shedding, load shifting, and load modulation.

2.2.2 Definitions

Building energy flexibility or demand flexibility is a progressive form of demand-side management technique. It has received increased attention due to its capability to manage dynamic demand and renewable-powered supply conditions. It can also facilitate the usage of modern controllers such as model predictive controllers to

achieve optimized operation of buildings. However, due to the lack of an international framework for building energy flexibility, several definitions have been reported, which were mainly focused on specific tasks rather than a standardized definition.

In the report of the International Energy Agency (IEA) Annex 67, building energy flexibility was defined as the ability of a building to manage its demand and generation according to user needs, energy network requirements, and local climate conditions (Jensen et al. 2017). In a report published by the International Renewable Energy Agency (IRENA), demand flexibility was defined as part of the demand that can be altered (i.e. reduced, increased, or shifted) in a specific period of time via reshaping the load profiles to match renewable energy generation or via load shifting and peak demand reduction (Matevosyan et al. 2019). In a report prepared by the European Smart Grids Task Force, demand flexibility was categorized into implicit and explicit demand flexibility. Implicit demand flexibility was defined as the reaction of consumers to price signals by adapting their behaviors to save energy costs, while explicit demand flexibility was defined as the committed, dispatchable flexibility that can be traded on different energy markets, which needs to be facilitated and managed by an aggregator (European Smart Grids Task Force Expert Group 3, 2019). Although the above three definitions were slightly different from each other, they all focused on the same principle to change the demand profiles in a specific period of time using different flexibility types (e.g. on-site generation, load shifting, load shedding, peak demand reduction, and load modulation) to meet the requirements of power grids and reduce building operational cost.

2.2.3 Interactions between different stakeholders

Different stakeholders, including the policy makers/government, service providers/aggregators, and consumers, are involved in successfully implementing a building energy flexibility plan. Consumers can be divided into residential and non-residential classes. The residential class further includes single-family and multi-family spaces, whereas the non-residential class can be divided into the industrial and non-industrial sectors. A report published by Expert Group 3 (EG3) of the European Smart Grids Task Force further characterized service providers as balance responsible party (BRP), balance service provider (BSP), congestion/grid capacity management service provider (CMSP), distribution system operator (DSO) and transmission

system operator (TSO) (European Smart Grids Task Force Expert Group 3 2019).

Fig. 2.2 shows a generalized implementation plan for demand flexibility by considering the interactions between different stakeholders. The government body is responsible for suggesting a demand flexibility plan and approving the respective budget. The budget and plan are shared with the aggregators. Consumers are directly linked with aggregators, and the stability of a demand flexibility plan highly depends upon the consumers and aggregators. With the constantly rising energy demand, complex patterns of energy consumption, and renewable energy-based generation, the demand flexibility plan needs to be updated regularly. For that purpose, the aggregator is responsible for closely monitoring external variables such as weather conditions, end-user demand trends, and generation patterns. Based on this data, energy and market analysis needs to be performed to help fine-tune building energy flexibility objectives. Sharing this information with the government authority will help achieve optimized flexibility and future improvements in the generation and transmission systems.

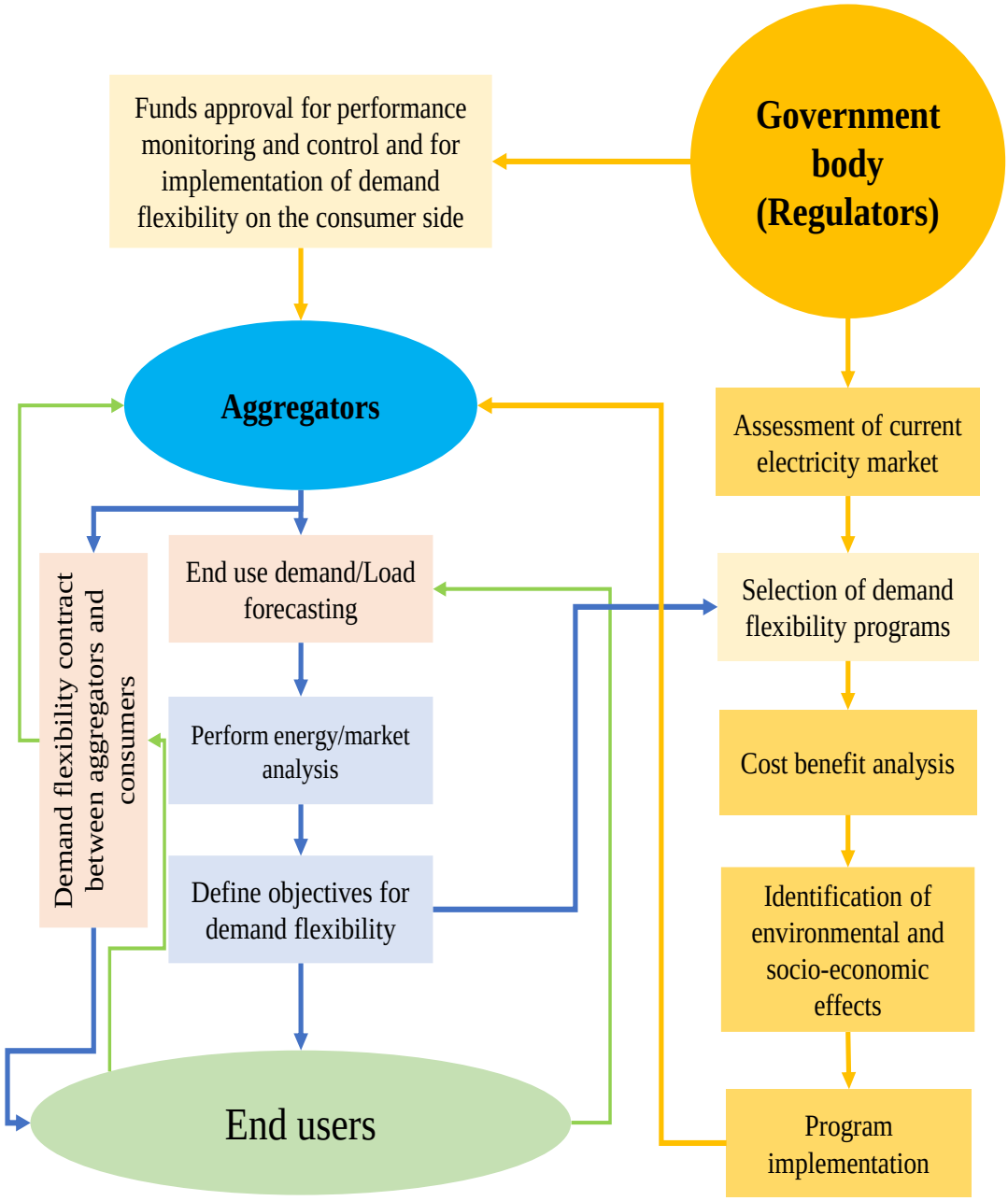

Fig. 2.2 Role of different stakeholders in implementing a building energy flexibility plan.

2.2.4 General procedure for energy flexibility implementation and optimization

Fig. 2.3 illustrates a general procedure to implement a building energy flexibility plan on the consumers'/end-users' side. This six-step strategy includes defining desired objectives, load categorization, data collection, identification of energy flexible measures, quantifying energy flexibility, and optimizing energy flexible measures.

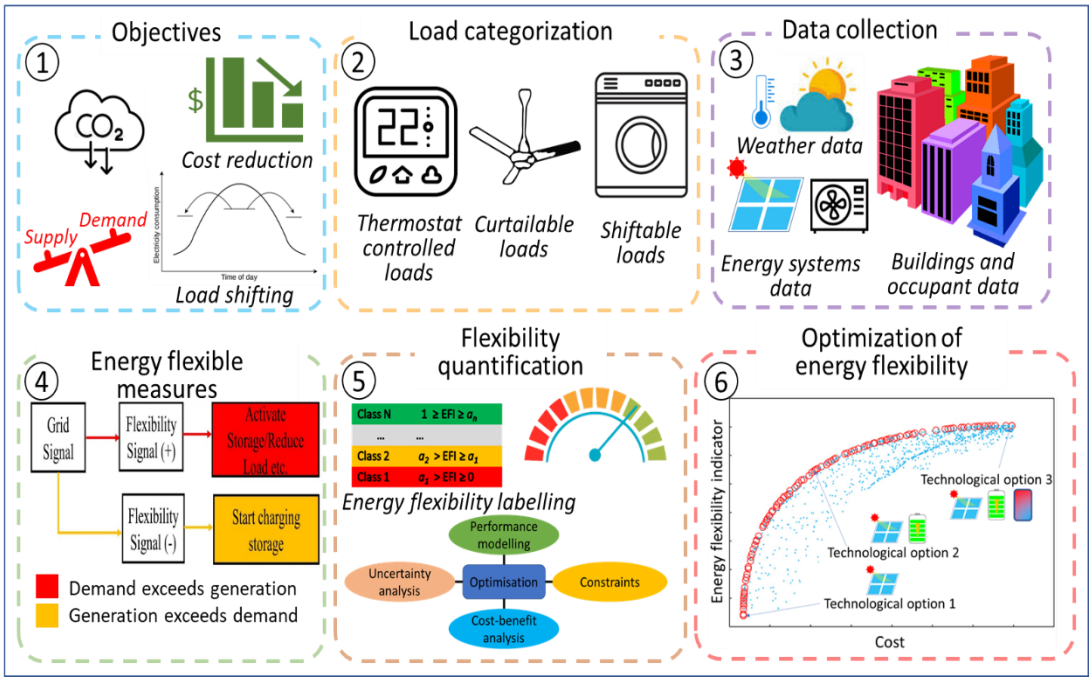

Fig. 2.3 Implementation plan of demand flexibility for end-users.

Different objectives, including grid stability, increased share of renewable energy resources in the total energy mix, cost reduction, increased self-consumption, load reduction, load shifting, and emissions reduction, can be used to form an energy flexibility plan on the demand side. For example, distributors may be interested in improving grid stability and achieving peak demand reduction, while regulators may be interested in reducing emissions and increasing the renewable energy share in the national energy mix. On the consumer side, an increase in self-consumption and cost reduction can be considered to be the leading objectives. Building load categorization is necessary to better understand the load characteristics to meet all these objectives. A building can have different types of loads, including shiftable and non-shiftable loads, thermostatically and non-thermostatically controlled loads, and curtailable and non-curtailable loads. Load categorization can help identify flexible sources inside a building. This step can also help identify different energy flexible measures in Step 4. The next step is to collect data related to buildings and building energy systems. The primary data can include but is not limited to weather data, building materials data, energy bill data, occupancy schedule, equipment usage data, electricity usage profiles, gas usage profiles, hot water consumption data, desired thermal comfort temperatures, and share of renewable and non-renewable consumption/generation. Once data collection is completed, energy flexible measures, such as identifying and

implementing optimal controllers, storage in building thermal mass, storage in the sensible/latent thermal energy storage tanks, electrical energy storage, setpoint changes, delayed operation, and preheating/precooling can be applied. To gauge the effectiveness of the energy flexible measures, quantification of the energy flexible measures is an important process. Various energy flexibility indicators (EFIs) suitable for a particular application can be used for quantification purposes. Details about EFIs and quantification methods are presented in Section 2.4.1 and Section 2.4.2, respectively. Lastly, optimization can be carried out to identify and determine the optimal sizes of energy flexible systems. Different technological options and combinations can also be compared to optimize the flexibility potential of the building (Ren et al. 2021).

2.2.5 Sources of energy flexibility in buildings

Identification of energy flexible sources in buildings is essential to unlocking the flexibility potential of buildings. Different types of buildings and building energy systems offer different levels of flexibility. Both residential and non-residential buildings have several sources of energy flexibility. However, residential buildings can provide more tolerance and susceptibility to an energy flexibility plan (Reka & Ramesh 2016). For instance, load shifting in the industrial sector can disrupt production, but it will not cause much disruption in residential buildings. Potential sources of building energy flexibility are illustrated in Fig. 2.4. Buildings can supply flexible services in different ways, such as the utilization of building thermal mass, changes in the operating schedules and setpoints of HVAC systems, optimization of charging and discharging of electrical and thermal energy storage, and shifting of plug loads (e.g. electrical appliances). This adaptable behavior is an important element in providing unique opportunities for effective demand-side management and thermal comfort of occupants, particularly under extreme weather conditions.

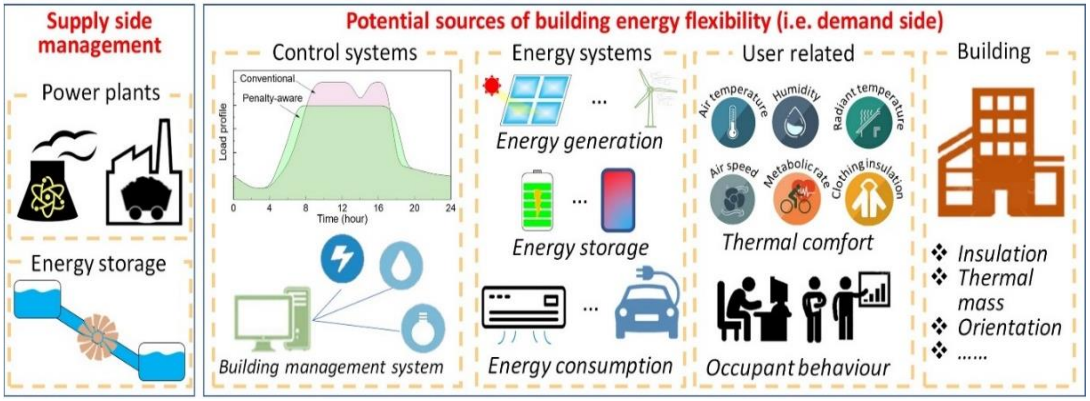

Fig. 2.4 Potential energy flexible sources from buildings for demand-side management.

Building energy flexible sources can be divided into three categories, including generation sources, consumption sources (loads), and storage sources. The potential energy flexible sources for residential buildings are illustrated in Fig. 2.5. Shiftable loads are the loads that can be completely or partially shifted from the peak demand period to the off-peak demand period without significantly compromising the thermal comfort of occupants and impacting the operation of essential equipment and facilities, while non-shiftable loads are the loads that cannot be shifted to the off-peak demand period without disrupting the occupants' thermal comfort and other building functional requirements. Similarly, curtailable loads are the loads that can be reduced during peak demand periods, while non-curtailable loads are the loads that cannot be modulated during peak demand periods without disrupting the thermal comfort of building occupants and the operation of essential equipment. Building loads identified either as shiftable or curtailable can be considered part of a flexibility plan in business-as-usual cases, i.e. no thermal or electrical energy storage and/or no self-generation available for the building. Other energy flexible sources presented in Fig. 2.5, such as energy generation using solar photovoltaic (PV) panels and solar thermal collectors, and energy storage technologies such as thermal energy storage in building thermal mass and sensible and latent heat storage tanks, and electrical energy storage can be used to provide flexibility to the non-flexible loads. Non-shiftable or partially shiftable loads can be made shiftable using thermal or electrical energy storage technologies. For instance, heat pumps can be used to charge TES systems during the off-peak demand hours, and the building cooling/heating load during the peak demand hours can be covered by discharging TES. In general, using energy storage and onsite

energy generation systems can significantly enhance the flexibility potential of a building. These systems are essential for reducing building emissions and optimizing grid operation. An energy flexibility plan for a residential building without storage and self-generation can often compromise the comfort of the occupants.

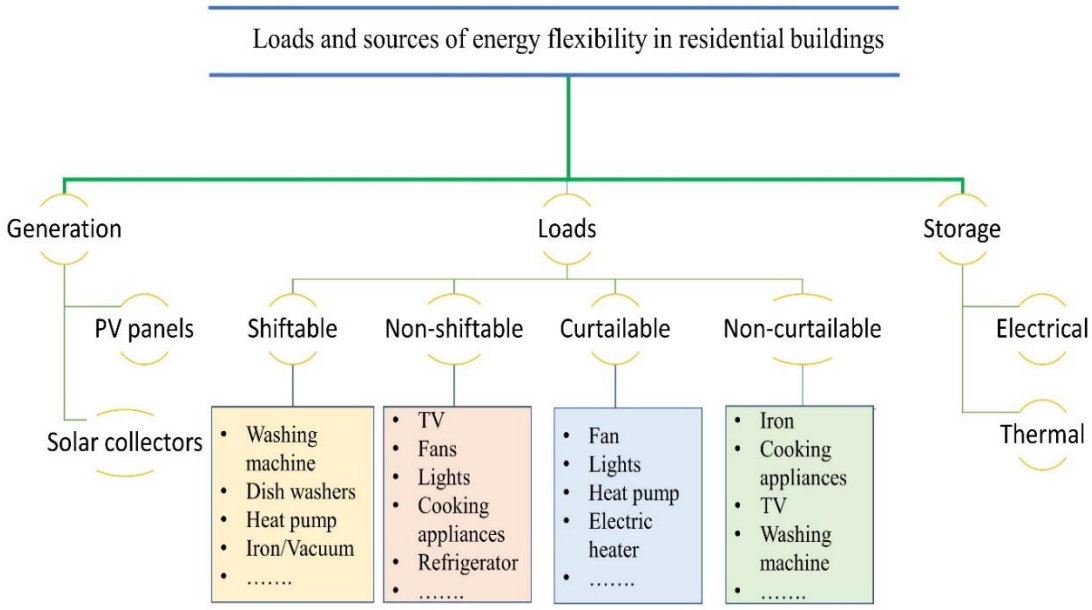

Fig. 2.5 Categorization of energy flexible sources in residential buildings.

2.3 Thermal energy storage for enhanced building energy flexibility

Energy storage is the core of building energy flexibility. Energy storage in the form of building thermal mass, electrical battery storage, and thermal storage has shown high potential in enhancing the energy flexibility of buildings and building energy systems (Luthander et al. 2015; Saffari et al. 2018; Uddin et al. 2018). A review of thermal energy storage for increased demand flexibility and performance improvement of buildings and building energy systems is provided below.

2.3.1 Thermal energy storage in building applications

TES systems for buildings are mainly characterized as latent and sensible heat storage systems. Because of the high energy density, latent heat storage systems can provide increased building energy flexibility. Phase change materials (PCMs) are preferred as latent heat storage materials. There are many PCMs commercially available, and they can be generally categorized into organic, inorganic, and eutectic PCMs. Organic PCMs such as paraffin wax have been widely used as heat storage materials. Paraffin

has shown non-segregation and negligible super-cooling properties, and has proven to be chemically stable. Although organic PCMs have been a priority for heat storage applications, problems such as high cost, low thermal conductivity, and particularly combustibility are among the main challenges to be addressed. This can be potentially tackled using inorganic PCMs such as salt hydrates. Salt hydrates are relatively cheap, available with a wide range of phase change temperatures, and have high thermal conductivity and high specific heat. The major limitations associated with salt hydrates are segregation after multiple cycles, super-cooling, and reactivity with specific metals (Abhat 1983). Such issues can be mitigated using nucleating agents and non-reactive metals (Sharma et al. 2004). Thermal energy can be stored in the building's thermal mass or a separate TES system, such as the PCM tank, that can aid in enhancing the energy flexibility of building energy systems. Different applications of TES in buildings are presented in Fig. 2.6.

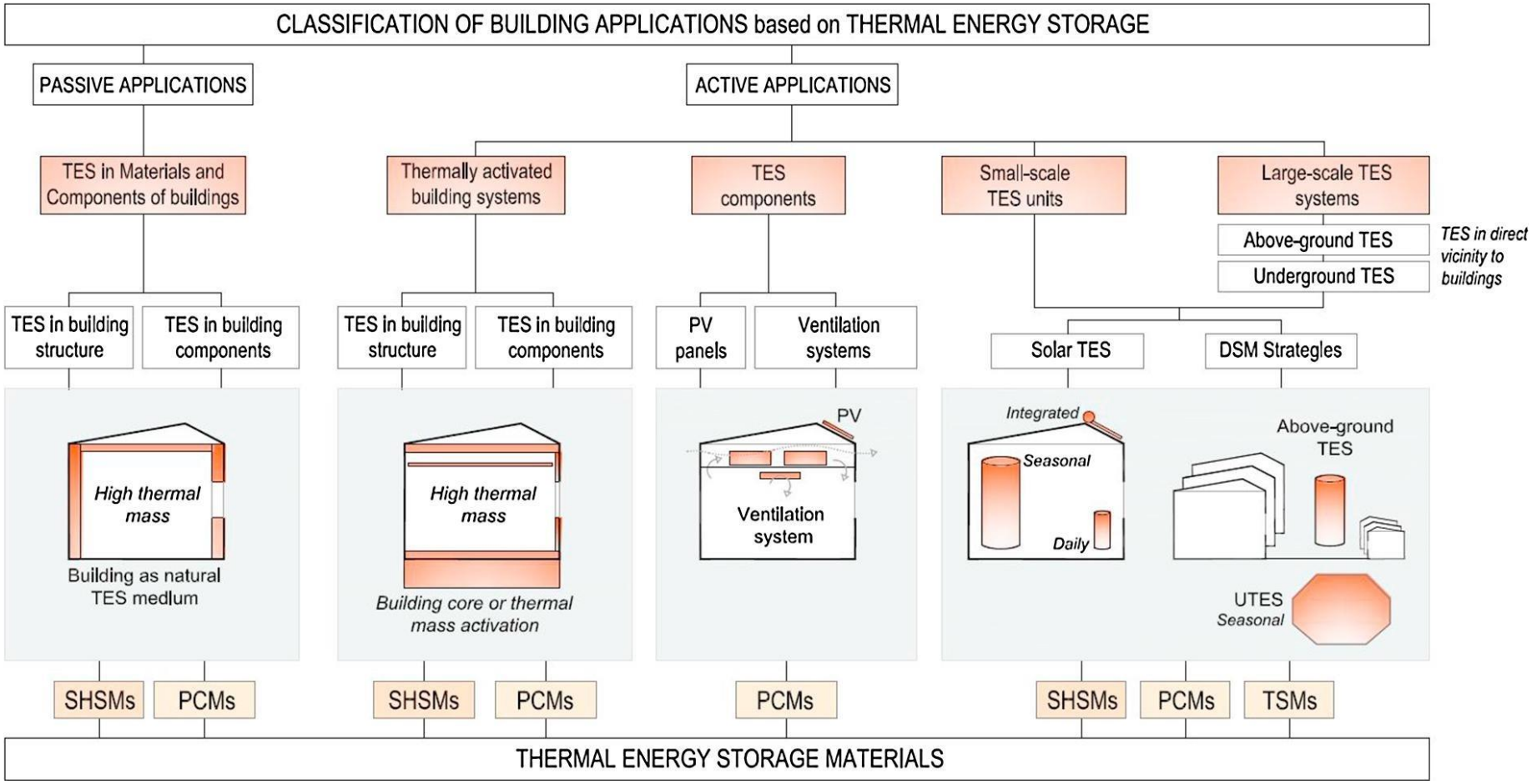

Fig. 2.6 Different applications of TES in buildings [SHSMs: Sensible heat storage materials, TSMs: Thermochemical energy storage material] (Lizana et al. 2017).

2.3.2 Thermal energy storage for demand management and performance improvement of buildings and building energy systems

Fig. 2.7 shows a general representation of thermal energy storage as a building energy flexible source along with some other flexible sources, in which a TES system can provide demand flexibility to a building or building energy system through charging and discharging processes based on the requirement of the grid. During the period of excessive power generation i.e. time period when power generation exceeds the demand, TES systems can support the grid using excessive energy for charging the heat storage materials, and during the period when demand exceeds generation, charged energy of the TES system can be utilized by the building, thus reducing the overall energy consumption of the building.

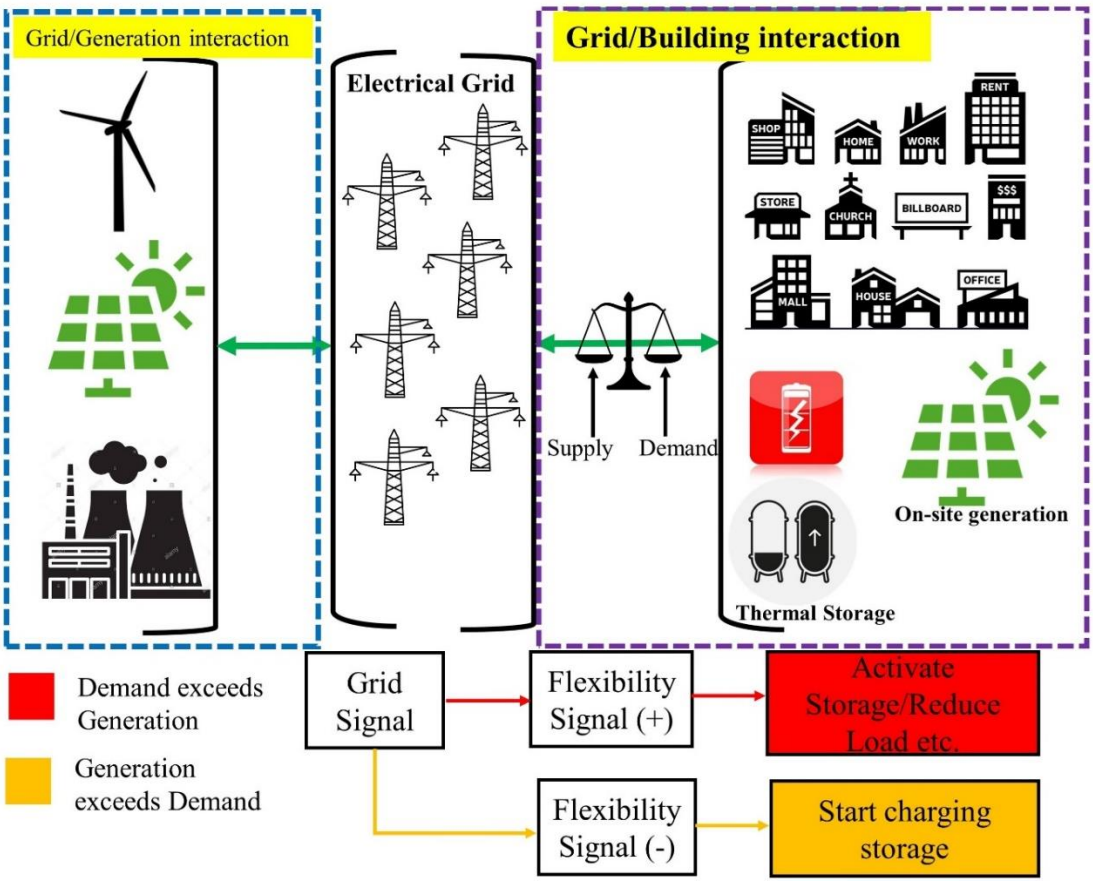

Fig. 2.7 A generalized representation of building energy flexibility.

Two patterns can be used to characterize demand flexibility. Either energy generation can exceed consumption, or consumption can exceed generation. Both manifestations can be converted into signals (Stinner et al.2016), as depicted in Table 2.2.

Table 2.2 Signals for the grid and building interaction.

Grid Signal	Flexibility
-ve (Demand has exceeded generation)	+ve (Activate flexibility options like discharge storage, set-point changes, etc.)
+ve (Generation has exceeded demand)	-ve (Start charging storage etc.)

A comprehensive review of the TES systems for demand management has been provided in Table 2.3, proving that using thermal energy storage in building applications can reduce building operational costs, peak load, and carbon emissions.

Table 2.3 Thermal energy storage for demand management.

Ref.	Energy storage type			Application		Energy storage duration		Evaluation		Significant findings
	Sensible heat storage	Latent heat storage	Thermochemical heat storage	Heating / Domestic hot water	Cooling	Long-term thermal energy storage (Seasonal)	Short-term thermal energy storage	Theoretical analysis or Simulation	Experimental	
(Paksoy et al. 2000)	✓			✓	✓	✓		✓		▪ 3000 MW electricity saving ▪ 2100 tons/year reduction in CO_2 emissions
(Lundh & Dalenbäck 2008)	✓			✓		✓		✓		▪ 3000 kWh electricity demand reduction per unit
(Öztürk 2005)		✓		✓		✓		✓	✓	▪ 40% net energy savings ▪ 4% exergy efficiency
(Buchholz et al. 2009)			✓	✓	✓	✓	✓		✓	▪ Cost reductions achieved
(De Schepper et al. 2019)	✓			✓	✓		✓	✓	✓	▪ Recovery of thermal energy up to 90%
(Vigna et al. 2019)	✓			✓			✓	✓		▪ 14% energy demand reduction ▪ Higher thermal mass does not necessarily increase the energy flexibility index

Ref.	Energy storage type			Application		Energy storage duration		Evaluation		Significant findings
	Sensible heat storage	Latent heat storage	Thermochemical heat storage	Heating / Domestic hot water	Cooling	Long-term thermal energy storage (Seasonal)	Short-term thermal energy storage	Theoretical analysis or Simulation	Experimental	
(Foteinaki et al. 2020)	✓			✓			✓	✓		▪ Cost reduction of up to 15% during the heating season ▪ 40-87% energy demand reduction during morning peak hours
(Luc et al. 2020)	✓			✓			✓	✓		▪ Achieved load shifting between 41 and 51%
(Le Dréau & Heiselberg 2016)	✓			✓			✓	✓		▪ 25 kWh/m^{2}year heat can be modulated for poorly insulated buildings during peak price period ▪ Well-insulated buildings enable modulation of a smaller amount of heat for long time periods
(Hall & Geissler 2015)	✓			✓			✓	✓		▪ Construction type greatly influences the flexibility potential of the building
(Guo et al. 2022)	✓			✓			✓	✓		▪ Nearly 62% reduction in energy consumption
(Balint & Kazmi 2019)	✓			✓			✓	✓		▪ 25% variation (in both positive and negative directions) in energy flexibility depending on smart controllers and occupant behavior
(Johra et al. 2019)	✓	✓		✓			✓	✓		▪ The energy flexibility index was increased by 111 and 35% with PCM wallboards for low-

Ref.	Energy storage type			Application		Energy storage duration		Evaluation		Significant findings
	Sensible heat storage	Latent heat storage	Thermochemical heat storage	Heating / Domestic hot water	Cooling	Long-term thermal energy storage (Seasonal)	Short-term thermal energy storage	Theoretical analysis or Simulation	Experimental	
										insulation and high-insulation light-structure houses, respectively ▪ 42% increase in building time constant because of indoor items and furniture in the built environment
(Trinkl & Zörner 2008)		✓		✓			✓	✓		▪ Solar energy covered 78% of the heat required
(Han et al. 2008)		✓		✓			✓	✓		▪ Latent heat storage provided great flexibility ▪ The operating performance of the heat pump increased by 12.3% using the latent heat storage
(Kelly et al. 2014)	✓	✓		✓			✓	✓		▪ Load shifting increased heat pump electricity consumption ▪ Load shifting by heat pump utilization should be carefully synchronized
(Kuboth et al. 2019)	✓			✓			✓	✓	✓	▪ Average heat pump COP increased by 22% ▪ 34% average reduction in heat pump operational cost
(Pean et al. 2019)	✓			✓	✓		✓	✓	✓	▪ Cost reduction of up to 7% ▪ Decrease in CO_2 emissions by 3-17%

Ref.	Energy storage type			Application		Energy storage duration		Evaluation		Significant findings
	Sensible heat storage	Latent heat storage	Thermochemical heat storage	Heating / Domestic hot water	Cooling	Long-term thermal energy storage (Seasonal)	Short-term thermal energy storage	Theoretical analysis or Simulation	Experimental	
(Hutty et al. 2020)	✓		✓	✓			✓	✓		▪ Adsorption was too costly for load peak shaving alone ▪ 14% reduction in peaks with either water storage or adsorption
(Hirmiz et al. 2019)	✓	✓		✓			✓	✓		▪ The low-temperature heat exchanger can be combined with thermal energy storage to increase the COP of the heat pump ▪ Peaks were sustained between 2 to 6h with a proper storage capacity
(Baeten et al. 2017)	✓			✓			✓	✓		▪ Up to 11% energy production reduction can be reached ▪ Extra storage tanks reduced generation capacity, yet consumer costs increased significantly
(Ren et al. 2021)		✓		✓	✓		✓	✓		▪ Heat pump solar contribution (i.e. energy consumption provided by PV/heat pump total energy consumption) up to 100% can be achieved ▪ Energy consumption for heat pumps can also increase by approximately 5-fold because of using thermal energy storage under a demand-side management strategy

Ref.	Energy storage type			Application		Energy storage duration		Evaluation		Significant findings
	Sensible heat storage	Latent heat storage	Thermochemical heat storage	Heating / Domestic hot water	Cooling	Long-term thermal energy storage (Seasonal)	Short-term thermal energy storage	Theoretical analysis or Simulation	Experimental	
(Y. Li et al. 2021)	✓			✓	✓		✓	✓		▪ 76% decrease in grid electricity demand for heat pump ▪ Peak load shaving by 45%
(Xu et al. 2021)		✓		✓			✓	✓	✓	▪ The system with LHTES provided 22 to 26% better performance ▪ Up to 5% reduction in operational cost ▪ 14% reduction in CO2 emissions
(Lizana et al. 2018)	✓	✓		✓			✓	✓		▪ Cost reductions of up to 20 and 25% for end-user and retailers, respectively ▪ CO2 emissions remained almost constant ▪ High payback period, roughly 10 years

Overall, using TES in buildings can be a valuable tool for reducing energy consumption and improving the flexibility potential of buildings and building energy systems. Still, it is important to carefully consider the potential limitations and challenges before implementing such systems.

2.3.3 Near-optimal selection of PCMs for TES systems

Since there are numerous PCMs available, the selection of an optimal PCM for a particular application is a challenging and time-consuming task, and it often turns out to be a multi-criteria decision problem as several properties such as thermal conductivity, latent heat of fusion, and phase change temperature can affect the performance of a TES system. Such problems can be potentially solved using multi-criteria decision analysis (MCDA) methods. The potential input variables often used in the multi-criteria selection of near-optimal PCMs can be as follows (Whiffen & Riffat 2013).

- Desirable properties with high values: Specific heat, latent heat of fusion, availability, chemical stability, density, recyclability, thermal conductivity, nucleation, and crystal growth rates, and phase transition stability.
- Desirable properties with low values: Volume changes during phase transition, vapor pressure, and cost.
- Other properties: Complete reversible freezing and melting cycles, melting temperature within the application range, negligible corrosiveness, supercooling, toxicity, combustibility, and explosiveness.

The application of MCDA for decision-making has been spread to various fields (Kolios et al. 2016; Muhsen et al. 2019; Stojčić et al. 2019). The prominent MCDA methods include: Weighted sum method (WSM), Weighted product method (WPM), Analytic hierarchy process (AHP), VIseKriterijumska Optimizacija I Kompromisno Resenje (VIKOR), Preference ranking organization method for enrichment evaluation (PROMETHEE), The technique for order of preference by similarity to the ideal solution (TOPSIS), Elimination et choixtraduisant la realité (ELECTRE), and Complex proportional assessment (COPRAS) (Beltrán & Martínez-Gómez 2019; Kolios et al. 2016; Stojčić et al. 2019). These methods have their respective advantages and limitations. Care should be taken when selecting a method for a

specific application, as the decision-making process can be complex. Comprehensive knowledge is also required in quantifying the data, defining alternatives, and assigning qualitative attributes. Attributes can increase the complexity of the decision-making process because of their mutuality, severance, and degree of completeness (Kolios et al. 2016).

The use of MCDA techniques to select an optimal PCM from a small list of commercial PCMs has been reported in many studies. Socaciu et al. (2016), for instance, applied the AHP method to characterize the performance of ten commercially available PCMs and identified the optimal PCM to ensure thermal comfort inside a vehicle. Phase change temperature, latent heat of fusion, sensible heat, thermal conductivity, densities in the liquid and solid forms, and maximum operating temperature were considered attributes in the decision-making. Weights for different attributes were assigned using the Saaty 9-point scale. Xu et al. (2017) applied the AHP and TOPSIS methods to select the best PCM for a heat storage unit, which was integrated with a solar absorption chilling system. The results showed that the method can successfully rank PCMs by considering their thermodynamic properties, and integration of the PCM into the solar cooling system can enhance its overall performance. Anilkumar et al. (2021) used different MCDA techniques for the optimal selection of PCMs for solar box cookers. The results showed the high performance of the selected PCM, and it was also found that the top-performing PCM required less quantity compared with other selected PCMs. Fernandez et al. (2010) used the Ashby approach to selecting the top-performing sensible heat storage materials with phase change temperatures ranging between 150 ^{o}C and 200 ^{o}C. Rathod & Kanzaria (2011) used AHP in combination with TOPSIS and Fuzzy TOPSIS methods to identify the best PCM from a list of nine PCMs. This method successfully ranked the PCMs, and TOPSIS proved to be suitable for performance rating, while Fuzzy TOPSIS performed better when ratings were vague, and the accuracy requirement was not high. Das et al. (2021) used TOPSIS for the selection of a PCM to provide thermal comfort in vehicles. The best PCM from a list of twenty-six PCMs was determined. Yang et al. (2018) introduced a methodological concept for PCM selection. This method included the integration of the AHP method for subjective weight assignment, the entropy information method for objective weight assignment,

and TOPSIS as the MCDA tool. The use of the top-ranked PCM integrated with a ground source heat pump system showed a positive impact on the system's performance. Beltrán & Martínez-Gómez (2019) selected and analyzed the performance of PCMs for building wallboards and roofs. The optimal PCM was selected from a list of nine PCMs using TOPSIS, VIKOR, and COPRAS-G, respectively. Small variations were observed in the results of using these three methods. The results from the aforementioned studies showed that MCDA can be a useful tool for accurate PCM ranking.

Although the existing studies successfully implemented MCDA tools for PCM ranking, a rational ranking strategy that can also consider the qualitative characteristics of PCMs, including the strategies to convert qualitative characteristics into quantitative factors and handle multiple characteristics of PCMs for weight assignment purposes, has not been reported.

2.4 Energy flexibility indicators and quantification methods

2.4.1 Indicators

EFIs are considered to be an important component in a flexibility plan to gauge the performance and effectiveness of energy flexibility measures and provide insights for better decision-making. A building energy flexibility plan includes cross-sectoral and multi-system interactions. Many EFIs have been formulated and used to evaluate the flexibility potential of various energy flexible systems involved in an energy flexibility plan. As presented in Section 2.2.5, the flexibility on the building side is dependent on three main sources, including energy generation, energy storage, and shiftable and/or curtailable loads. Hence, the formulated EFIs should be able to evaluate the performance of these sources and the effect of these sources on the overall flexibility potential of a building. Five key factors, including time, power/energy, capacity/amount, cost, and efficiency/effectiveness, have been frequently used in the formulation of building EFIs. Each of these factors can be used to present several aspects of building energy flexibility. For instance, the capacity factor can be used to estimate the amount of energy shifted, and it can also be used to estimate the charging state of a TES system after providing flexibility to a building. All of these factors should be evaluated using appropriate EFIs to gauge the success of a flexibility plan.

Among these five key factors, time is the most important parameter to formulate EFIs, as a flexibility plan is highly dependent on the response time, activation time, and demand response period. Hence, to formulate an EFI, the temporal domain of the flexibility plan should be considered. Details about these factors are presented in Table 2.4.

Table 2.4 Summary of key factors used in the formulation of building EFIs.

Key factor	Description
Time	• Demand response period, i.e. flexibility activation period • Response time • Charging / Discharging periods • …
Power/energy	• Energy-savings potential • Self-generation potential • Self-consumption potential • Power reduction potential • Power shifting/shedding potential • …
Capacity/amount	• Storage capacity • Amount of emissions reduced • Comfort compromised • Maximum hourly surplus • Maximum hourly deficit • …
Cost	• Cost reduction potential
Efficiency/effectiveness	• Effectiveness of a flexibility plan • Flexible energy efficiency • Storage efficiency • ….

These key factors can be used to formulate different EFIs such as optimum cost factor, available structural storage capacity, rebound energy, flexibility index of aggregated demand, power shifting capability, loss of load probability, and many other EFIs as those reported in (Airò Farulla et al. 2021; Marszal-Pomianowska et al. 2019). Table 2.5 summarizes the major flexibility indicators that can be used to evaluate the flexibility potential of a building and building energy flexible systems, and their interaction with the power grid.

Table 2.5 Summary of EFIs developed for building demand flexibility.

Application	Indicator	Factors covered					Formulation and description
		Time	*Power*	*Cost*	*Capacity*	*Efficiency*	
Building level	Demand response potential (Yin et al. 2016)	✓	✓		✓		$DR_i = \frac{P_{i,b} - P_{i.DR}}{P_{i,b}}$ where i represents the i[th] appliance, $P_{i,b}$ is the average baseline power during a DR event, and $P_{i,DR}$ is the power consumption using flexible measures.
	Self-sufficiency (Salom et al. 2014)	✓	✓		✓		$\gamma_l = \frac{\int_{t1}^{t2} \min [G(t) - S(t) - \zeta(t), l(t)]dt}{\int_{t1}^{t2} l(t)dt}$ where ζ represents energy losses, G is the generation, l is the building demand and S is the storage.
	Self-consumption (Salom et al. 2014)	✓	✓		✓		$\gamma_s = \frac{\int_{t1}^{t2} \min [G(t) - S(t) - \zeta(t), l(t)]dt}{\int_{t1}^{t2} G(t)dt}$
	Flexibility factor (Zhou & Cao 2020)	✓	✓		✓		$FF_{f,e} = \frac{E_{f,e}^{+} - E_{f,e}^{-}}{E_{f,e}^{+} + E_{f,e}^{-}}$ $FF_{d,e} = \frac{E_{d,e}^{+} - E_{d,e}^{-}}{E_{d,e}^{+} + E_{d,e}^{-}}$ where f and d are forced and delayed, respectively; + and – indicate the system operated with and without using energy flexible measures, respectively.
	Flexibility index (Junker et al. 2018)	✓	✓	✓	✓		$FI = 1 - \frac{C^1}{C^0}$; $C^1 = \sum_{t=0}^{N} \sigma_t \ u_t^1$; $C^0 = \sum_{t=0}^{N} \sigma_t \ u_t^0$ where C represents the cost, u_t^1 and u_t^0 respectively represent energy consumption at time t under the penalty aware control and penalty-ignorant control, and σ_t is the penalty on the energy consumption at time t.

Application	Indicator	Factors covered					Formulation and description
		Time	*Power*	*Cost*	*Capacity*	*Efficiency*	
	Flexibility indicator of aggregate demand (Sajjad et al. 2016)		✓		✓		$\mathrm{F}_{\Delta t_s}^{(a)} = 2 \times \min_{\forall \omega_{\Delta t_s}^{(a)}} (\omega_{\Delta t_s}^{(a)}, (1-\omega_{\Delta t_s}^{(a)})),$ $with\ \mathrm{F}_{\Delta t_s}^{(a)} \epsilon\ [0,1]$ where $\omega_{\Delta t_s}^{(a)}$ and $(1-\omega_{\Delta t_s}^{(a)})$ represent the binomial probability of increase and non-increase in demand respectively, and *a* represents the number of aggregating customers.
	Percentage flexibility level (Sajjad et al. 2016)		✓		✓		$\psi_{\Delta t_{s\%}}^{(a)} = \frac{\overline{\Delta p}_{\Delta t_s+}^{(a)} - \overline{\Delta p}_{\Delta t_s-}^{(a)}}{\bar{p}_{\Delta t_s}^{(a)}} \left(\frac{\mathrm{F}_{\Delta t_s}^{(a)}}{2}\right) \times 100$ where $\overline{\Delta p}_{\Delta t_s+}^{(a)}$ and $\overline{\Delta p}_{\Delta t_s-}^{(a)}$ are the mean load variations for the increase and non-increase in demand respectively, and $\bar{p}_{\Delta t_s+}^{(a)}$ is the mean aggregate demand.
	Energy flexibility (Stinner et al. 2016)	✓	✓		✓		$EF(t) = \int_{t1}^{t2} \left(P_{flex}(t) - P_{inflex}(t)\right) dt$
	Power shifting flexibility (Tang & Wang 2021)	✓	✓		✓		$r_{shift} = \frac{P_{shifted}}{P_{demand}}$
	Rebound energy (Kathirgamanathan et al. 2020)	✓	✓		✓		$E_{rb} = \int_{-\infty}^{l_{DR,start}} (P_{DR} - P_{ref}) dt + \int_{l_{DR,end}}^{+\infty} (P_{DR} - P_{ref}) dt$ where DR represents the demand response event.
	Flexible energy efficiency (Kathirgamanathan et al. 2020)		✓			✓	$\eta_f = \left\lvert \frac{E_f}{E_{rb}} \right\rvert \times 100\%$
Grid	Grid interaction index (Salom et al. 2011)	✓	✓		✓		$f_{grid} = STD\left[\frac{E_i}{Max\lvert E_i \rvert}\right]$ where *E* is the net energy export to the grid at time interval *i*, and STD is the representation of standard deviation.

Application	Indicator	Factors covered					Formulation and description
		Time	*Power*	*Cost*	*Capacity*	*Efficiency*	
	One percent peak power (Verbruggen & Driesen 2015)	✓	✓		✓		$OPP\ (kW) = \frac{P_{1\%\ Peak}}{\Delta t(h)/100}$
	Absolute grid support coefficient (Klein et al. 2017)	✓	✓		✓		$GSC = \frac{\sum_{i=1}^{n} P_{el}^{i} G^{i}}{P_{el}\bar{G}}$ where P_{el}^{i} and G^{i} respectively represent the electricity consumption and value of the grid signal at the time step i, n represents the total number of time steps, and P_{el} and $\bar{G}$ are the average values in a period of interest.
Building energy systems	The flexibility of building thermal mass (Chen et al. 2019)	✓	✓		✓	✓	$F_{TM} = \frac{\sum_{i=1}^{n} \alpha_i C_i \Delta T}{t_{DR} COP_{HVAC}}$ where α_i is the heat release ratio of thermal mass, ΔT is the thermal comfort temperature range, C_i is the total heat capacity of thermal mass, and COP is the HVAC Coefficient of performance.
	Flexibility of HVAC systems (Chen et al. 2019)	✓	✓		✓	✓	$F_{HVAC} = F_{TM} + \frac{\left[k_0 P_{lights} + \left(\frac{\rho_a V_r c_a}{t_{DR}} + U_A + \dot{m} c_a\right)\Delta T\right]}{COP_{HVAC}}$ where $k_0 P_{lights}$ is the heat gain reduction from lights, and $\rho_a, V_r, c_a, U_A and\ \dot{m}$ represent the air density, volume of the thermal zone, air specific heat, overall heat transfer coefficient, and mass flow rate of fresh air, respectively.
	Shifting efficiency of building thermal mass (Le Dréau & Heiselberg 2016)				✓	✓	$\eta = \frac{\Delta Q_{discharged}}{\Delta Q_{charged}}$

Application	Indicator	Factors covered					Formulation and description
		Time	*Power*	*Cost*	*Capacity*	*Efficiency*	
	Flexibility of thermal storage tanks (Chen et al. 2019)	✓	✓		✓	✓	$F_{T.S} = \frac{\left[\frac{\rho_w V_{tank} c_w \left(T_{tank,t_0} - T_{tank,t_{DR}}\right)}{t_{DR}}\right]}{COP_{HVAC}}$ where T_{tank} represents the temperature of the tank.
	Flexibility of electrical battery based load (Tulabing et al. 2016)	✓			✓		$F_{ES} = \frac{(t_{use} - t) - \left(t_f - t\right)}{t_{use} - t}$ where t, t_{use} and t_f respectively represent the current time, the time when the fully charged battery will be used and the expected time to finish charging based on charging status.
	Flexibility of lights (Chen et al. 2019)		✓		✓		$F_{lights} = k_0 P_{lights}$ where P_{lights} represents the lights load and k_0 represents the lights dimming rate with the value of one indicating that lights can be completely turned off.
	Flexibility of appliances (Chen et al. 2019)	✓	✓		✓		$F_{app} = \sum_{i=1}^{n} P_i(t).K_i(t)$ where $P_i(t)$ and $K_i(t)$ respectively represent the power and flexibility state of the appliance.
	Flexibility of occupant behavior (Chen et al. 2019)	✓	✓		✓	✓	$F_{OB} = \frac{\Delta T_{extra}(\sum_{i=1}^{n} \frac{\alpha_i C_i}{t_{DR}} + \frac{\rho_a V_r c_a}{t_{DR}} + U_A + \dot{m}c}{COP_{HVAC}}$ where ΔT_{extra} represents the difference between the upper limit of the recommended temperature range and the maximum temperature that occupants can accept for cooling applications.

Application	Indicator	Factors covered					Formulation and description
		Time	*Power*	*Cost*	*Capacity*	*Efficiency*	
	Flexibility index of combined cooling, heating, and power system (Zhou et al. 2021)		✓		✓		$FI = \left(w_{gas} \frac{U_{gb}^{no} - U_{gb}}{U_{gb}^{no}} + w_{grid} \frac{P_{grid}^{no} - P_{grid}}{P_{grid}^{no}} \right) \times 100$ where w represents weight, U_{gb} and P_{grid} respectively represent natural gas usage of the boiler and interactive power (i.e. sum of power purchased from and sold to the grid) between the system and grid, and U_{gb}^{no} and P_{grid}^{no} respectively represent the fuel consumption of the gas boiler and interactive power without storage devices.
	Flexibility of wind power-based system (Ma et al. 2013)	✓	✓		✓		$F_{E.A} = \sum_{i \epsilon A}^{n} \left[\frac{P_{max}(i)}{\sum P_{max}(i)} \times \frac{0.5[P_{max}(i) - P_{min}(i)] + 0.5[Ramp(i)]}{P_{max}(i)} \right.$ where $P_{max}(i)$ and $P_{min}(i)$ respectively represent the maximum capacity and the minimum stable generation of the conventional generator i. $0.5[Ramp(i)]$ represents the average value of ramp up and ramp down.

Although EFIs developed to date can represent the flexibility potential of a building or building energy systems under dynamic conditions and specific flexibility plans, some have limitations in providing collective information related to the interactions between different stakeholders. Under an energy flexibility plan, if an EFI is just to provide information about a single objective, such as cost reduction or demand reduction, it may then only provide limited opportunities for operational improvements. Furthermore, a specific value of flexibility obtained in a building cannot guarantee similar results in other buildings because of disregarding external variables such as weather conditions, occupant behavior, and state of energy systems in formulating the EFIs. Hence, EFIs should be further developed to present a broader aspect of the flexibility domain.

2.4.2 Quantification methods

Quantifying building energy flexibility is important for assessing the potential for reducing energy demand and improving the overall efficiency of building energy systems. By measuring and tracking key indicators such as energy consumption and demand, energy savings, and the effectiveness of demand management programs, building owners and managers can identify opportunities for improving energy flexibility and reducing energy costs. In addition, quantification can provide valuable information for policymakers and regulators to develop effective energy policies and support the transition to a more flexible and resilient energy network. Overall, quantifying building energy flexibility can help drive the adoption of energy-efficient technologies and practices, and contribute to the sustainability and environmental performance of buildings. Furthermore, quantification of building energy flexibility is also vital to assign a numeric value to the performance of an energy flexibility plan. A standardized quantification method can be used to evaluate and optimize the flexibility potential of a building, and it can also be used to compare the performance of a building with other buildings under similar energy flexibility plans. As shown in Fig. 2.8, eight main factors, including power grid requirement, utility tariff, flexibility types, demand response strategies, energy flexible measures, constraints, uncertainties, and the selection and aggregation of EFIs, govern the development of a quantification method.

To support power grid operation, an energy flexibility plan must control the kVA demand of the building according to the requirement of the power grid. kVA is a measure of apparent power and helps maintain the frequency of the power generation system according to the pre-set limits. To maintain the frequency, a grid-responsive building should be able to increase or decrease its consumption according to the grid needs, which can be achieved by optimizing and controlling the operation of building energy flexibility sources. Service providers monitor and predict generation and demand patterns and develop different tariffs accordingly, focusing on cost penalties and consumer benefits. These tariff profiles are then used to facilitate the development of different demand response programs and flexibility types, such as load shifting, load shedding, and load covering. Buildings working under a flexibility plan can respond with different capacities and at different periods of time to these demand

response programs by controlling the operation of energy flexible systems while considering system constraints and uncertainties. The performance of energy flexible measures needs to be evaluated by appropriate EFIs in relation to other factors. Furthermore, aggregation is required if multiple EFIs are used to quantify the overall response of the building to the grid requirement.

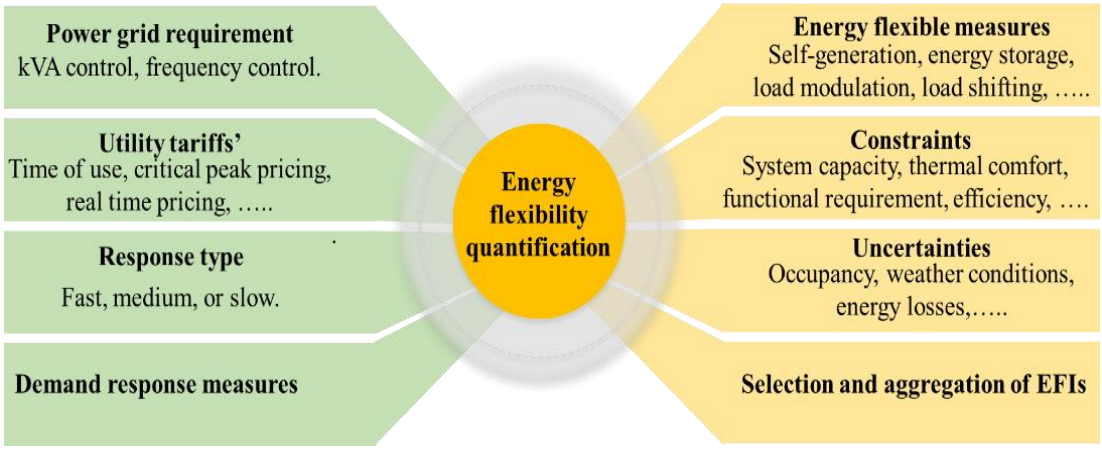

Fig. 2.8 Factors for quantification of building energy flexibility.

A number of building energy flexibility quantification methods or frameworks have been reported in the open literature, which were mainly developed to quantify the flexible response of buildings or building energy systems according to the need of a specific study. For instance, Yin et al. (2016) proposed a demand response estimation framework to quantify the flexibility potential of residential and commercial buildings using setpoint changes. Based on the physical models developed, the demand response potential of thermostatically controlled loads was first determined, and a simplified strategy based on a set of regression models which used hour of the day, setpoint change, and outdoor air temperature as the inputs was then developed and used to estimate demand response potential. Stinner et al. (2016) developed a methodology to quantify the flexibility potential of building energy systems with integrated thermal energy storage. The developed method can compare different flexibility options for building energy systems via the calculation of temporal flexibility, power flexibility, and energy flexibility through simulations. It was claimed that one of the main features of this methodology was the aggregation potential of the flexibility measures. Tang & Wang (2021) presented a methodology, as shown in Fig. 2.9, to quantify the flexibility potential of grid-responsive buildings. The flexibility capacities and

flexibility ratios were proposed and used as the flexibility indicators, which eventually resulted in generating a five-dimensional flexibility performance map. The results from a case study showed that this strategy can help achieve up to a 21% reduction in electricity costs.

Chen et al. (2019) presented the quantification of energy flexibility offered by building thermal mass, HVAC systems, lighting, appliances, and occupant behaviors based on their mathematical expressions and using the flexibility ratio as the indicator. Zhou et al. (2021) developed a strategy, as shown in Fig. 2.10, to quantify and optimize the flexibility potential of a combined cooling, heating, and power system using a new flexibility index, which can reflect system design and operational performance. The flexibility enhancement was achieved through the optimization of system configuration and the use of appropriate operation strategies. It was shown that the flexible components in the system can well handle the uncertainties due to renewable energy generation and power demand.

Perera et al. (2019) introduced a quantification method to evaluate the energy systems flexibility, as shown in Fig. 2.11. An MCDA method was used to aggregate different flexibility indicators in order to develop a single quantification function. A number of probabilistic scenarios for different grid conditions, energy demand, and renewable energy generation were simulated. It was concluded that more than 45% renewable energy covering with respect to the annual demand can be achieved. However, a decrease in the flexibility level was observed if the renewable energy penetration level was above 30%.

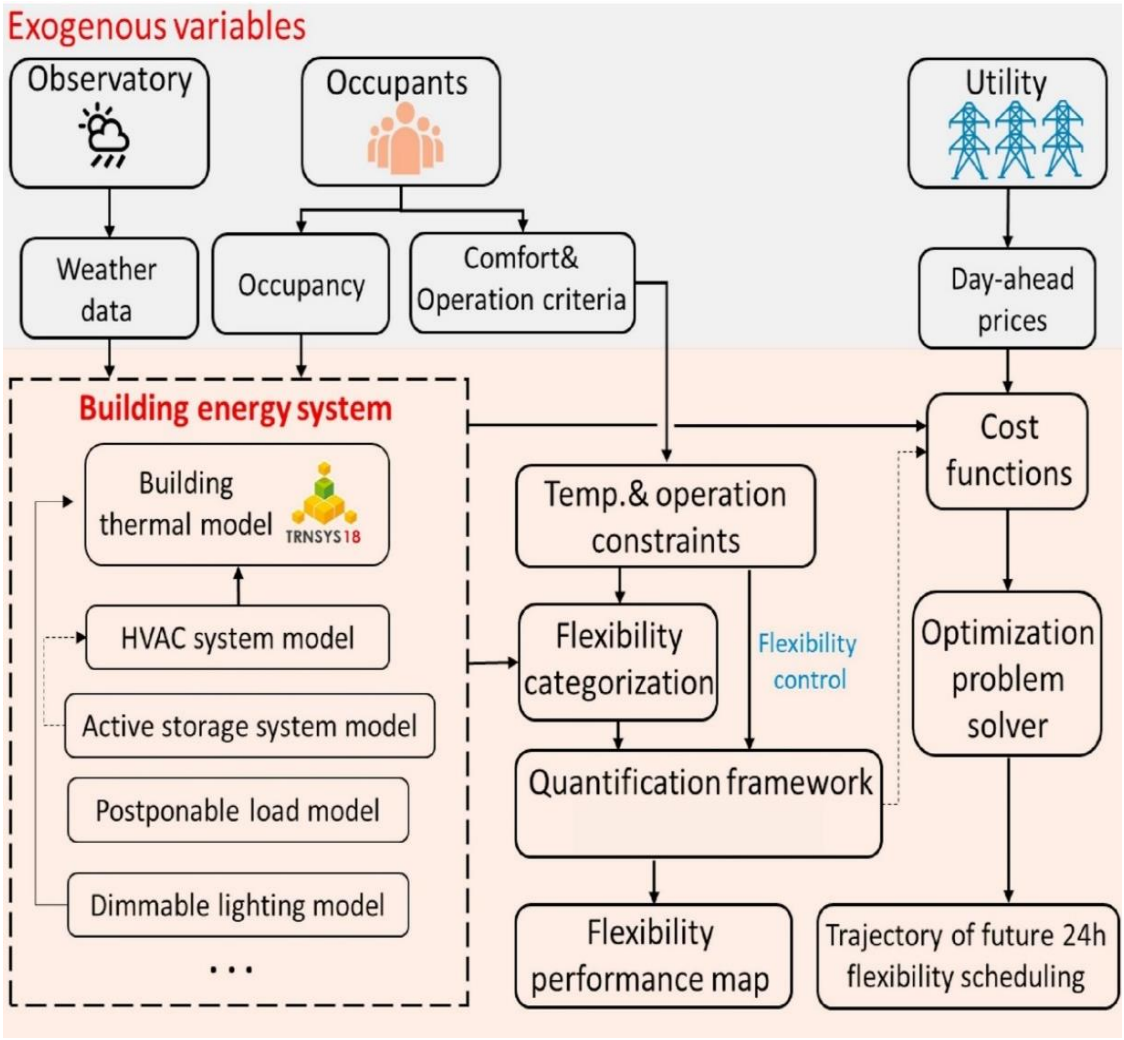

Fig. 2.9 A strategy for energy flexibility quantification and schedule optimization (Tang & Wang 2021).

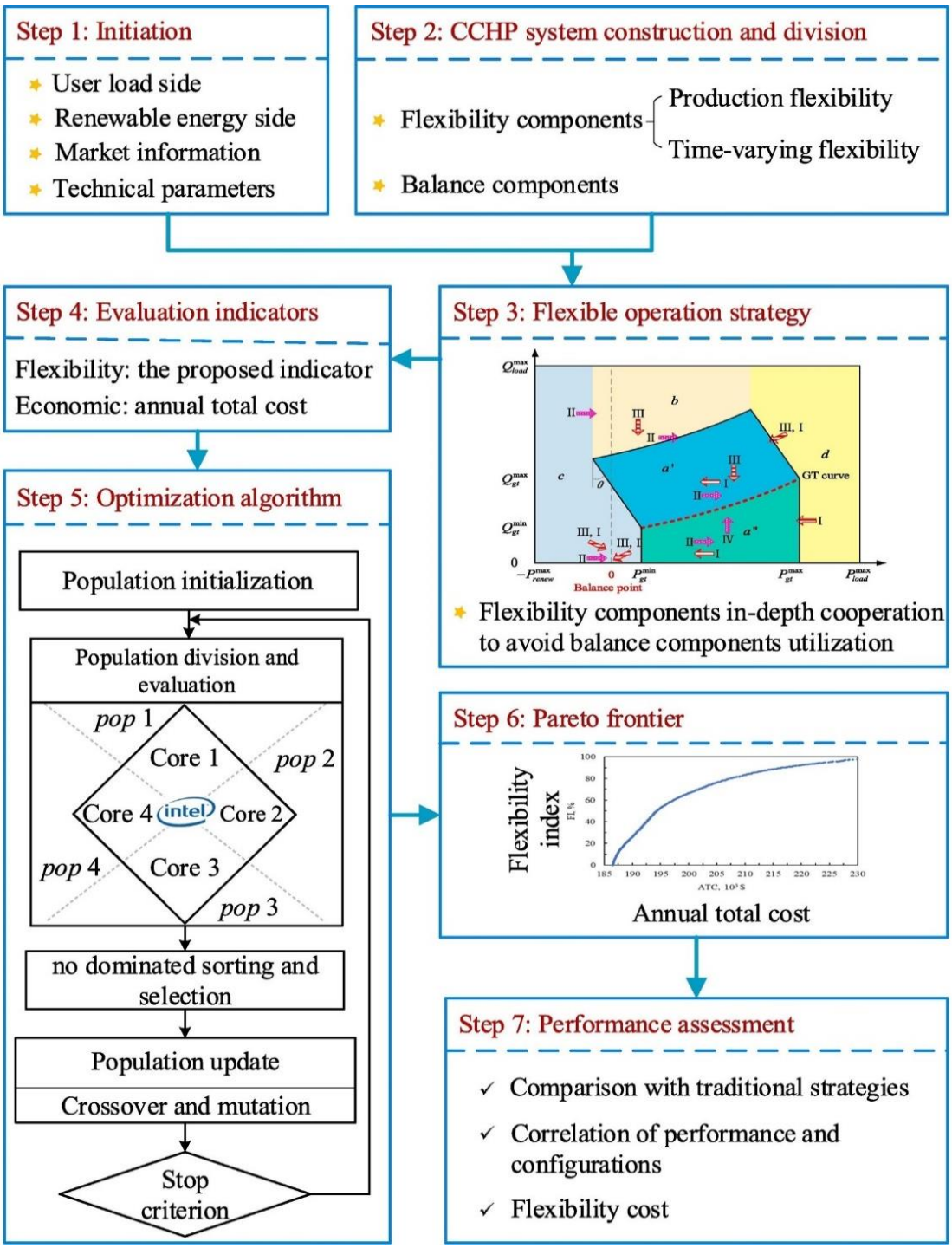

Fig. 2.10 A strategy to evaluate and optimize the flexibility potential of a hybrid combined cooling, heating, and power system (Zhou et al. 2021).

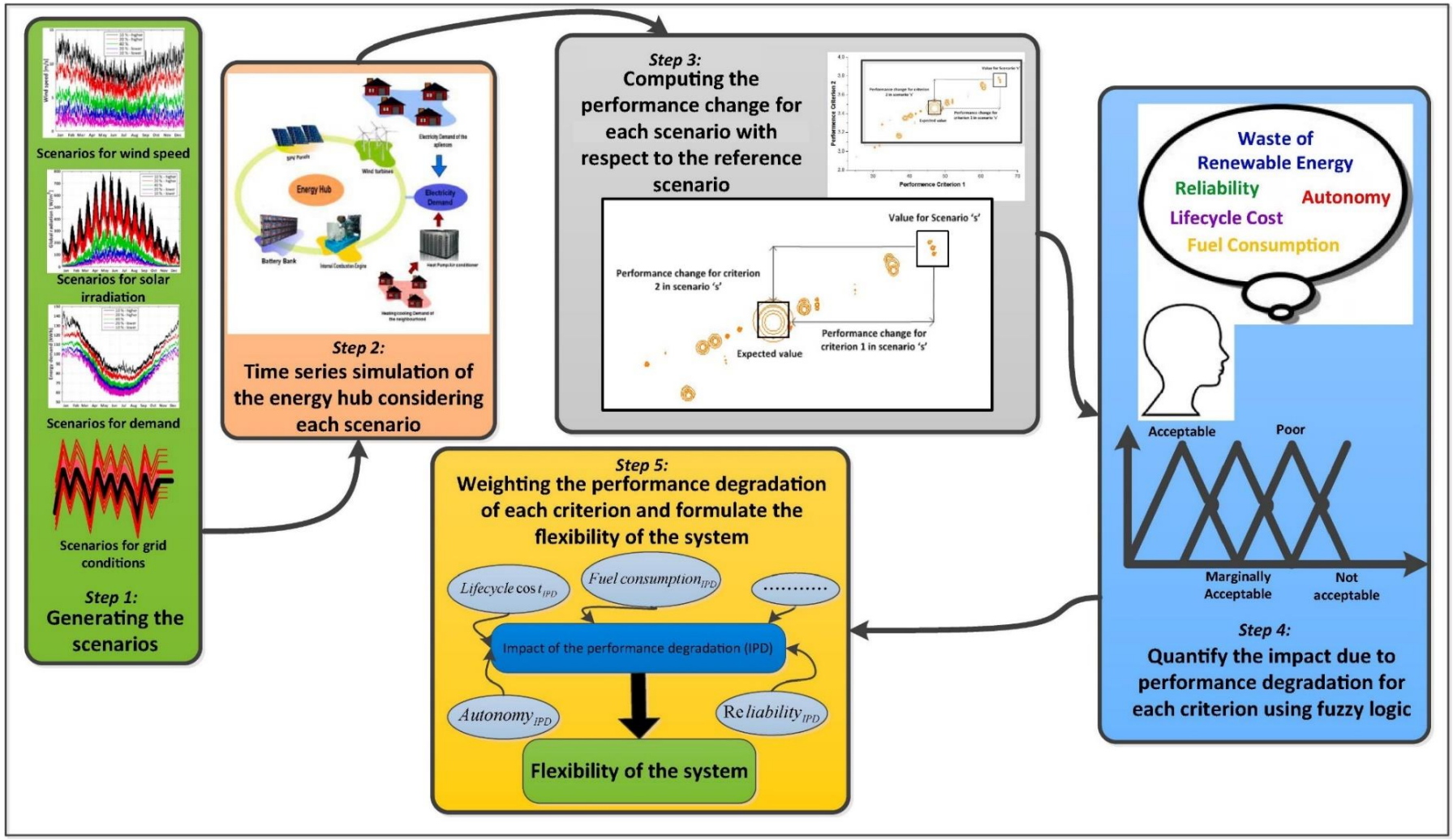

Fig. 2.11 A method to evaluate system flexibility for distributed energy system design (Perera et al. 2019).

Bampoulas et al. (2021) presented a framework to characterize and quantify the energy flexibility of residential buildings considering possible interactions between different energy systems. Storage capacity, storage efficiency, and self-consumption were used as the EFIs to generate daily energy flexibility maps, which can be used to quantitatively compare and evaluate the energy flexibility potential of different energy flexible options. De Coninck & Helsen (2016) used a bottom-up approach to quantifying building energy flexibility, in which the range of flexibility was graphically represented in a cost curve. This method can quantify both the amount of energy that can be shifted and the cost associated with the energy shifting. Homaei & Hamdy (2021) introduced an energy flexibility quantification method by taking into account the trade-off between survivability and energy flexibility under the time-of-use tariffs. Different building flexibility indexes, including the cost-effective flexibility index, survivability, savings index, and passive survivability index, were used to formulate the quantification method.

Although a range of methods have been introduced for building energy flexibility quantification, the majority of these methods were developed for a particular application, and different EFIs were used to meet the demand for that particular application. There is no one-size-fits-all method that can be employed for different types of buildings and various energy-flexible sources based on the priorities of different stakeholders. Therefore, a generic quantification method is needed but the development of such a method in principle is quite challenging due to the unique characteristics of each building and its energy-flexible systems, and flexibility types required, as well as various constraints imposed for different applications.

Conclusively, the evaluation of building energy flexibility is essential to identifying opportunities for increased energy flexibility. It can be attained using EFIs, which are capable of quantifying the achieved level of energy flexibility of participating systems by considering their characteristics and external variables such as environmental conditions, penalty signals, occupant comfort, and grid needs. EFIs can also aid in developing a contractual framework among different stakeholders, such as end-users and service providers (Kathirgamanathan et al. 2020). An effective EFI matrix should be able to identify the flexibility mix and factors that affect the flexibility level of a building, and what footprint flexible operation leaves on the pre and post-flexibility

operation of the building. It should also highlight the role of an individual system in enhancing the overall building energy flexibility and provide information regarding the temporal performance of the system, i.e. how long a system takes to react to the flexibility need; how long it works without disrupting occupant comfort; how frequently it can respond to sudden changes; and how long-lasting impact it leaves on the pre and post-flexibility operation of the building. Such a detailed flexibility evaluation framework can lead to achieving optimized flexibility in buildings.

2.5 Prediction of building energy consumption and energy flexibility

Prediction of the energy flexibility offered by buildings or building energy systems can help the building owners and operators better understand their buildings' potential to provide grid services. It can be used to optimize the use of building energy systems and earn revenue by participating in grid service markets. It can also save money for the building owners and support the stability of the grid by providing prior information about the demand patterns. Based on this information, grid operators can robustly manage the flow of electricity and avoid power outages or other disruptions that can ensure the grid's reliability to meet the dynamic energy needs of customers, even under abrupt weather changes.

2.5.1 Prediction models

An accurate prediction of building energy consumption can reduce the operational costs of building energy sources through better control and improved energy management (Lei et al. 2021). Prediction of energy consumption of buildings and building energy systems can be achieved using white-box, black-box and grey-box models (Yu et al. 2022).

2.5.1.1 White-box models

White-box model-based approaches are based on physics-based models and primarily depend on heat transfer principles. These approaches do not require historical data on buildings or building energy systems. Instead, they need detailed information about building and building energy systems parameters, including the external and internal factors affecting the performance of these systems. External factors are mainly environmental conditions, occupant behavior, and disturbances, whereas internal factors are system geometry, materials, compositions, capacity, and other thermo-

physical characteristics. Conventionally, these approaches have been widely used for performance assessment and forecasting of energy profiles because of interpretability, accuracy, diversity, and no need for historical data. Some limitations also exist, such as the need for detailed information about the system and unavoidable small prediction errors because of occupant activities. A major advantage of these models is the flexibility to test a system under different scenarios (Yu et al. 2022).

2.5.1.2 Black-box models

Black-box models are mainly data-driven models that use statistical techniques to establish a connection between independent and target variables based on historical data (Zhang et al. 2022). Prediction using data-driven models is mainly accomplished using classification and regression technologies. Regression establishes a set of continuous attributes by linking them with associated variables in the dataset and offers descriptive and predictive features. Some of the leading algorithms for regression are artificial neural networks, and support vector, linear, polynomial, and stepwise regressions. In regression models, continuous variables are predicted, whereas classification is mainly used to predict discrete class labels. Some of the classification models are CIT, K-Nearest Neighbors, random forest, support vector machine, and logistic regression. Many data analytics models can be used for both regression and classification (Li 2020).

Because of the introduction of building management systems, a large dataset of buildings and building energy systems are readily available, which increases the effectiveness of this strategy for the effective predictability of target variables. However, the over-reliance of these models on data is also a limitation of these models. Furthermore, these methods do not explain the physical principles of the systems, and hence require strong domain knowledge for drawing effective conclusions about complex systems.

2.5.1.3 Grey-box models

Grey-box models are designed to address the shortcomings of white and black-box models. These models tend to exploit the increased predictive capabilities of data-based models while offering physical insights into the behavior of the system (Pitchforth et al. 2021). These models can be developed by integrating data-driven

models into the white-box models. Table 2.6 provides a summary of the comparison among these approaches.

Table 2.6 Comparison among different energy prediction approaches.

Technique	Advantages	Limitations
White box	➢ High interpretability, allowing a clear understanding of decisions. ➢ Easy to validate and debug due to its explicit nature. ➢ Useful for decision-making in critical applications.	➢ May have limitations in handling complex relationships. ➢ Requires expert domain knowledge for model design.
Black Box	➢ High predictive power due to complex modeling capabilities. ➢ Ability to capture intricate patterns and non-linear relationships. ➢ Ability to handle large data sets.	➢ Limited insights into the underlying physical processes. ➢ May ignore system limitations and constraints while suggesting optimum solutions.
Grey Box	➢ Offers a balance between transparency and predictive power. ➢ Better interpretability than black box models. ➢ Can incorporate domain knowledge for improved performance.	➢ May not capture all complexities of the system. ➢ Demands strong domain knowledge.

2.5.2 Prediction of energy flexibility

Although the methods mentioned above have been widely used for performance assessment and energy forecasting of buildings and building energy systems, the prediction of energy flexibility has not been performed in most of the studies. Accurately predicting the energy flexibility potential can offer enhanced demand management opportunities while unlocking opportunities for optimization of the supply side (Zhang et al. 2021).

Vesa et al. (2020) performed a study to predict the energy flexibility of data centers for participating in demand response programs. The authors acclaimed this study as one of the initial studies, which was focused on predicting energy flexibility along with energy consumption of the data center instead of just predicting the energy

consumption patterns. A genetic heuristic prediction model was used to determine the optimal ensemble of a set of neural network prediction models to minimize the uncertainty for demand response participation and prediction error. The model showed a mean absolute percentage error of around 6% and proved safe participation of the data centers in the demand response program. Zhang et al. (2021) performed a study to predict the energy flexibility of a building using a decision tree model, and highlighted the importance of forecasting the energy flexibility potential of a building that can offer dynamic, subjective, and uncertain characteristics for demand response events. It was stated that such prediction can guide aggregators for better bidding in energy markets. The proposed method proved to be effective in demand forecasting. Hu et al. (2021) predicted the energy flexibility offered by aggregated electric vehicles and domestic hot water systems in smart grids using the temporal convolution network-combined transformer technique. The results proved that this method was effective in unlocking the demand-side flexibility to provide a reserve to grids. Firoozi et al. (2021) used recurrent neural networks and long short-term memory models to forecast energy flexibility at a local energy community level. The results proved the effectiveness of the proposed method in predicting energy flexibility and energy consumption at the community level.

Available literature showed that existing research was mainly focused on energy consumption forecasting/prediction, and very few studies have focused on energy flexibility prediction. Among the existing studies, data-driven or black-box models were frequently used for prediction purposes. Meanwhile, the literature highlighted a lack of models for forecasting energy flexibility offered by buildings and building energy systems, especially HVAC systems.

2.6 Summary

A literature review related to the role of data analytic techniques for performance assessment of building HVAC systems, building energy flexibility fundamentals and the role of TES systems and near-optimal selection of PCMs in enhancing the energy flexibility of the buildings and building HVAC systems were provided. EFIs and quantification methods, along with the prediction models to predict the flexibility potential and energy consumption of the buildings and building energy systems were also summarized. The key findings from the literature review are summarized below:

1) Performance improvement in building HVAC systems can be achieved by tracking the operational improvement opportunities that can be achieved using advanced data analytics and visualization techniques. A detailed analysis, including energy profiling, performance benchmarking, and establishing relations between system performance and operational parameters at different part load ratios, can help achieve improved HVAC performance. However, a comprehensive performance evaluation method and indicator are desirable to effectively trace the performance improvement and degradation at different operational stages of HVAC systems.

2) Building energy flexibility or demand flexibility is a key component in supporting the transition towards sustainable energy resources from fossil fuel-based power generation. This can help reduce building energy costs, power usage, and emissions without much infrastructural upgradation and investments. Among different energy flexible sources, PV, TES, and HVAC systems have shown high potential to be used as a leading source of energy flexibility in buildings. However, rational strategies to implement and optimize the flexibility potential of buildings and building energy systems are still desirable.

3) Near-optimal selection of PCMs is important to enhance the performance and energy flexibility of buildings and building energy systems with integrated thermal energy storage. PCMs have several qualitative and quantitative characteristics, and the selection of a near-optimal PCM is a multi-criteria decision analysis problem. Hence, an MCDA-based ranking model that can be used to select near-optimal PCMs for desired applications considering both the qualitative and quantitative characteristics of PCMs can enhance the performance of TES systems without any technical improvement in the design of these systems. Such systems can also effectively enhance the flexibility potential of buildings and building energy systems.

4) Different stakeholders are involved in the successful implementation of a flexibility plan. Hence, it is important to quantify the flexibility offered by

buildings and building energy systems based on the interactions between these stakeholders. However, the available literature lacks such quantification methods and indicators. A framework that can be used to develop and aggregate flexibility indicators can provide opportunities to overcome this challenge and identify opportunities to improve the flexibility potential of buildings and building energy systems.

5) It is also vital to predict the flexibility potential of buildings and building energy systems to support grid optimization. The existing studies were mainly focused on predicting the energy consumption of buildings and building energy sources. A rational model that can predict the flexibility potential of buildings and building energy systems can help service providers for optimum bidding in energy markets and stabilize the operation of power generation and distribution systems.

Chapter 3 A data-driven performance assessment strategy for centralized chiller systems using data mining techniques and domain knowledge

The literature review in Chapter 2 demonstrated that the heating, ventilation, and air-conditioning (HVAC) systems are one of the main sources of energy consumption in buildings. An accurate performance evaluation of these systems, particularly chillers, is critical for improving their efficiency and economic performance. Current practices for evaluating the performance of HVAC or chiller systems primarily rely on performance assessment indicators such as Coefficient of performance (COP), which do not offer detailed information about performance degradation under dynamic operating conditions. It was also discussed that data mining techniques can provide detailed insights into performance improvement opportunities of building energy systems, which can offer economic benefits to building owners. Moreover, data visualization strategies can provide in-depth details about the energy usage patterns of these systems and further support energy-flexible decision-making. This chapter introduces a rational data-driven performance assessment strategy for centralized chiller systems using data mining techniques and domain knowledge. The effects of the selected operating variables on the system performance are analyzed through quantitative and qualitative analysis. The links among these variables are also established using different data analytic techniques. In addition, energy usage patterns are also recognized using advanced visualization techniques.

3.1 Methodology

3.1.1 Outline of the proposed strategy

The outline of the proposed strategy is shown in Fig. 3.1. This strategy consists of four steps, which are data collection, data cleaning, energy profiling of the chiller system, and data analysis. All steps in the proposed strategy are performed by incorporating the domain knowledge to provide better insights into the data analyses. The performance of chiller systems is often affected by the operating parameters such as inlet and outlet temperatures of the chilled water across the chiller evaporator, inlet and outlet temperatures of the cooling water across the chiller condenser, mass flow rates of the chilled water and cooling water, and the power consumption of chillers,

air handling units, water pumps, and cooling towers. A substantial amount of the operational data of the chiller system was first collected, which is generally available from the building management systems (BMS). Density-based spatial clustering of applications with noise (DBSCAN) algorithm was then applied to the collected data to detect and remove the outliers from the raw data, which is further explained in Section 3.1.2. In the third step, the energy profiling of the chiller system was carried out to identify the distinctive patterns in the operation of the chiller system. In this chapter, the energy consumption patterns of the chiller system were first visualized in a calendar view heat map for preliminary analysis. The Conditional inference tree (CIT) model was then used for chiller power ratio (CPR) classification based on temporal variations. The last step is data analysis which involves qualitative and quantitative analysis. The processed data were first quantitatively analyzed in this step using the Agglomerative hierarchical clustering (AHC) and CIT models. Quantitative analysis established the relationships between the selected chiller operating variables and chiller performance in terms of COP and COP Destruction (COPD), respectively. Secondly, the Association rule mining (ARM) model was applied to qualitatively analyze the relationships among the chiller performance indicators and selected operating variables. Association rules were established to demonstrate the collective effect of the variables on the system performance. It is worthwhile to note that the method developed in this chapter can be used for the performance assessment of any chiller system with little changes but different domain knowledge may be required depending on the complexity of the chiller system and the potential operating issues involved.

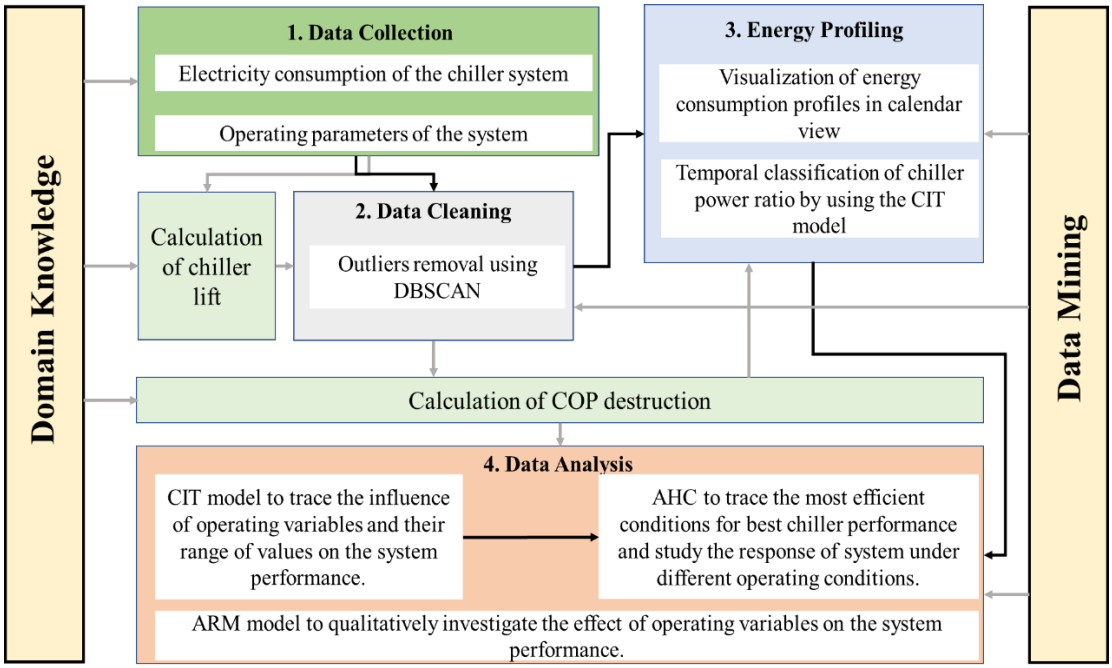

Fig. 3.1 Outline of the strategy.

In the study, the COP of the system is considered as the ratio of the heat removed from the chilled water across the chiller evaporator and total electricity input of the chiller compressors, and chilled water and cooling water pumps that are dedicated to the chillers. The COP can be calculated using Eq. (3.1).

$$COP = \frac{\dot{m}_e \times c_P \times \left(T_{in,e} - T_{o,e}\right)}{E_c + E_p} \tag{3.1}$$

where $\dot{m}$ stands for mass flow rate, T and E stand for temperature and input power respectively, the subscripts e, c, p, in and o stand for evaporator water loop, compressor, pump, inlet, and outlet, respectively, and c_P represents specific heat of the water.

To enhance the accuracy of the chiller performance evaluation, COPD, as expressed in Eq. (3.2) was introduced as a new performance indicator. It represents the quality of COP and determines how far the system performs from the respective ideal performance i.e. Carnot COP. For instance, 50% COP Destruction shows that, ideally, the system has the capacity to improve its performance by 50%. This indicator, in combination with COP can provide better details to identify the effectiveness of a system as compared to the use of COP alone. Higher values of COPD indicate an

inefficient operation. Sometimes negative values of COPD and values close to 100% may be resulted because of the sudden changes in the operating conditions, and these values in principle should be discarded.

$$COPD = \frac{[(\frac{T_{o,e}}{T_{in,c}-T_{o,e}})-COP)]}{(\frac{T_{o,e}}{T_{in,c}-T_{o,e}})} \times 100\% \quad (3.2)$$

3.1.2 Data cleaning using DBSCAN

Data cleaning, as a substantial part of the data processing, can exclude the outliers from the collected data before further analysis in order to enhance overall performance assessment. In this chapter, the outliers were defined as the observations in which the CPR and chiller lift (i.e. the temperature difference between the cooling water leaving the condenser and chilled water leaving the evaporator) were considerably different from most of the other observations. The DBSCAN algorithm was used in this chapter for outlier detection. As a density-based algorithm, DBSCAN can identify the data points with a low density of neighbors as outliers (Ester et al. 1996). Compared to other commonly used statistics-based outlier detection methods (e.g. generalized extreme studentized deviate test and interquartile range test), DBSCAN performs better if the data do not obey the specific probability distributions. To conduct the outlier detection using DBSCAN, the density of each data point in the dataset was first estimated by counting the number of neighbors around the estimated data points in a specified radius (ε). The data points were then classified into three types based on the specified radius (ε) and the threshold of the density (k). The three types of data points include core points, border points, and noise points. A core point is a data point whose density exceeds the threshold (i.e. k). A border point is a data point whose density is lower than k while the distance between it and a core point is smaller than ε. A noise point is a data point that is neither a core point nor a border point and is identified as an outlier.

In this chapter, CPR and chiller lift data were first rescaled to 0 mean and 1 deviation. All the data points were then plotted on a two-dimensional scatter plot. Each point in the scatter plot of DBSCAN stands for an observation at a specific time interval. The value of ε was chosen using a k-distance graph (Ester et al. 1996). After the estimation

of the density for each data point, the noise points were identified and removed from the dataset for further analysis.

3.1.3 Conditional inference tree

The CIT is a well-known classification technique, which generates a tree-like model comprising a set of if-then rules. Compared to the widely known decision tree generation algorithms such as Classification and Regression Tree (CART), the major benefit of CIT is that the bias in the classification results can be avoided due to significant tests in the variable selection process. Additionally, the CIT algorithm has the advantage of controlling the tree size, which avoids cross-validation and tree pruning (Hothorn et al. 2006). The first step in the development of a decision tree using the CIT model is to test the global null hypothesis of independence between the explanatory variables and response variables. If explanatory variables have no significant influence on the response variables, the process will be terminated, i.e. null hypothesis will not be rejected. Otherwise, a partial null hypothesis will be used to test the independence between each response variable and the explanatory variables. Explanatory variables with the strongest association with the response variable are then added to the model. A binary split in the selected explanatory variable is then implemented in the next step. The goodness of a split is evaluated using Eq. (3.3) (Hothorn et al. 2006).

$$A_{opt} = \underset{A}{\operatorname{argmax}}\, c\left(x_j^A, \partial_j^A, \vartheta_j^A\right) \tag{3.3}$$

where x^A is a metric to measure the incongruity among the two split samples, ∂^A represents the conditional expectation and ϑ^A represents the covariance.

In this chapter, a decision tree was used to identify the chiller operating routine and to model the relationships between the system performance in terms of COP and COPD, and multiple operating parameters. CIT was employed for tree generation that was dependent on temporal variations and system variables. CIT helped identify the temporal variations-based operational behavior of the chiller system. Specific months, days of week, and hours were detected when the system operated above a specific CPR. Such assessment helps identify the building energy consumption patterns that further improve the system's performance. In the data analysis step, CIT also provided

a detailed insight into the performance variation of the chiller system based on the different operating conditions.

3.1.4 Agglomerative hierarchical clustering

Ward's method-based AHC algorithm was used to analyze the performance of the chiller based on the operating conditions. AHC is a bottom-up clustering strategy. In this chapter, a total of 6 variables were analyzed, including the water temperature differences across evaporator and condenser, CPR, chiller PLR, and chiller performance in terms of COP and COPD. All these 6 variables at a specific time were labeled as a single observation. Initially, each observation was treated as a separate cluster, the observations (clusters) close to each other were then identified and merged into larger clusters. The process continued until all clusters were merged into a single cluster. The merging process is represented using a dendrogram (i.e. a tree-like structure). The dendrogram can then assist in determining the optimal number of clusters that can be achieved by cutting the dendrogram at a specific height. The dissimilarity measure is an important component in a hierarchical clustering algorithm. In this chapter, Euclidean distance (ED) was used as the dissimilarity measure as it has the advantage of measuring the dissimilarity based on magnitude.

3.1.5 Association rule mining

ARM discovers the relationships in large datasets (Zhu et al. 2012). It has been effectively used in the fields of bioinformatics (Leung et al. 2010), medical diagnosis (Almansory 2018), and marketing (Kaur & Kang 2016), and has also been proven to be effective in analyzing building operational data (Fan et al. 2015). The representative setup of an association rule is like A→B, where A and B represent separate sets of items or events. For example, the rule {high PLR of the HVAC system}→{efficient performance of the HVAC system} advocates that a relationship exists between the variation in the PLR and the performance of the system. Two indicators, i.e. support and confidence, are used to measure the strength of an association rule. Support represents how frequently a rule is applicable within the constraints of a dataset, whereas confidence determines how frequently "A" will appear if "B" appears. The Apriori method was used in this chapter to discover the association rules. The Apriori algorithm consists of two steps, including frequent item

set generation and rule generation. In the frequent item set generation step, all the item sets that satisfy the threshold of support are identified. In the rule generation step, all the high-confidence rules are extracted from the frequent item sets identified in the previous step. In this chapter, the thresholds of support and confidence were set as 0.2 and 0.8, respectively, so that the identified high-frequency association rules are within a controllable number for further analysis and interpretation using domain knowledge.

3.2 Performance test and evaluation of the developed strategy

3.2.1 Description of the case study chiller system

In this chapter, a centralized chiller system (Fig. 3.2) installed in a multi-functional university building cluster was used to test and evaluate the performance of the developed strategy. The building cluster consists of three independent buildings (A, B and C) with three floors each (Fig. 3.2a). The total floor areas of buildings A, B and C are 1,420 m^2, 2,265 m^2 and 2,190 m^2, respectively. AHU-A1-P, AHU-B1-P and AHU-C1-P are used to serve the perimeter zones. AHU-A1-C, AHU-B1-C and AHU-C1-C are used to serve the central zones in the ground level and Level 1 of building A, Levels 1 & 2 of building B and Level 1 of building C, respectively (Fig. 3.2b). AHU-C2-E and AHU-C2-W are used to condition the east and west zones of level 2 of building C, respectively. The fitness centre in building B, kitchen in building C and the reception are conditioned by the fan coil units FCU-F, FCU-K and FCU-R, respectively. FCU A2-1 and FCU A2-2 are used to condition Level 2 of building A, and FCU BG-1 and FCU BG-2 serve the ground floor of building B. The ground floor of building C is conditioned by the packaged units. The building occupancy pattern is nearly identical for most of the year, as the building concerned mainly consists of offices, a cafeteria, and a gym that are operational almost all the year. Two identical scroll chillers with a cooling capacity of 220 kW each were used. When the cooling load was less than 220 kW, one chiller was in operation. Otherwise, two chillers were in operation. R407c is used as the refrigerant. The system is equipped with two chilled water pumps with a rated power of 2.7 kW each and two cooling water pumps with a rated power of 3.8 kW each. The supply air is conditioned through several air handling units (AHUs) and fan coil units (FCUs) (Fig. 3.2b). Two cooling towers with a heat removal capacity of 357 kW and input power of 2.2 kW were also part of the system. Variable speed drive (VSD) pumps and fans are employed in the system to enhance

energy performance. Chilled water and cooling water pumps were operated based on the operation of their dedicated chillers. Both cooling towers were put in operation if either or both of the chillers were operating.

The operation data of the chiller system was collected from the BMS, and the main data were recorded every 30 minutes.

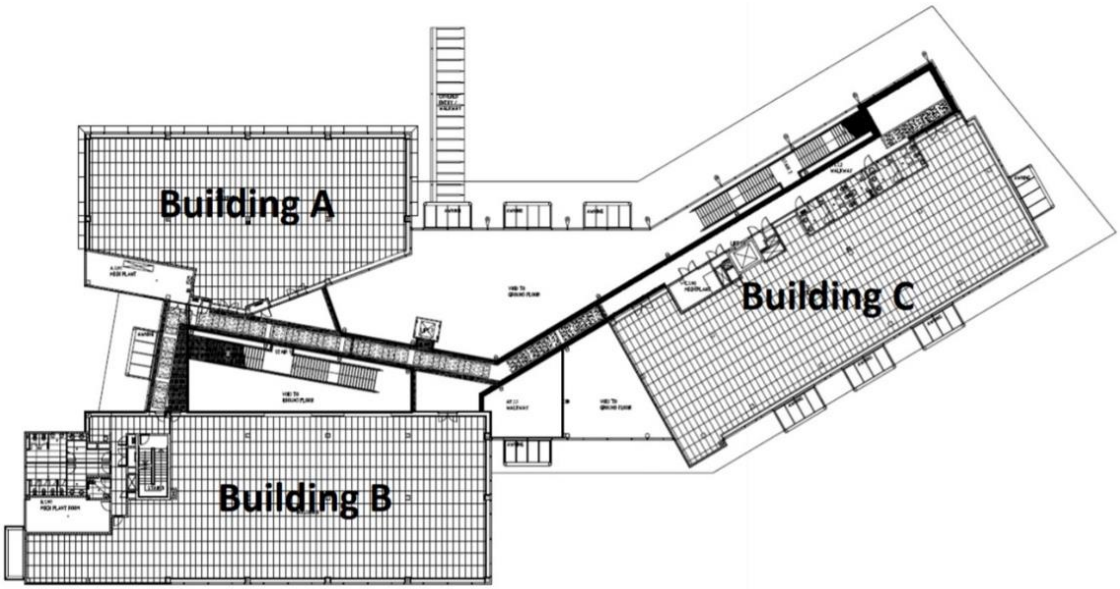

a) Building layout

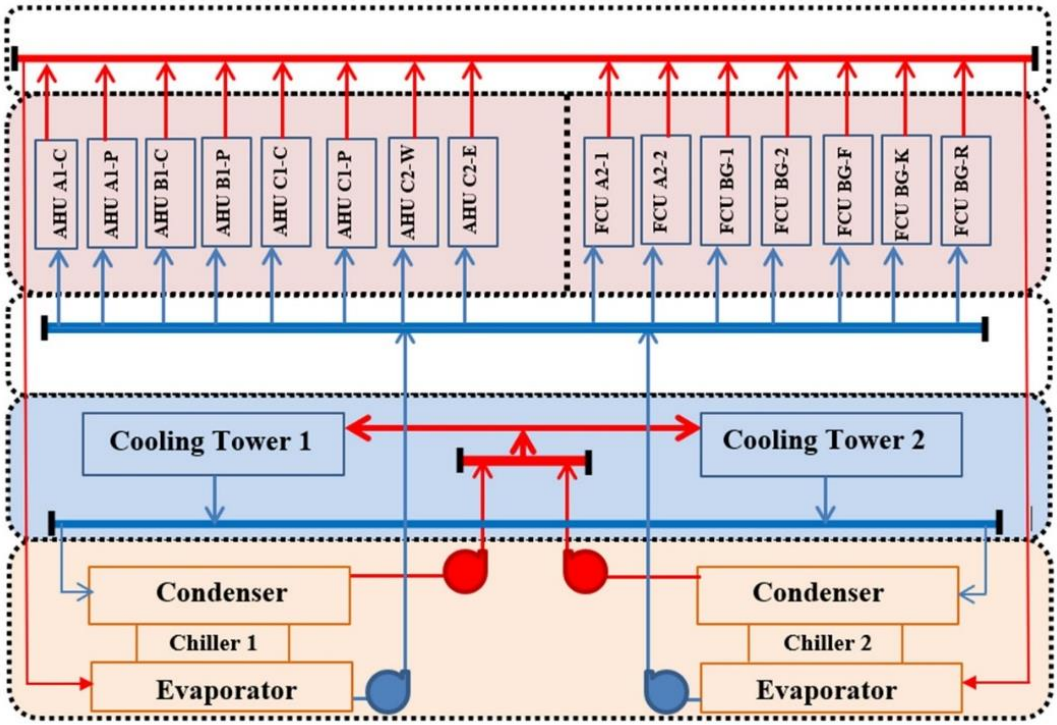

b) Line diagram of the chiller system

Fig. 3.2 Illustration of the centralized chiller system.

The operating variables of the chiller system, including the inlet and outlet temperatures of the chilled water across the chiller evaporator, inlet and outlet temperatures of the cooling water across the chiller condenser, mass flow rates of the chilled water and cooling water, power consumption of chillers, air handling units, water pumps, and cooling towers were collected from the BMS. The data were collected from November 2017 to October 2018 with ½ hour intervals, and a total of 17,520 observations were used in this chapter. Fig. 3.3a shows an example of the retrieved data in a week from 4th to 10th December 2017. It can be observed that the highest power usage of the system generally occurred from 9:00 to 16:00 during weekdays. The power consumption of the AHUs remained similar irrespective of the chiller operation. The power consumption of the water pumps was around 4.0 kW when one chiller was operating, while it was increased to 8.0 kW when both chillers were operating. Although the pumps are equipped with variable speed drives, they were mostly operated at a constant speed. The COP of the chiller system was then calculated using Eq. (3.1) and is illustrated in Fig. 3.3b.

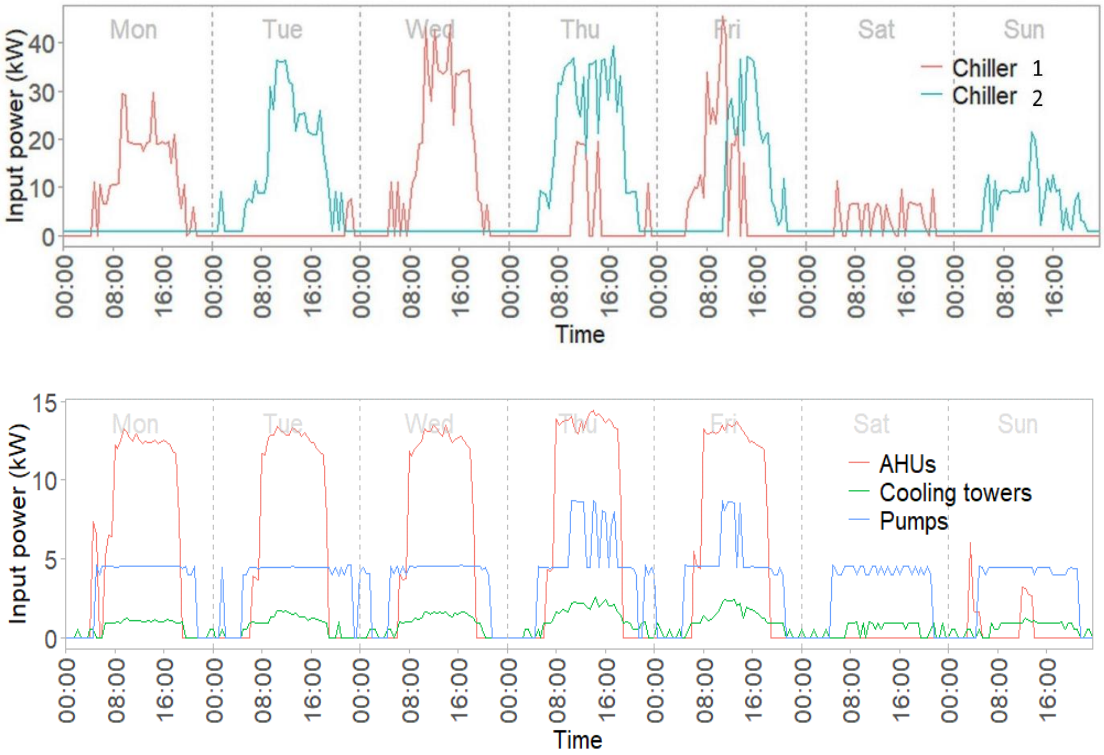

a) Power consumption of different components

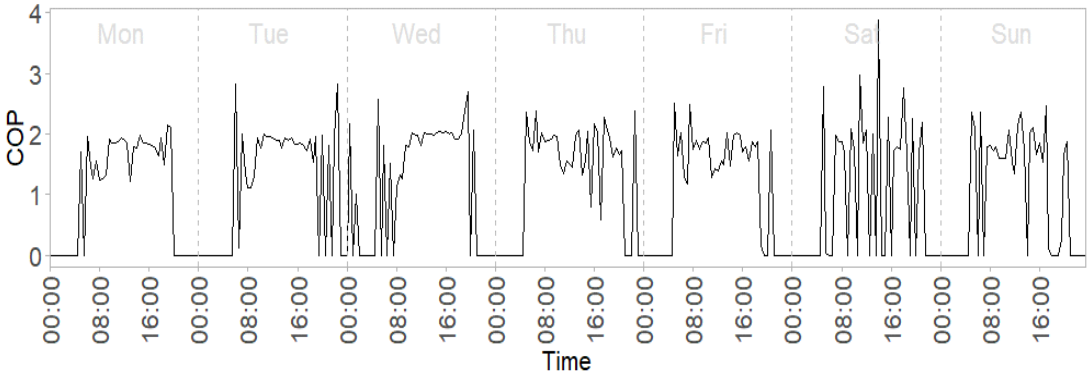

b) COP of the system

Fig. 3.3 Illustration of the retrieved and calculated variables in a week.

3.2.2 Data pre-processing

DBSCAN was first used for data cleaning. As introduced in Section 3.1.2, the parameter ε in the DBSCAN was determined using a *k*-distance graph (Fig. 3.4a). A *k*-distance graph showed the dissimilarity from each data point to its k^{th} nearest neighbor in increasing order, and a sharp variation in the value of the dissimilarity corresponded to a suitable value of ε (i.e. 0.075 in this chapter). The outliers identified via the DBSCAN are illustrated in Fig. 3.4b with the blue dots. The observations that corresponded to these outliers were removed. After the data cleaning, 17,314 observations were retained.

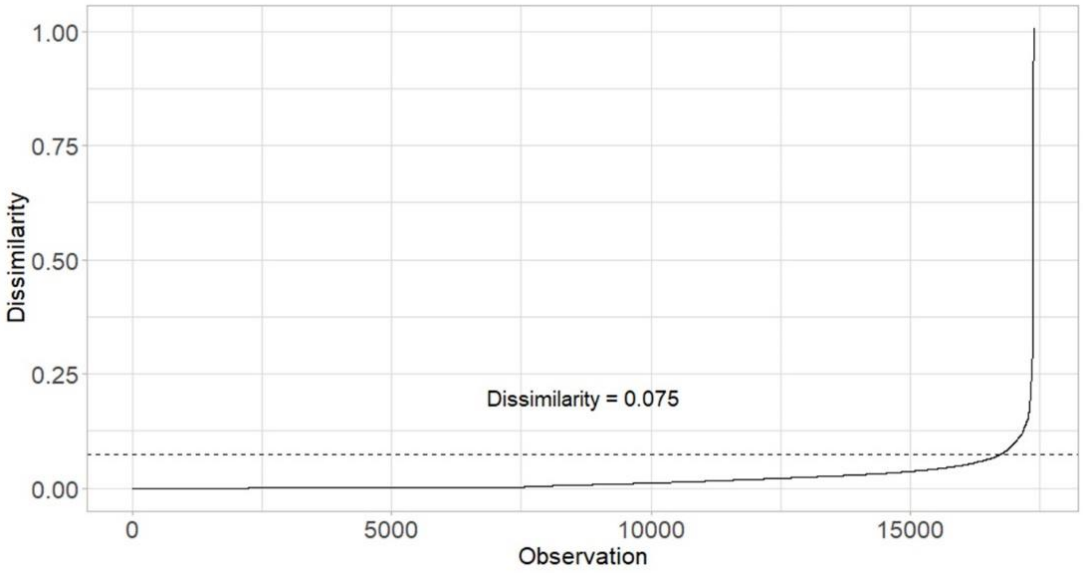

a) *k*-distance diagram

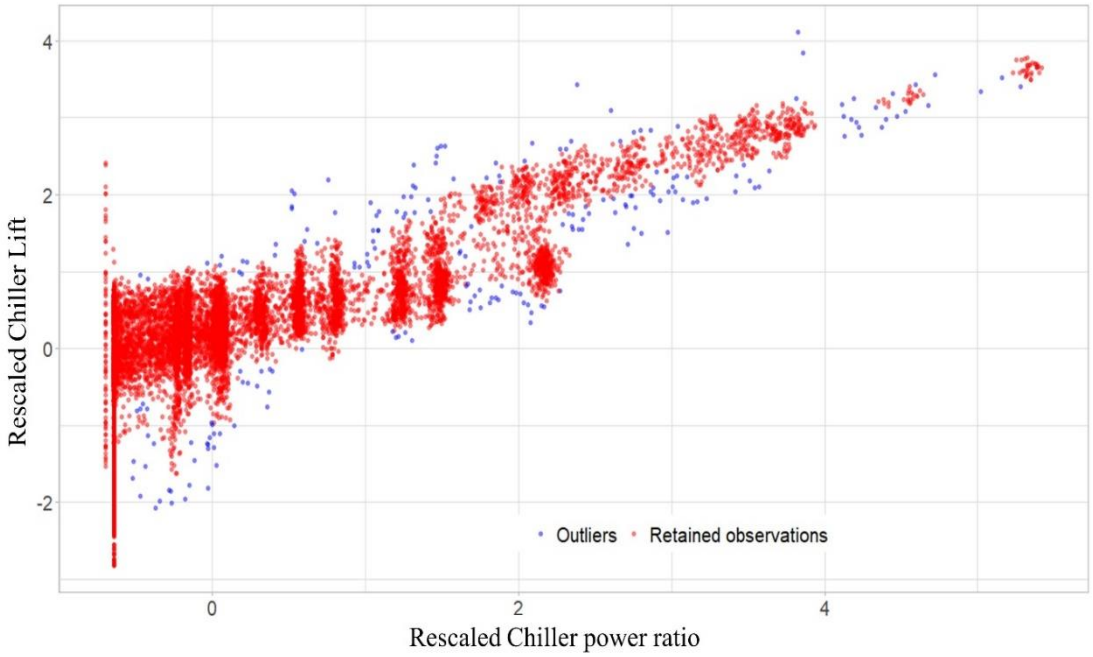

b) Result of the outlier detection

Fig. 3.4 Outlier detection using DBSCAN.

3.2.3 Energy profiling of the chiller system

Fig. 3.5 shows the daily mean energy consumption of each component in the chiller system for 12 consecutive months. All these components are variable speed drives. The dark grey blocks in Fig. 3.5 indicated the days with no data recorded or the data with outliers that have been removed from the raw data, whereas the blue shaded blocks showed that each component in the chiller system was operated below 50% of its rated power and the dark yellow shaded blocks showed each component in the chiller system operated above its 50% rated power. In the city where the case study system is located, the cooling demand generally starts rising in October and remains high till April next year. Therefore, the chillers were frequently used during these months for space cooling. Fig. 3.5a and Fig. 3.5b indicate the power usage patterns of the two chillers for 12 consecutive months, from November to October of the next year. A comparison between both figures indicated that the chillers were rarely operated at their full rated power. Moreover, the cooling demand below 220 kW was met by operating one chiller only. For instance, only chiller 1 was operating at nearly 75% of its rated power on 30th October (Fig. 3.5a and Fig. 3.5b). It can be observed from Fig. 3.5d that the cooling tower operation was directly linked with the chiller

operation and the power consumption patterns of the condenser water pumps and chilled water pumps were nearly identical throughout the year. As shown in Fig. 3.5c, AHUs were generally in operation on working days throughout the year. It is noted that the power consumption of AHU-C2-E and AHU-C2-W was not included in Fig. 3.5, because these two AHUs are constant volume and their separate power consumption data were not available. In the cold season, building heating was achieved using a boiler system. As Wollongong, Australia, has mild weather and sometimes cooling is still needed during winter months, the chillers were therefore also operated during the cold season when needed. In general, the energy required for the perimeter zones was considerably higher than that for the central zone of each building.

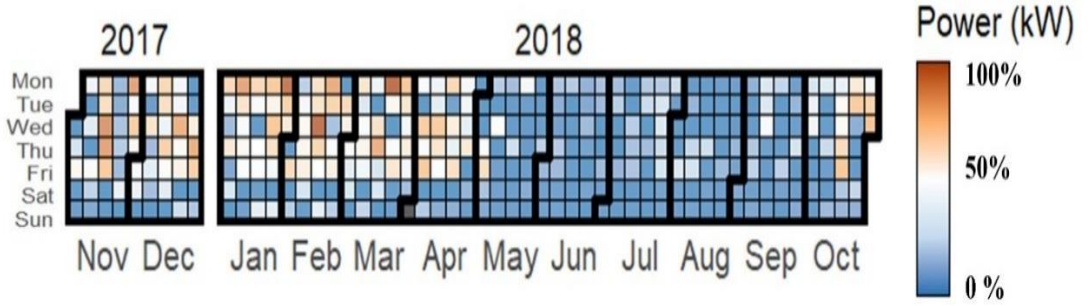

a) Chiller 1

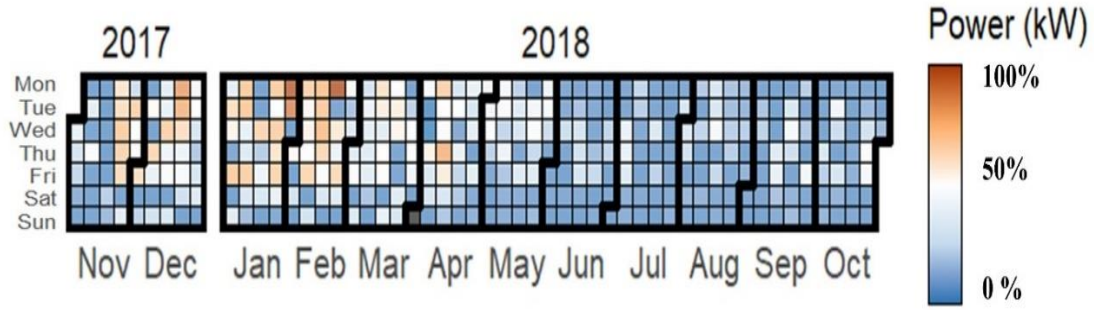

b) Chiller 2

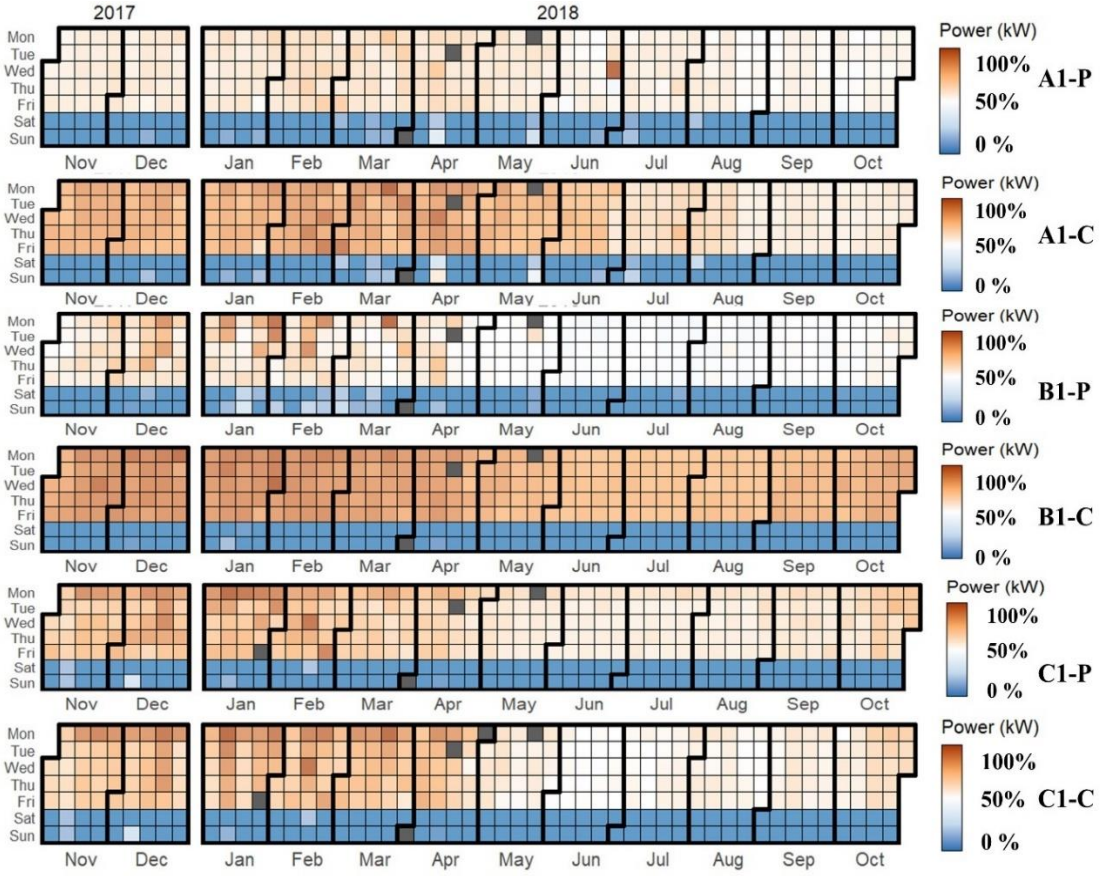
2017
2018
Mon
Tue
Wed
Thu
Fri
Sat
Sun
Nov
Dec
Jan
Feb
Mar
Apr
May
Jun
Jul
Aug
Sep
Oct
Power (kW)
100%
50%
0 %
A1-P
A1-C
B1-P
B1-C
C1-P
C1-C

c) AHUs

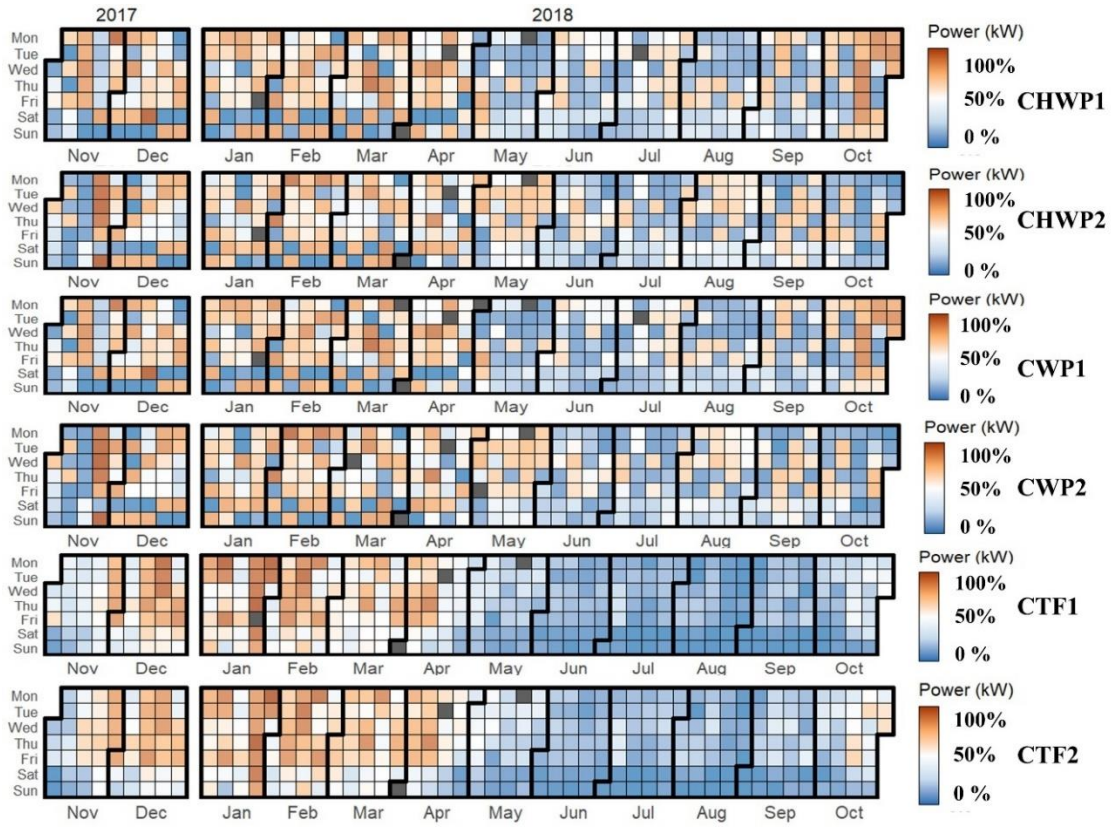

d) Water pumps and cooling tower fans

Fig. 3.5 Heat-map of daily power ratio of main components in the chiller system in a calendar view.

The energy profiles of the chiller system were further explored using the CIT model. The CIT models illustrated the variations in the CPR with respect to the months, days of week (DoW), and hours of the day. The input data used for the CIT model generation consisted of the response variables and explanatory variables. The response variable used was whether the CPR of the chiller exceeds its 25%. The explanatory variables included the month, DoW, and hours of the day. The generated CIT model is presented in Fig. 3.6, in which the green bars indicated the percentage of the data observations with the CPR equal to or higher than 25%, whereas the red bar showed the CPR below 25%. The chiller system was most frequently operated from 8:00 to 18:00 during weekdays of the last three and the first four months of the next year. The presence of the green bars in the winter months showed that the chillers were also occasionally operated in the winter months. Clear segregation of the operating conditions achieved from this model can be used to develop optimal control strategies for chiller systems as per temporal variations in the load demand.

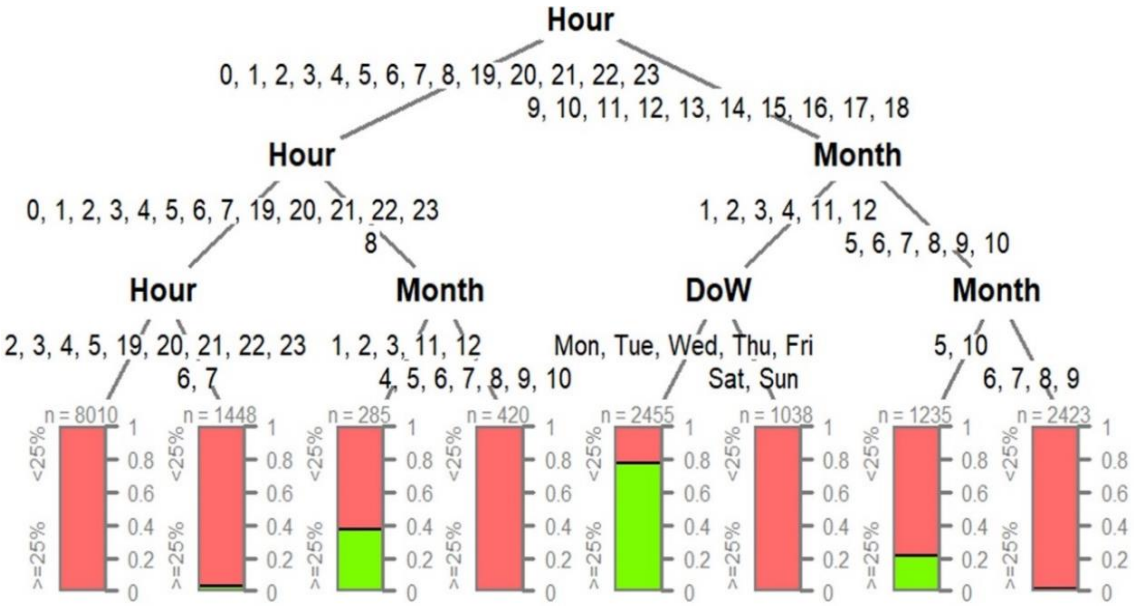

Fig. 3.6 Temporal classification of the CPR (Green bars indicated the percentage of the data observations with the CPR equal or higher than 25%, whereas the red bar shows the CPR below 25%).

3.3 Quantitative Analysis

To increase the reliability of the analysis, only the observations recorded during the office hours of the cooling months were further quantitatively analyzed using the AHC and CIT. As the system performance is affected concurrently by multiple parameters, both AHC and CIT were hence adopted to examine the effect of four variables (i.e. CPR, chiller PLR, and water temperature differences across the evaporator (TDE) and condenser (TDC)) on the two performance indicators of COP and COPD.

Fig. 3.7 and Fig. 3.8 illustrate the effect of the CPR, chiller PLR, and temperature differences across the evaporator and condenser on the system performance in terms of COP and COPD, respectively. COP and COPD datasets were divided into three categories with equal magnitude. Top, middle, and low 33.3% values were termed as high, medium, and low COP and COPD, respectively. The top 33.3% COP and bottom 33.3% COPD presented the best performance, i.e. the chiller can remove more heat at a relatively lower power input as compared to that under other conditions. Low COP and high COPD indicated poor or low chiller performance. The results from Fig. 3.7 showed that a high COP can result when the temperature difference across the

evaporator was above 5.1 ºC at low and medium CPR conditions. At some low CPR conditions, the evaporator temperature difference between 3.1 ºC and 5.1 ºC also resulted in a high COP. However, lower chiller performance was resulted when the water temperature difference across the evaporator was below 3.1 ºC at some low and medium CPR conditions, and that across the evaporator was below 4.1 ºC at some medium CPR conditions. At high CPR conditions, the temperature difference at the evaporator below 5.1 ºC generally resulted in low system performance, whereas the best performance was achieved when the temperature difference across the evaporator was above 6.4 ºC and that across the condenser was above 6.0 ºC. In contrast, the water temperature difference across the condenser below 6.0 ºC and that across the evaporator below 6.4 ºC generally resulted in low performance at high CPR conditions. Overall, the results from Fig. 3.7 indicated that the system COP was most strongly influenced by the temperature difference across the evaporator among the variables considered.

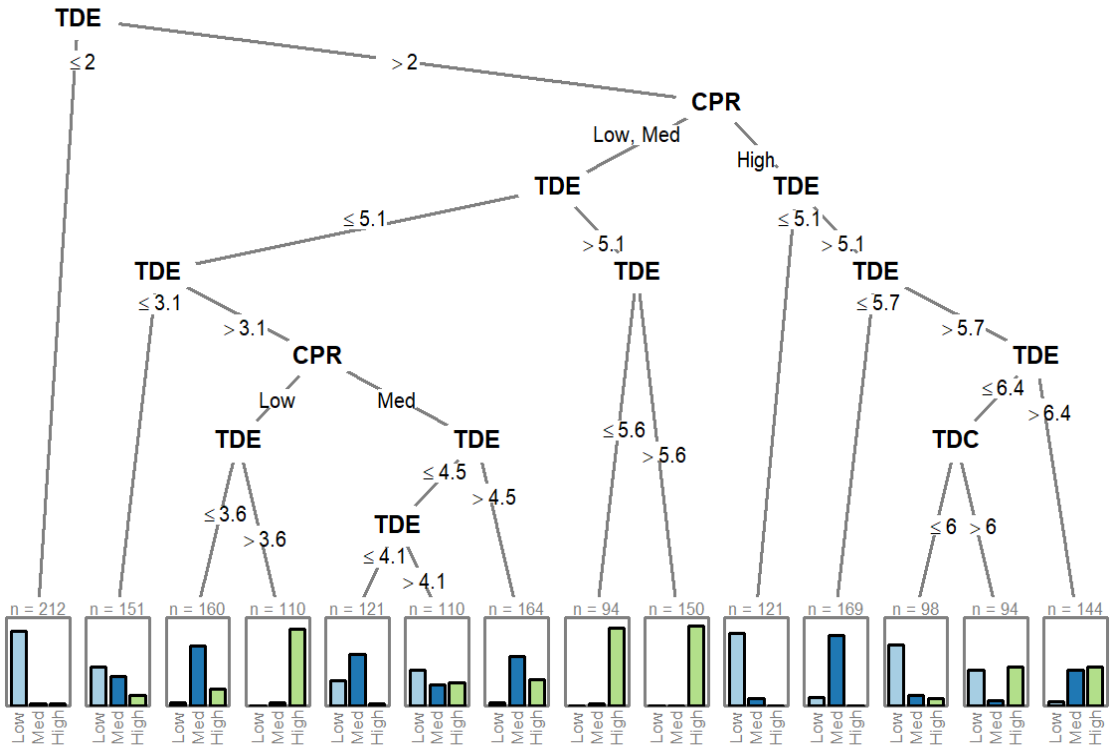

Fig. 3.7 Relationship between the system COP and the operating parameters.

The effect of the operating parameters on the COPD (Fig. 3.8) showed that the system performed worst when the temperature difference across the evaporator was below

3.1 ºC. At low CPR conditions, the combination of the water temperature difference across the evaporator above 3.6 ºC and that across the condenser below 4.4 ºC provided better performance. At high CPR conditions, the best performance was achieved when the temperature difference across the condenser was above 6.3 ºC and that across the evaporator was above 6.5 ºC. At low and medium CPR conditions, the system showed high performance when the temperature difference across the condenser was above 4.4 ºC and that across the evaporator was above 4.8 ºC. The above analysis showed that the temperature difference across the evaporator had the strongest relationship with COPD.

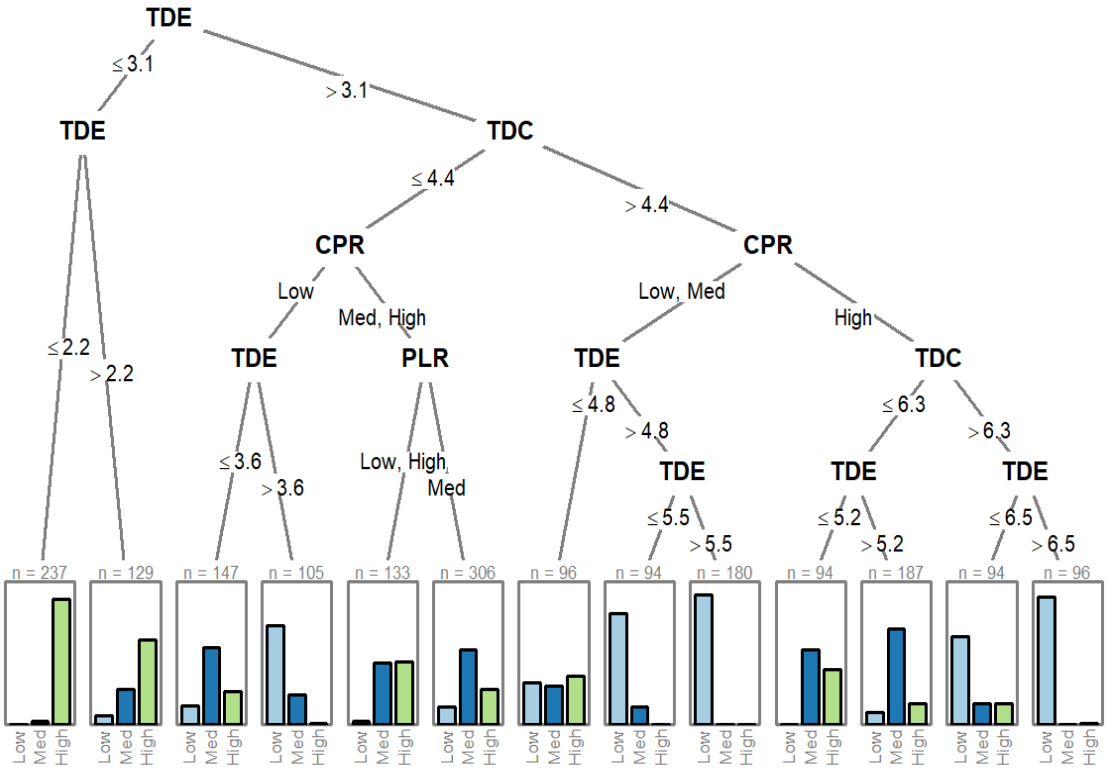

Fig. 3.8 Relationship between the system operating parameters and COP Destruction.

A comparison between Fig. 3.7 and Fig. 3.8 showed that to achieve a good performance, the system should be operated at high CPR conditions. However, high performance can also be achieved at some low and medium CPR conditions. For instance, the system showed better performance (i.e. high COP and low COPD) when the water temperature difference across the evaporator was above 3.6 ºC at some low CPR conditions and above 4.8 ºC at some medium CPR conditions. Similarly, for some high CPR conditions, the temperature difference across the evaporator above

6.4 ^{o}C resulted in better performance. High COP at low CPR conditions more frequently resulted in high COPD. Moreover, the water temperature difference across the evaporator below 3.1 ^{o}C generally resulted in low performance. The quantitative numbers from the CIT model can be used as the constraint conditions for performance optimization and assisting the development of optimal control schemes for this chiller system.

Although the CIT model is computationally fast to identify the optimum operating conditions, CIT can just establish links for the most strongly interlinked variables, and with the increase in the number of variables, weaker connections get ignored. For instance, CIT was unable to establish a link between the chiller PLR and system performance by considering the operational variables. Hence, for a further detailed evaluation of the interconnection between the chiller operating variables and performance variables, hierarchical clustering was used. Fig. 3.9a shows the dendrogram of all six observations, including four operating variables and two performance indicators, which were all merged into a single observation. Every single observation was identified as an individual cluster. Seven main clusters were formed and identified, which were labeled with different colors. The sub-clusters in the same cluster had similar trends but were distinct from those in the other clusters. Fig. 3.9b displays the relationship between four variables and two performance indicators with 0 mean and 1 standard deviation. The mean and median values of each variable are summarized in Table 3.1.

Table 3.1 Mean and median of each variable [K: Kelvin].

	TDE (K)	**TDC (K)**	**PLR (%)**	**CPR (%)**	**COPD (%)**	**COP**
Mean	4.4	4.1	44.4	53.8	71.8	3.2
Median	4.7	4.1	47.4	49.8	74.2	3.1

The best performance was reported in cluster 2, in which chiller PLR, CPR, water temperature differences across the evaporator and condenser, and COP were considerably above their respective mean values and COPD was below its mean value. The worst performance was reported in cluster 6 and cluster 7, with each operating variable and COP below its mean values and COPD above its mean value. These two clusters showed that operating the system at low CPR conditions (i.e. less than zero of the rescaled value in Fig. 3.9) will generally cause high irreversibility in the system.

The clustering results indicated that the chiller performance had a strong relationship with the temperature difference across the evaporator and chiller PLR, and had a relatively weak relationship with the temperature difference across the condenser. For instance, the temperature difference across the condenser in cluster 1 was higher than that of cluster 2, however, the chiller performance in cluster 2 was higher than that in cluster 1. The major reason behind this was, in cluster 2, higher PLR values and higher temperature differences across the evaporator were achieved at relatively low CPR conditions compared to cluster 1. The results of cluster 3, cluster 4, and cluster 5 indicated that at high CPR conditions, a low-temperature difference across the evaporator can cause large COP destruction. The overall results indicated that to achieve the best performance, the chillers should be operated with PLR above 45% and CPR above 50% with the water temperature differences across the condenser and evaporator above their mean values. The best-performing cluster can be set as a benchmark to achieve optimized operation. The clustering results also validated the results of the CIT model but with better insights. The above results showed that the combination of the CIT model and AHC can help achieve optimized operation without opting for extensive conventional optimization models.

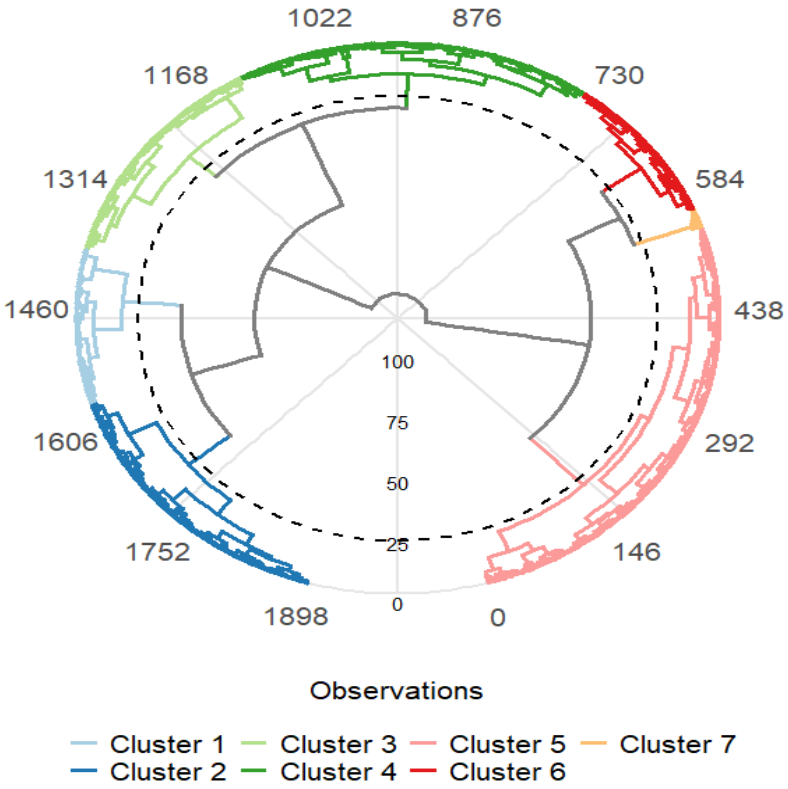

a) Dendrogram

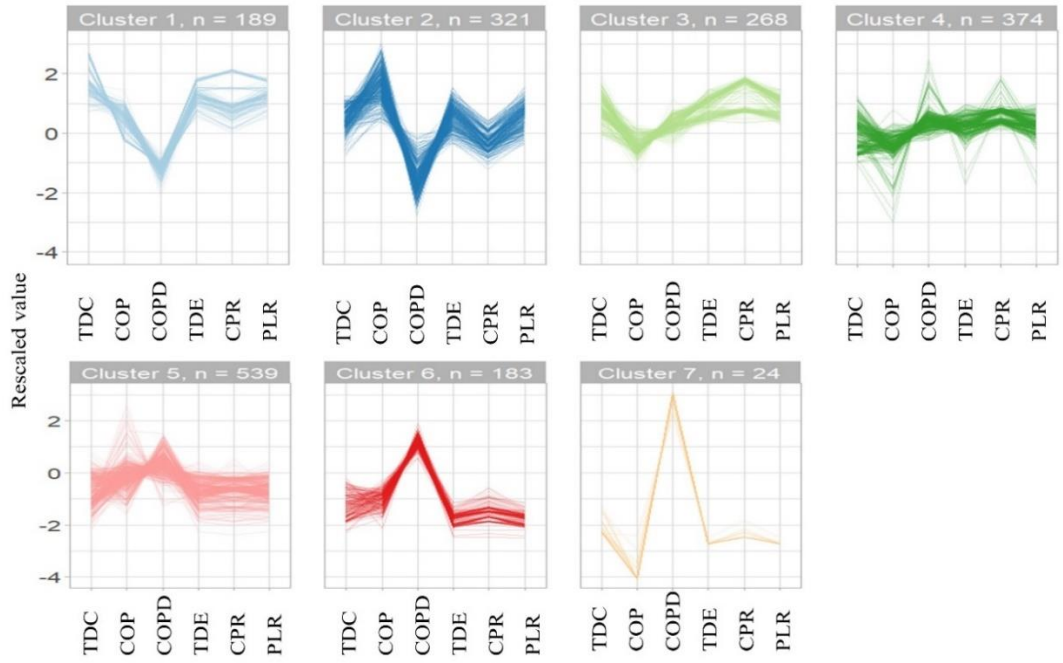

b) Profiles of the observations

Fig. 3.9 Relationships between the performance indicators and operating variables in the identified clusters.

3.4 Qualitative Analysis

ARM was used for further knowledge discovery from the processed data. Using the ARM model, a total of 57 sets of rules among COP, PLR, CPR, water temperature differences across the evaporator and condenser, and COPD were generated, as shown in Table 3.2. Antecedent and consequent were the first half and second half of a rule discovered by the association analysis. For example, in a rule {A, B} ⇒ {C}, A and B are antecedents, and C is consequent. “High” means higher than the median value and “Low” means lower than the median value. For example, one rule established in Table 3.2 with antecedent “CPR=High, COPD=High” and consequent “COP=Low” had the support of 0.20 and confidence of 0.88. This indicated that the system COP was low when the system had high COP destruction at high CPR conditions. 0.20 support indicated that 20% of the total data had this rule and a confidence of 0.88 indicated that 88% of the time dataset followed this rule.

The ARM model identified various combinations of the rules from the dataset. The system showed high performance (e.g. high COP and low COPD) when the water temperature differences across the evaporator and condenser, and PLR were

concurrently higher than their respective median values. The overall results from the AHC, CIT, and ARM models indicated that the system performed better when PLR was above 45%, CPR was above 50%, and the temperature differences across the evaporator and condenser were above their median values.

Table 3.2 Set of the rules generated from the ARM model.

Antecedent	Consequent	Support	Confidence
TDE=Low	PLR=Low	0.5	1
PLR=High	TDE=High	0.5	1
TDC=High	TDE=High	0.42	0.84
TDC=Low	TDE=Low	0.42	0.84
COP=Low	COPD=High	0.42	0.84
COP=High	COPD=Low	0.42	0.84
TDC=Low	PLR=Low	0.42	0.84
PLR=High	TDC=High	0.42	0.84
PLR=High, TDC=High	TDE=High	0.42	1
PLR=Low, TDC=Low	TDE=Low	0.42	1
PLR=High	CPR=High	0.41	0.82
CPR=Low	PLR=Low	0.41	0.82
TDE=High	CPR=High	0.41	0.82
TDE=High, CPR=High	PLR=High	0.41	1
TDE=Low, CPR=Low	PLR=Low	0.41	1
CPR=Low	TDE=Low	0.41	0.82
TDC=Low, CPR=Low	PLR=Low	0.37	0.99
TDC=Low, CPR=Low	TDE=Low	0.37	0.99
PLR=Low, COPD=High	TDE=Low	0.35	1
PLR=High, COPD=Low	TDE=High	0.34	1
TDC=High, CPR=High	PLR=High	0.33	0.89
TDC=High, CPR=High	TDE=High	0.33	0.89
TDC=High, COPD=Low	TDE=High	0.31	0.91
TDC=High, COPD=Low	PLR=High	0.31	0.91
COP=High, PLR=High	TDE=High	0.31	1
COP=Low, PLR=Low	TDE=Low	0.31	1
TDC=Low, COPD=High	TDE=Low	0.29	0.85
TDC=Low, COPD=High	PLR=Low	0.29	0.85
COP=Low, TDE=Low	COPD=High	0.29	0.94
COP=Low, PLR=Low	COPD=High	0.29	0.94
COP=High, TDC=High	COPD=Low	0.29	0.96
COP=High, TDE=High	COPD=Low	0.28	0.92
COP=High, PLR=High	COPD=Low	0.28	0.92
COP=Low, TDC=Low	COPD=High	0.27	0.92
CPR=Low, COPD=High	PLR=Low	0.27	1
CPR=Low, COPD=High	TDE=Low	0.27	1
COP=High, TDC=High	TDE=High	0.27	0.9
COP=High, TDC=High	PLR=High	0.27	0.89

Antecedent	Consequent	Support	Confidence
COP=High, TDC=High, TDE=High	COPD=Low	0.26	0.97
COP=High, PLR=High, TDC=High	COPD=Low	0.26	0.97
CPR=High, COPD=Low	PLR=High	0.26	0.95
COP=Low, TDC=Low	TDE=Low	0.26	0.86
CPR=Low, COPD=High	TDC=Low	0.26	0.94
CPR=High, COPD=Low	TDE=High	0.26	0.94
COP=Low, TDC=Low	PLR=Low	0.26	0.85
COP=Low, PLR=Low, TDC=Low	COPD=High	0.24	0.94
CPR=High, COPD=Low	TDC=High	0.23	0.86
TDC=High, CPR=High, COPD=Low	PLR=High	0.23	0.98
TDC=High, CPR=High, COPD=Low	TDE=High	0.23	0.98
COP=Low, CPR=Low	PLR=Low	0.23	1
COP=Low, CPR=Low	TDE=Low	0.23	1
CPR=Low, COPD=Low	COP=High	0.22	0.95
COP=High, CPR=High	PLR=High	0.22	0.96
COP=High, CPR=High	TDE=High	0.22	0.96
COP=Low, CPR=Low	COPD=High	0.22	0.95
COP=Low, CPR=Low	TDC=Low	0.21	0.95
CPR=High, COPD=High	COP=Low	0.2	0.88

Overall, the results showed that data mining techniques can help identify both efficient and inefficient operating conditions of chiller systems. Temporal classification obtained using the heatmaps and CIT model can be used to assess the operational behavior of the chiller system. The result obtained from the analyses showed that several operational alternatives can achieve a similar level of high performance under the same working conditions, and this can provide the controller with a certain flexibility in decision-making. These results in conjunction with the known operational behavior of the system can help implement better operational strategies for chiller systems. Moreover, the data cleaning process and introduction of COPD indicator can increase the reliability of the performance assessment process. It is worthwhile to note that the results reported in this chapter were generated based on the data collected from the case study system under the given climate. The results and the association rules might be different when the strategy developed is applied to a different chiller system at a different climate condition. However, the performance assessment strategy introduced can be adapted to evaluate the performance of other building energy systems.

3.5 Summary

This chapter presented a data-driven strategy for the performance assessment of a chiller system using data mining and visualization techniques. The chiller performance was evaluated based on the operating variables using AHC, CIT, and ARM. The collective effect of the operating variables on the system performance was studied. This strategy used DBSCAN to detect and remove the outliers in the collected data. CIT was used to classify the chiller power ratio based on temporal variations. The CIT model and AHC were used to quantitatively analyze the effect of the operating variables on the performance of the system. A new performance indicator, COPD was introduced to represent the quality of the COP. The introduction of this performance indicator enhanced the reliability of the performance assessment process. ARM was used for knowledge discovery by interlinking system performance indicators and operational variables. The overall results indicated that to achieve better operating performance, the chiller system studied should be operated with PLR above 45%, CPR above 50%, and the water temperature differences across the evaporator and condenser above their respective median values. A total of 57 sets of rules among COP, PLR, water temperature differences across the evaporator and condenser, CPR, and COP Destruction were established through association analysis. It was found that the system performance decreased when the PLR and water temperature differences across the condenser and evaporator were concurrently below their median values. The results from the ARM model also validated the results obtained from the AHC and CIT model. It was found that the temperature differences across the evaporator most strongly influenced the system performance. The quantitative results showed a range of operating conditions that can be selected for better operation. Similarly, the results generated by the ARM model also showed that under a given condition, several alternatives can achieve a better operational performance of the chiller system. The developed method can be used to assess the performance of any HVAC system, and the generated results can be used to develop energy-flexible and energy-efficient control strategies for chiller systems.

Chapter 4 A characteristic-oriented strategy for ranking and near-optimal selection of phase change materials for thermal energy storage in building applications

The literature review in Chapter 2 demonstrated the benefits of thermal energy storage (TES) to enhance the energy flexibility of buildings and building energy systems. It was also summarized that latent heat storage materials, especially phase change materials (PCMs), have shown better performance compared with other thermal energy storage technologies at the building level. Moreover, the selection of near-optimal PCMs for building applications is critical to enhance the performance of TES systems and it is a multicriteria decision problem that can be handled using the Multicriteria decision analysis (MCDA) techniques. This chapter introduces a Weighted product method (WPM) based ranking strategy for near-optimal selection of PCMs for thermal energy storage in building applications. Criteria to convert qualitative attributes into quantitative values and a weight assignment process to handle multiple characteristics of PCMs are also introduced. The impact of better-ranked PCM on the energy flexibility potential of a heating, ventilation, and air-conditioning (HVAC) system with integrated TES is analyzed as well.

4.1 Methodology

4.1.1 Outline of the research method

The proposed strategy for PCM ranking is presented in Fig. 4.1. It consists of three main steps, including model development, performance testing, and results verification. In the first step, based on the selected qualitative and quantitative characteristics, a strategy to convert qualitative characteristics into numeric values was introduced, which will be presented in Section 4.1.3. The WPM and a weight assignment process were then used to develop a PCM ranking model, which will be presented in Section 4.1.4. In the second step, the performance of the ranking model developed was tested through two different case studies, in which the first case study was focused on the ranking of a range of building applications-related PCMs based on their thermodynamics properties, whereas the second case study was conducted to select a near-optimal PCM for a ground source heat pump system with integrated TES, based on several qualitative and quantitative characteristics of PCMs including the

cost. An insight into the ranking results of the first case study was also provided using advanced visualization and data analytic techniques. In the last step, two PCMs from the ranking results were selected and used to provide energy flexibility to operate an HVAC system in order to verify the results. The simulation of each PCM was carried out separately under the same working conditions, and the results obtained were compared with the ranking results. In the second case study, the results verification was achieved by comparing the obtained results with that from a pre-published study with the same dataset and conditions.

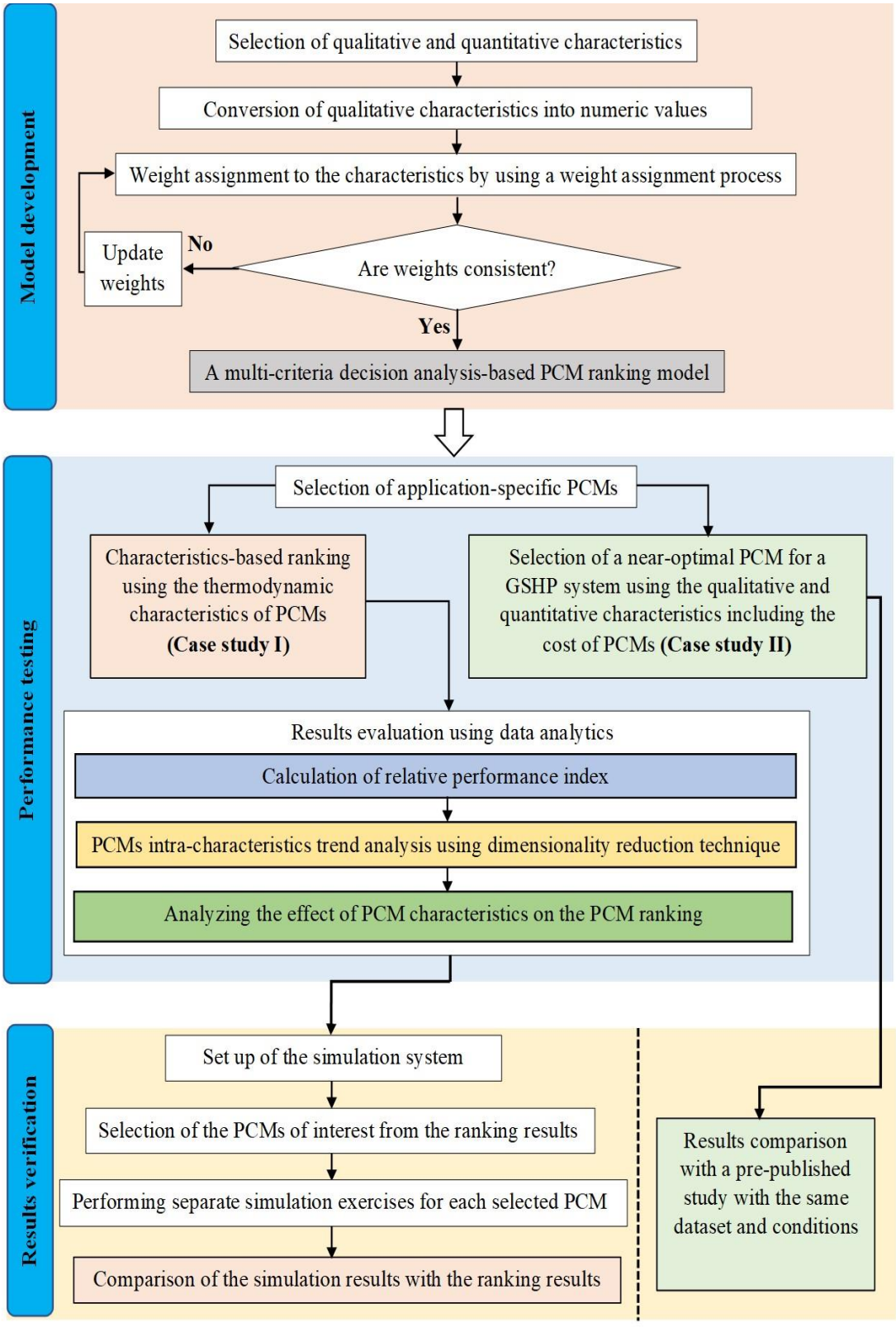

Fig. 4.1 Outline of the developed strategy.

4.1.2 Weighted product method

The WPM is a dimensionless analysis method. The vector representation of this method is shown in Fig. 4.2 (Mateo 2012). For multi-criteria decision analysis, this method initially labels each attribute as an objective function. Each objective function is first scaled from 0 to 1. The scaling process is shown in the second step of Fig. 4.2, i.e. vector scaling by identifying each attribute either as a minimization function or a maximization function. A desirable attribute should be handled as a maximization function, while an undesirable attribute should be handled as a minimization function. Once scaled, each objective function becomes non-dimensional, and this transforms multi-dimensional objective functions into a single dimension. Each objective function is then assigned a specific weight. In the one-dimensional space, a vector with the maximum length is considered the best, and that with the minimum length is considered the least effective option. The length of the vector can be determined using Eq. (4.1), whereas Eq. (4.2) and Eq. (4.3) can be used respectively for maximization and minimization purposes (Mateo 2012).

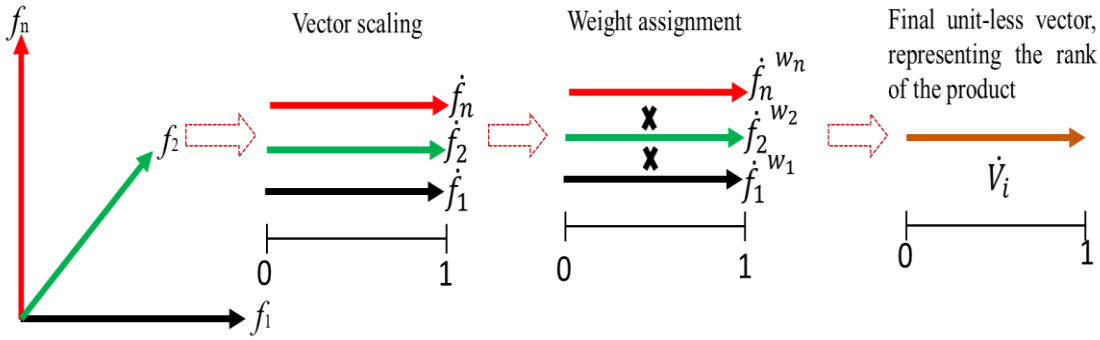

Fig. 4.2 Vector representation of the WPM (Mateo 2012).

$$\dot{V}_i = \prod_{j=1}^{n} \dot{f}_{ij}^{\,w_{ij}}, \text{ for i=1,2,3,…..,m.} \tag{4.1}$$

$$\dot{f}_{ij} = {f_{ij}}\Big/{\max f_j} \tag{4.2}$$

$$\dot{f}_{ij} = {\min f_j}\Big/{f_{ij}} \tag{4.3}$$

where $\dot{V}_i$ represents the length of the final vector, $\dot{f}_{ij}$ represents the scaled objective function, in which i represents an object that is being ranked and j represents a specific

attribute of the i^{th} object, $\max f_j$ and $\min f_j$, respectively represent the maximum and minimum values of the j^{th} attribute in the whole dataset, w represents the weight of each property, and $\prod$ is the symbol of multiplication.

4.1.3 Conversion of qualitative characteristics into numeric values

A ranking model was developed that can consider qualitative and quantitative attributes of PCMs in the characteristics-based ranking of PCMs. The ranking of the quantitative properties is relatively easy as these properties can be mutually scaled. However, qualitative functions cannot be scaled, and hence need to be converted into quantitative factors. Table 4.1 summarizes the strategy to assign a numeric value to the qualitative characteristics based on the respective significance and intensity of importance that was achieved using the standard Saaty scale ('The Analytic Hierarchy Process' 1990). It also highlights the significance of the required property/characteristic and the respective intensity of importance on a relative scale.

Table 4.1 Strategy to convert qualitative properties into quantitative factors.

Significance	**Intensity of importance**								
	Extremely high	**Very high**	**High**	**Above avg.**	**Avg.**	**Below avg.**	**Low**	**Very low**	**Extremely low**
Desirable	0.9	0.8	0.7	0.6	0.5	0.4	0.3	0.2	0.1
Undesirable	0.1	0.2	0.3	0.4	0.5	0.6	0.7	0.8	0.9

Table 4.2 shows the conversion of the qualitative characteristics into the quantitative factors using Table 4.1. Because of using the inverse function for the desirable and undesirable characteristics in these tables, the characteristic normalization process was further simplified. With the help of Table 4.2, only the maximization function (Eq. (4.2)) can be used to achieve normalization for the qualitative characteristics, which effectively increases the computational performance of this method for ranking of PCMs. The same strategy can be used to convert additional qualitative characteristics into quantitative factors.

Table 4.2 Conversion of qualitative characteristics into quantitative factors.

Qualitative Characteristics	Quantitative Conversion								
	Extremely high	**Very high**	**High**	**Above avg.**	**Avg.**	**Below avg.**	**Low**	**Very low**	**Extremely low**
Phase transition stability (ϕ)	0.9	0.8	0.7	0.6	0.5	0.4	0.3	0.2	0.1
Chemical stability (ↄ)	0.9	0.8	0.7	0.6	0.5	0.4	0.3	0.2	0.1
Reversible freeze melt cycles (rm)	0.9	0.8	0.7	0.6	0.5	0.4	0.3	0.2	0.1
Recyclable (ϒ)	0.9	0.8	0.7	0.6	0.5	0.4	0.3	0.2	0.1
Volumes changes (V)	0.1	0.2	0.3	0.4	0.5	0.6	0.7	0.8	0.9
Vapor pressure changes (p)	0.1	0.2	0.3	0.4	0.5	0.6	0.7	0.8	0.9
Corrosiveness (ς)	0.1	0.2	0.3	0.4	0.5	0.6	0.7	0.8	0.9
Toxicity (ŧ)	0.1	0.2	0.3	0.4	0.5	0.6	0.7	0.8	0.9
Combustibility (ℱ)	0.1	0.2	0.3	0.4	0.5	0.6	0.7	0.8	0.9
Supercooling (ƨ)	0.1	0.2	0.3	0.4	0.5	0.6	0.7	0.8	0.9
Explosiveness (∃)	0.1	0.2	0.3	0.4	0.5	0.6	0.7	0.8	0.9

4.1.4 Formulation of the PCM-ranking model

Based on the Weighted product method (Section 4.1.2), a ranking model was formulated to support the performance-based ranking of PCMs, as depicted in Eq. (4.4). The majority of the qualitative and quantitative characteristics were considered in this model, and this model has the flexibility to include or exclude any variable.

$$R_i = \prod[\dot{\rho_{s_1}}^{w_{\rho s}}, \dot{\rho_{l_1}}^{w_{\rho l}}, \dot{k_{s_1}}^{w_{ks}}, \dot{k_{l_1}}^{w_{kl}}, \dot{c_{Ps_1}}^{w_{cps}}, \dot{c_{Pl_1}}^{w_{cpl}}, \dot{Q_{L_1}}^{w_{Q_L}}, \dot{C_1}^{w_C}, \dot{T_1}^{w_T}, \dot{\exists_1}^{w_\exists}, \dot{\digamma_1}^{w_\digamma}, \dot{ŧ_1}^{w_ŧ}, \dot{\varsigma}^{w_\varsigma}, \dot{V_1}^{w_V}, \dot{p_1}^{w_p}, \dot{ↄ_1}^{w_ↄ}, \dot{\phi_1}^{w_\phi}, \dot{rm_1}^{w_{rm}}, \dot{ƨ_1}^{w_ƨ}, \dot{\Upsilon_1}^{w_\Upsilon}] \quad (4.4)$$

where R represents the rank of the PCM, ρ, k, c_p, Q_L, C, and T represent density, thermal conductivity, specific heat, latent heat of fusion, cost, and melting temperature, respectively, dot (.) above each letter represents normalization that can be achieved using Eq. (4.2) or Eq. (4.3), and the subscripts *s* and *l* represent solid and liquid, respectively.

As the weight assignment is considered to be a critical part of the ranking process, the weights can be assigned using the Analytic hierarchy process (AHP) method. A total of 20 properties were considered in Eq. (4.4) that generated a 20 x 20 matrix. Considering the mutuality of the properties, the number of attributes in the AHP matrix can be reduced. As shown in Table 4.3, three clusters were formed based on domain knowledge and considering the interconnection between inter-cluster properties.

Table 4.3 Formation of the clusters for weight assignment.

Clusters	**Cluster 1**	**Cluster 2**	**Cluster 3**
Characteristics	$w_{\rho_s}, w_{\rho_l}, w_{k_S}, w_{k_l}, w_{C_{P_S}}$, $w_{C_{P_l}}, w_{Q_L}, w_C, w_T$	w_p , w_{rm}, w_ϕ, w_F	$w_\supset$, w_ζ, w_t, w_V, $w_\exists$, $w_\wr$, w_Y

The properties in cluster 1 can be given more importance for weight assignment purposes as they tend to have the maximum influence on the performance of a specific material (Anilkumar et al. 2021; Das et al. 2021; Rathod & Kanzaria 2011; Socaciu et al. 2016). Cluster 2 can be given average importance as these properties have slightly less influence as compared to the properties in cluster 1, but most of these properties strongly influence the pre-selection process, and most of them can be improved by taking certain measures. Cluster 3 can be given the lowest importance, as the adverse effect of these properties can be mitigated by taking certain measures (Sharma et al. 2004). Because of the inter-cluster mutuality, cluster 2 and cluster 3 can be assigned the same inter-cluster weights but different intra-cluster weights. Similarly, liquid and solid states of the properties in cluster 1 can be assigned with the same weight. The pairwise matrix (Fig. 4.3), Eq. (4.5), and Eq. (4.6) can be used to assign specific weights to each property using the Saaty scale and the AHP method.

$$\begin{bmatrix} & \mathrm{k} & \rho & c_P & T & Q_L & C & Cl2 & Cl3 \\ \mathrm{k} & 1 & P_{\mathrm{k}/\rho} & P_{\mathrm{k}/c_P} & P_{\mathrm{k}/T} & P_{\mathrm{k}/Q_L} & P_{\mathrm{k}/C} & P_{\mathrm{k}/Cl2} & P_{\mathrm{k}/Cl3} \\ \rho & {}^{1}/_{P_{\mathrm{k}/\rho}} & 1 & P_{\rho/c_P} & P_{\rho/T} & P_{\rho/Q_L} & P_{\rho/C} & P_{\rho/Cl2} & P_{\rho/Cl3} \\ c_P & {}^{1}/_{P_{\mathrm{k}/c_P}} & {}^{1}/_{P_{\rho/c_P}} & 1 & P_{c_P/T} & P_{c_P/Q_L} & P_{c_P/C} & P_{c_P/Cl2} & P_{c_P/Cl3} \\ T & {}^{1}/_{P_{\mathrm{k}/T}} & {}^{1}/_{P_{\rho/T}} & {}^{1}/_{P_{c_P/T}} & 1 & P_{T/Q_L} & P_{T/C} & P_{T/Cl2} & P_{T/Cl3} \\ Q_L & {}^{1}/_{P_{\mathrm{k}/Q_L}} & {}^{1}/_{P_{\rho/Q_L}} & {}^{1}/_{P_{c_P/Q_L}} & {}^{1}/_{P_{T/Q_L}} & 1 & P_{Q_L/C} & P_{Q_L/Cl2} & P_{Q_L/Cl3} \\ C & {}^{1}/_{P_{\mathrm{k}/C}} & {}^{1}/_{P_{\rho/C}} & {}^{1}/_{P_{c_P/C}} & {}^{1}/_{P_{T/C}} & {}^{1}/_{P_{Q_L/C}} & 1 & P_{C/Cl2} & P_{C/Cl3} \\ Cl2 & {}^{1}/_{P_{\mathrm{k}/Cl2}} & {}^{1}/_{P_{\rho/Cl2}} & {}^{1}/_{P_{c_P/Cl2}} & {}^{1}/_{P_{T/Cl2}} & {}^{1}/_{P_{Q_L/Cl2}} & {}^{1}/_{P_{C/Cl2}} & 1 & P_{Cl2/Cl3} \\ Cl3 & {}^{1}/_{P_{\mathrm{k}/Cl3}} & {}^{1}/_{P_{\rho/Cl3}} & {}^{1}/_{P_{c_P/Cl3}} & {}^{1}/_{P_{T/Cl3}} & {}^{1}/_{P_{Q_L/Cl3}} & {}^{1}/_{P_{C/Cl3}} & {}^{1}/_{P_{Cl2/Cl3}} & 1 \end{bmatrix}$$

Fig. 4.3 AHP matrix for relative weight assignment, where P represents the priority number of a numerator over the denominator using the Saaty scale, and *Cl* represents a cluster.

Once the weights are determined using the AHP matrix, individual weights can be adjusted for each property using Eq. (4.5). Weight adjustment is needed to assign weights to inter-cluster values.

$$\mathrm{W}_{adj_j} = \frac{\Omega_j}{\sum(\mathrm{z}_k\Omega_k, \mathrm{z}_\rho\Omega_\rho, \mathrm{z}_{cp}\Omega_{cp}, \mathrm{z}_T\Omega_T, \mathrm{z}_{QL}\Omega_{QL}, \mathrm{z}_C\Omega_C, \mathrm{z}_{Cl2}\Omega_{Cl2}, \mathrm{z}_{Cl3}\Omega_K)} \tag{4.5}$$

where Ω_j and W_{adj_j}, respectively represent the individual weight determined by the AHP matrix and the adjusted weight of the j[th] characteristic, and z represents the number of characteristics merged for a relative characteristic. For instance, in this case, for the first 3 characteristics, z was 2, as liquid and solid-state properties were merged. For the next 3 properties, z was 1, and it was 4 and 7 for cluster 2 and cluster 3, respectively. Furthermore, each weight can be normalized using Eq. (4.6), in which the summation sign represents the sum of weights of all characteristics, and the obtained value of the weight should be used in Eq. (4.4).

$$\mathrm{w}_j = \frac{\mathrm{W}_{adj_j}}{\sum_{j=1}^{n} \mathrm{W}_{adj_j}} \tag{4.6}$$

It is worthwhile to note that the weight assignment process is flexible, and weights can be adjusted as per desired application. For instance, in an application where space

is limited, density can have high importance but with high space availability, less weight can be assigned to density.

4.2 Performance testing

4.2.1 Case study I: Ranking PCMs for different building applications based on major thermodynamic properties

To test the performance of the developed strategy, a sample dataset of 134 commercial PCMs as presented in Table 4.6 was established from commercial PCM websites (Axiotherm; Climator; PCP; Pluss; Rgees; Rubitherm). These PCMs were selected by considering their melting temperatures relating to building applications. The selected PCMs were divided into five application-specific categories based on the available literature (Agyenim et al. 2010; Akeiber et al. 2016; Oró et al. 2012; Tyagi & Buddhi 2007). The PCMs with melting temperatures ranging from -7 ^{o}C to 16 ^{o}C were considered for cooling or cold storage application as per literature (Oró et al. 2012). The PCMs with melting temperatures ranging from 17 ^{o}C to 28 ^{o}C were considered to be used in building envelopes to maintain indoor thermal comfort and reduce building heating/cooling demand as per the melting temperature range (Akeiber et al. 2016; Tyagi & Buddhi 2007). The PCMs from 29 ^{o}C to 44 ^{o}C were considered for heat storage applications (Agyenim et al. 2010). As the PCMs considered were commercially available and only the thermodynamic properties data is available, hence only thermodynamic properties were considered in the performance testing. Density, latent heat, specific heat, and thermal conductivity of the PCMs were considered the objective functions. Eq. (4.7) was derived from Eq. (4.4) and was used for the performance ranking of PCMs.

$$R_i = \prod [\dot{\rho}_1^{w_{\rho i}}, \dot{k}_1^{w_{ki}}, \dot{c_{P_1}}^{w_{Cpi}}, \dot{Q_{L_1}}^{w_{Q_{Li}}}], \text{ for i=1,2…..,134} \quad (4.7)$$

The weights for the selected variables were assigned by assuming the following two scenarios.

- Scenario I: The same size of the TES was considered, and therefore the storage capacity may be different depending on the characteristics of the material used. For this scenario, latent heat, density, and specific heat were given importance over thermal conductivity, as these characteristics are considered

to be essential for the high energy density of a TES system, and these characteristics were assigned the same priority number. Thermal conductivity was assigned with moderate importance value as it is important for effective heat transfer, but its effect on the heat storage capacity of a TES system is not significant.

- Scenario II: For building applications, fast charging and discharging are preferred to meet building heating and cooling demand. Therefore, in this scenario, thermal conductivity was given preference over all other selected characteristics.

The AHP matrix (Fig. 4.3) and Eq. (4.6) were used to calculate the weights for both application scenarios, and the results are summarized in Table 4.4.

Table 4.4 Pair-wise matrix of relative importance for individual weight assignment.

	Scenario 1					**Scenario 2**					**Consistency ratio**	**Normalized average weights**
	ρ	Q_L	**k**	c_P	**weight**	**ρ**	Q_L	**k**	c_P	**weight**		
ρ	1	1	3	1	0.3	1	1	1/2	1	0.2		0.25
Q_L	1	1	3	1	0.3	1	1	1/2	1	0.2	0.00	0.25
k	1/3	1/3	1	1/3	0.1	2	2	1	2	0.4		0.25
c_P	1	1	3	1	0.3	1	1	1/2	1	0.2		0.25

A low consistency ratio (CR << 0.1 (Saaty 2002)) validated the weight assignment process. Eq. (4.8) was used to calculate the consistency ratio (CR), in which the consistency index (CI) was calculated using Eq. (4.9).

$$CR = \frac{CI}{RI} \tag{4.8}$$

$$CI = \frac{\lambda_{max} - n}{n-1} \tag{4.9}$$

where RI represents the random consistency index, and its value was taken from the standard random consistency index (RI) table, i.e. 0.9 for n=4 ('The Analytic Hierarchy Process' 1990), and λ_{max} was 4.0, which was calculated using the standard formulation derived by Saaty (Saaty 2002).

Table 4.6 presents the list of the PCMs with their application-specific ranks. Ranks were assigned as per the vector length of the PCM, i.e. PCM with the maximum vector

length was ranked at the top, and that with the shortest length was assigned at the bottom of the ranking list. The top-ranked PCMs in each category were marked in bold and italics in Table 4.6. The values of these objective functions are summarized in Fig. 4.4 and Table 4.5. Fig. 4.4 is a boxplot of the data for each property of the organic and inorganic PCMs. The three horizontal lines in the box represent the first quartile (lower line), the median (middle line), and the third quartile (upper line) of the data, and the circles represent the outliers. The outliers above the box represent the PCMs with better thermodynamic properties, whereas the outliers below the box represent the PCMs with less effective properties. It is noted that inorganic PCMs mainly possess overall better thermodynamic properties compared with organic PCMs.

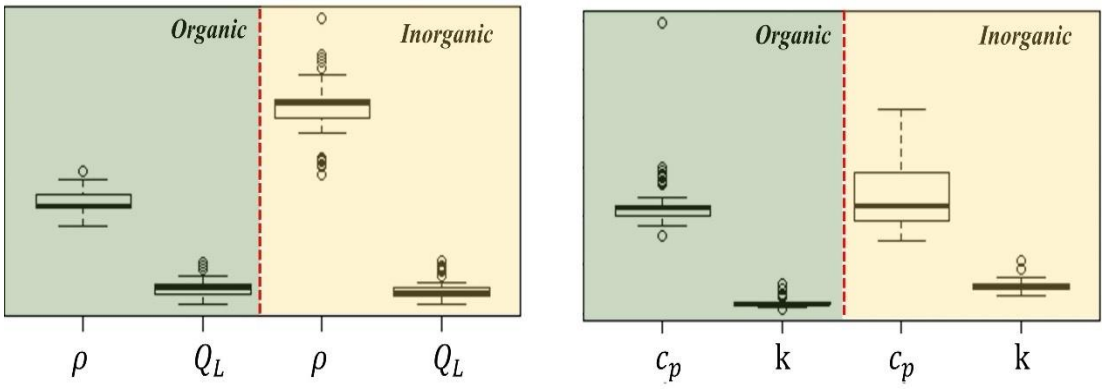

Fig. 4.4 Box plot of the thermodynamic properties of the selected PCMs.

Table 4.5 Statistical summary of the properties of the selected PCMs.

	Organic				**Inorganic**			
	ρ (kg/m^3)	**Q_L (kJ/kg)**	**c_p (kJ/kg.K)**	**k (W/m.K)**	**ρ (kg/m^3)**	**Q_L (kJ/kg)**	**c_p (kJ/kg.K)**	**k (W/m.K)**
Min.	650	102	1.60	0.10	1000	100	1.50	0.35
1st Quartile	770	170	2.00	0.18	1400	159	1.90	0.49
Median	780	215	2.18	0.20	1512	180	2.20	0.54
Mean	810	213	2.26	0.21	1455	200	2.44	0.56
3rd Quartile	862	235	2.22	0.22	1530	204	2.90	0.60
Max	1028	385	5.95	0.59	2100	395	4.19	1.08

Table 4.6 Commercial PCMs considered and their respective ranks [CS: Cooling storage, ESc: Building envelope application (space cooling), ES_{ch}: Building envelope application (space cooling or heating), ES_h: Building envelope application (space heating), HS: Heat storage].

Sr #	PCM	$T_{p.c}$ (°C)	ρ (kg/m^3)	Q_L (kJ/kg)	c_p (kJ/kg.K)	k (W/m.K)	Type	App.	Rank
1	HS7N	-7	1120	296	3.5	0.55	I.O	CS	8
2	PCM-7	-7	1100	290	2.1	0.5	I.O	CS	11
3	E-6	-6	1110	300	3.83	0.56	I.O	CS	5
4	ATS -6	-6	1100	360	3	0.6	I.O	CS	6
5	E-3	-4	1060	330	3.84	0.6	I.O	CS	2
6	HS3N	-3	1060	346	3.98	0.35	I.O	CS	9
7	ATS -3	-3	1100	330	3	0.6	I.O	CS	7
8	E-2	-2	1070	325	3.8	0.58	I.O	CS	3
9	***E0***	***0***	***1000***	***395***	***4.19***	***0.58***	***I.O***	***CS***	***1***
10	HS01	1	1010	350	3.9	0.55	I.O	CS	4
11	A2	2	765	230	2.2	0.21	O	CS	23
12	ATP 2	2	760	215	2	0.2	O	CS	36
13	A3	3	765	230	2.2	0.21	O	CS	24
14	OM03	3	835	229	1.91	0.15	O	CS	41
15	FS03	3	870	161	2.23	0.16	O	CS	42
16	A4	4	766	235	2.18	0.21	O	CS	21
17	A5	5	768	170	2.18	0.22	O	CS	39
18	M05P	5	760	216	2	0.51	O	CS	18
19	OM05P	5	763	242	5.95	0.37	O	CS	10
20	OM06P	6	762	252	2	0.21	O	CS	25
21	A6	6	768	185	2.17	0.21	O	CS	37
22	ATP 6	6	740	275	2	0.2	O	CS	22
23	A6.5	7	770	190	2.18	0.22	O	CS	32
24	A7	7	770	190	2.18	0.22	O	CS	33
25	C7	7	1400	123	2.4	0.59	I.O	CS	13
26	A8	8	770	180	2.16	0.21	O	CS	38
27	S8	8	1475	130	1.9	0.44	I.O	CS	19
28	A9	9	770	190	2.16	0.21	O	CS	35
29	A10	10	770	210	2.16	0.22	O	CS	29
30	S10	10	1470	170	1.9	0.43	I.O	CS	15
31	C10	10	1400	116	2.85	0.7	I.O	CS	12
32	A11	11	775	210	2.16	0.22	O	CS	28
33	A12	12	775	215	2.16	0.22	O	CS	26
34	ATP 12	12	800	245	2	0.2	O	CS	27
35	A13	13	775	225	2.16	0.22	O	CS	20
36	S13	13	1515	150	1.9	0.43	I.O	CS	17

Sr #	PCM	$T_{p.c}$ (°C)	ρ (kg/m^3)	Q_L (kJ/kg)	c_p (kJ/kg.K)	k (W/m.K)	Type	App.	Rank
37	A14	14	775	200	2.16	0.22	O	CS	31
38	PCM14	14	1750	145	1.5	0.5	I.O	CS	16
39	A15	15	780	205	2.16	0.18	O	CS	40
40	S15	15	1510	180	1.9	0.43	I.O	CS	14
41	A16	16	780	225	2.16	0.18	O	CS	34
42	ATP 16	16	770	245	2	0.2	O	CS	30
43	A17	17	780	235	2.18	0.18	O	ESc	31
44	S17	17	1525	155	1.9	0.43	I.O	Esc	18
45	S17	17	1525	160	1.9	0.43	I.O	Esc	15
46	PCM17	17	1800	147	1.5	0.5	I.O	Esc	17
47	A18	18	765	155	2.18	0.22	O	ESc	37
48	S18	18	1520	145	1.9	0.43	I.O	ESc	19
49	OM18P	18	735	233	2.2	0.59	O	ESc	13
50	OM18	18	870	212	2.69	0.1	O	ESc	28
51	ATP 18	18	760	270	2	0.2	O	ESc	29
52	$KF.4H_2O$	19	1455	246	1.62	0.5	I.O	ESc	11
53	A19	19	765	150	2.18	0.22	O	ESc	38
54	S19	19	1520	175	1.9	0.43	I.O	ESc	14
55	S19	19	1520	160	1.9	0.43	I.O	ESc	16
56	A20	20	770	160	2.2	0.22	O	ESc	35
57	S20	20	1530	195	2.2	0.54	I.O	ESc	8
58	ATP 20	20	840	220	3	0.2	O	ESc	24
59	RT 21	21	880	150	2	0.2	O	ESc	39
60	A21	21	770	160	2.2	0.22	O	ESc	36
61	S21	21	1530	220	2.2	0.54	I.O	ESc	4
62	S21	21	1530	170	2.2	0.54	I.O	ESc	10
63	OM21	21	891	174	2.85	0.14	O	ESc	33
64	C21	21	1400	134	2.94	0.75	I.O	ESc	3
65	HC 22	22	760	200	2	0.2	O	ESc	34
66	NE 23	22	770	342	2	0.2	O	ESc	25
67	A22	22	785	160	2.2	0.18	O	ESc	40
68	S22	22	1530	215	2.2	0.54	I.O	ESc	5
69	A22H	22	820	216	2.85	0.18	O	ESc	27
70	RT 21	22	880	190	2	0.2	O	ESc	32
71	SP 21 E	22	1500	160	2	0.6	I.O	ESc	12
72	HS22P	22	1540	185	3.04	0.56	I.O	ESc	2
73	HS22	22	1540	168	2.53	0.56	I.O	ESc	6
74	PCM 23	23	1300	170	1.6	0.45	I.O	ESc	20
75	GmbH 23	23	970	365	2	0.19	O	ESc	22
76	BASF 23	23	770	343	1.8	0.2	O	ESc	26
77	PCM 23	23	770	342	2.2	0.2	O	ESc	23
78	A23	23	785	155	2.2	0.18	O	ESc	41
79	S23	23	1530	200	2.2	0.54	I.O	ESc	7

Sr #	PCM	$T_{p.c}$ (°C)	ρ (kg/m³)	Q_L (kJ/kg)	c_p (kJ/kg.K)	k (W/m.K)	Type	App.	Rank
80	S23	23	1530	175	2.2	0.54	I.O	ESc	9
81	***HS23P***	***23***	***1540***	***185***	***3.05***	***0.9***	***I.O***	***ESc***	***1***
82	Weber 23	23	950	170	2.32	0.38	O	ESc	21
83	ATP 23	23	800	230	2	0.2	O	ESc	30
84	GmbH 24	24	880	150	2	0.2	O	ES_{ch}	13
85	A24	24	790	155	2.22	0.18	O	ES_{ch}	14
86	S24	24	1530	180	2.2	0.54	I.O	ES_{ch}	6
87	***HS24P***	***24***	***1820***	***185***	***2.26***	***0.9***	***I.O***	***ES_{ch}***	***1***
88	RT 25	24	880	230	2	0.2	O	ES_{ch}	12
89	HS24	24	1510	199	2.42	0.55	I,O	ES_{ch}	4
90	C24	24	1400	140	2.9	0.74	I.O	ES_{ch}	2
91	A25	25	785	150	2.22	0.18	O	ES_{ch}	15
92	S25	25	1530	175	2.2	0.54	I.O	ES_{ch}	9
93	S25	25	1530	180	2.2	0.54	I.O	ES_{ch}	7
94	SP 25 E2	25	1500	180	2	0.6	I.O	ES_{ch}	8
95	PCM25	25	1700	150	2.73	0.58	I.O	ES_{ch}	3
96	A26	26	790	230	2.22	0.21	O	ES_{ch}	11
97	SP 26 E	26	1500	190	2	0.6	I.O	ES_{ch}	5
98	BASF 26	26	770	385	1.6	0.2	O	ES_{ch}	10
99	PX 27	27	650	102	1.6	0.2	O	ES_h	7
100	RT 27	27	880	179	2	0.2	O	ES_h	6
101	A27	27	768	250	2.22	0.22	O	ES_h	4
102	S27	27	1530	185	2.2	0.54	I.O	ES_h	2
103	A28	28	789	265	2.22	0.21	O	ES_h	3
104	ATP 28	28	760	265	2	0.2	O	ES_h	5
105	***C28***	***28***	***1400***	***170***	***2.9***	***0.72***	***I.O***	***ES_h***	***1***
106	A29	29	810	225	2.22	0.18	O	HS	19
107	HS29	29	1530	190	2.62	0.38	I.O	HS	8
108	OM29	29	870	194	2.71	0.17	O	HS	16
109	FS29	29	950	158	2.1	0.17	O	HS	25
110	PCM29	29	1710	188	2.31	0.54	I.O	HS	2
111	SP 24 E	30	1500	190	2	0.6	I.O	HS	3
112	OM30	30	835	230	1.91	0.15	O	HS	26
113	FS30	30	960	172	2.77	0.34	O	HS	10
114	ATS 30	30	1300	200	2	0.6	I.O	HS	5
115	A32	32	845	120	2.2	0.21	O	HS	28
116	A32H	32	820	240	2.2	0.22	O	HS	13
117	S32	32	1460	220	1.9	0.51	I.O	HS	6
118	OM32	32	870	156	2.81	0.15	O	HS	23
119	***C32***	***32***	***1400***	***160***	***3***	***1.08***	***I.O***	***HS***	***1***
120	S34	34	2100	140	2.1	0.52	I.O	HS	4
121	HS34	34	1850	150	2.32	0.47	I.O	HS	7

Sr #	PCM	$T_{p.c}$ (°C)	ρ (kg/m^3)	Q_L (kJ/kg)	c_p (kJ/kg.K)	k (W/m.K)	Type	App.	Rank
122	OM35	35	870	202	2.78	0.16	O	HS	17
123	A36	36	790	130	2.37	0.18	O	HS	29
124	A36H	36	776	300	2.3	0.22	O	HS	11
125	ATP 36	36	800	240	2	0.2	O	HS	18
126	OM37P	37	880	218	2.2	0.13	O	HS	24
127	OM37	37	860	231	2.63	0.13	O	HS	20
128	A39	39	900	135	2.22	0.22	O	HS	21
129	A42	42	905	140	2.22	0.21	O	HS	22
130	OM42	42	863	221	2.78	0.1	O	HS	27
131	FS42	42	1028	187	2.91	0.36	O	HS	9
132	A43	43	780	280	2.37	0.18	O	HS	14
133	ATP 43	43	760	265	2	0.2	O	HS	15
134	S44	44	1584	100	1.61	0.43	I.O	HS	12

4.2.2 Results evaluation

The quantitative difference in the relative performance of the PCMs considered can be visualized in Fig. 4.5, in which the x-axis indicates the serial number of the PCMs in Table 4.6, and the y-axis represents the difference in the relative performance of the PCMs. Two clusters were formed, the upper cluster represents the majority of inorganic PCMs, whereas the lower cluster represents the majority of organic PCMs. The red circles in Fig. 4.5 represent the best PCM for each application. The relative performance was obtained using Eq. (4.10) as below.

$$\gamma_i = \left[1 - \frac{Max(V)}{V_i}\right] \times 100 \qquad (4.10)$$

where i = 1, ….., n represents the serial number of a PCM, and γ represents the relative performance index of a PCM in percentage.

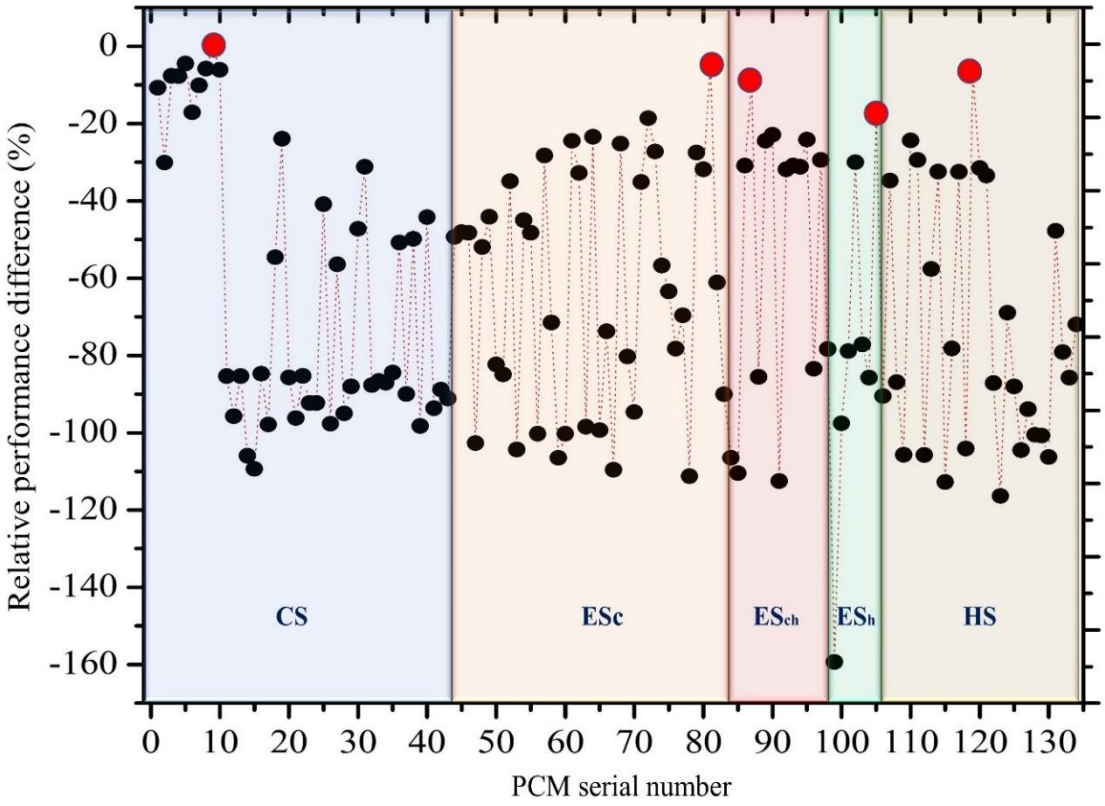

Fig. 4.5 Visualization of the relative performance of PCMs considered, where 0 represents the top-ranked and -160 represents the lowest-ranked PCM.

It is worthwhile to note that the color shadings in Table 4.6 and Fig. 4.5 were used to separate the data of the PCMs based on their preferable type of application and there is no statistical significance. The lines connecting the dots were just indications of the performance difference between the two consecutive PCMs.

To visualize all PCMs with the respective properties in a 2-dimensional space, the Principal component analysis (PCA) (Jolliffe 2002) was used for dimensionality reduction. Firstly, the whole dataset was considered as a matrix, and covariances were found for each data point. Secondly, eigenvectors and subsequent eigenvalues were calculated. All eigenvectors were then sorted based on the eigenvalues in decreasing order. After this step, the eigenvectors with low values were eliminated so as to achieve dimensionality reduction. In the same step, the feature vectors were formed. Lastly, the transpose of the feature vector was taken and multiplied with the transpose of the originally scaled data. This transformed *n*-dimensional data points into *k* dimensions, i.e. principal components. Four-dimensional properties were reduced to two dimensions using the PCA, as shown in Fig. 4.6, in which PC1 and PC2

respectively represent principal component 1 and principal component 2. The numbers in Fig. 4.6 illustrate the serial number of PCMs in Table 4.6. The PCMs outside ovals showed a distinctive performance in a few or all of the characteristics. The ovals covered 95% of the values of the dataset, and the rest 5% of the PCMs from each category were outside the ovals, representing the leading 5% performers in an individual or several characteristics. The red arrows show that density and conductivity are correlated, and the latent heat and specific heat are also correlated. The PCMs with serial numbers away from the origin in the direction of arrows indicate better characteristics than the PCMs close to the origin. Moreover, PCMs with a higher density, higher specific heat, and higher conductivity were mostly on the right side of the origin line, whereas those with higher latent heat were mostly on the left side of the origin.

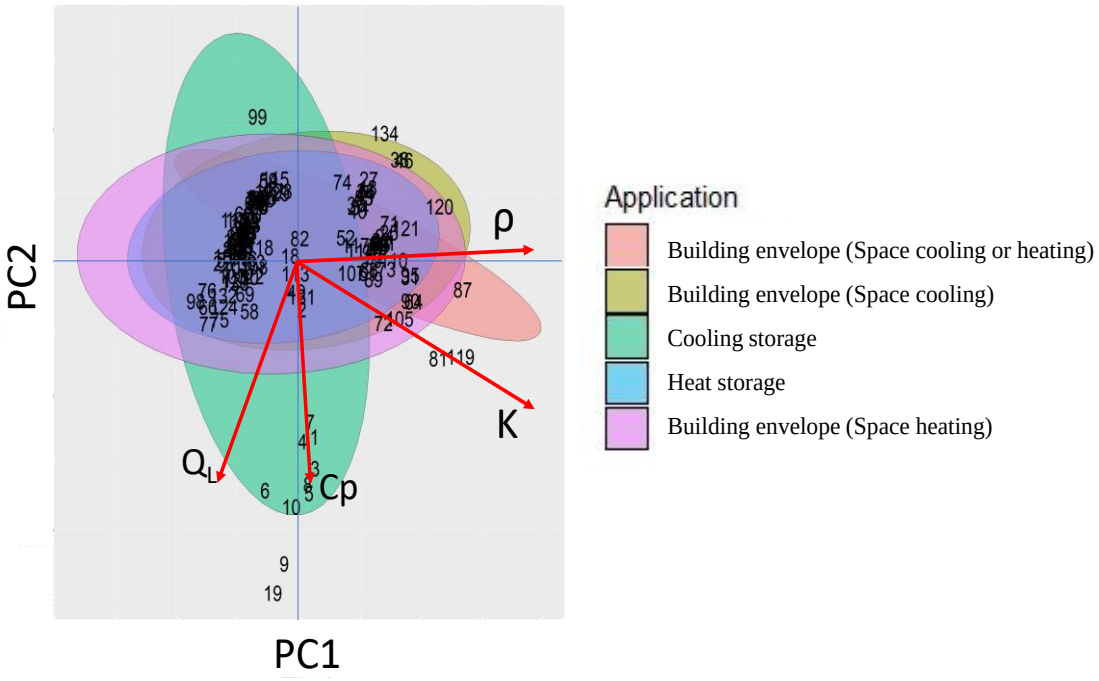

Fig. 4.6 Biplot of principal components (PCs) as per building-related applications.

The ranking in each category was further divided into three alphabetical levels, with "A" representing the top-performing PCMs and "C" representing the bottom-performing PCMs, from each category. Each level was assigned the same weight. The results obtained using the CITs algorithm (Awan et al. 2021) are shown in Fig. 4.7. For cooling storage applications (Fig. 4.7a), the PCMs with a density greater than 870 (kg/m^3), a solid thermal conductivity greater than 0.2 (W/m.K), and a specific heat

capacity greater than 2.2 (kJ/kg.K) were ranked as the top PCMs, whereas the majority of the PCMs with thermal conductivity, density, latent heat, and specific heat capacity that is not greater than 0.2 (W/m.K), 870 (kg/m^3), 205 (kJ/kg) and 2.2 (kJ/kg.K) respectively, were ranked at the bottom. A similar trend was also observed for the PCMs in building envelope applications (space cooling) (Fig. 4.7b), where the PCMs with thermal conductivity and density that were not greater than 0.4 (W/m.K) and 891 (kg/m^3) respectively, were ranked at the bottom. For heat storage applications (Fig. 4.7c), the PCMs with thermal conductivity greater than 0.2 (W/m.K), density greater than 950 (kg/m^3), and the majority of the PCMs with latent heat that was not greater than 221 (kJ/kg) were ranked as the top PCMs. For PCMs in building envelope applications (space heating and cooling, and space heating only), no significant difference in the data was observed. The PCMs for these categories were therefore ranked purely based on the vector transformation, as illustrated in Section 4.1.2.

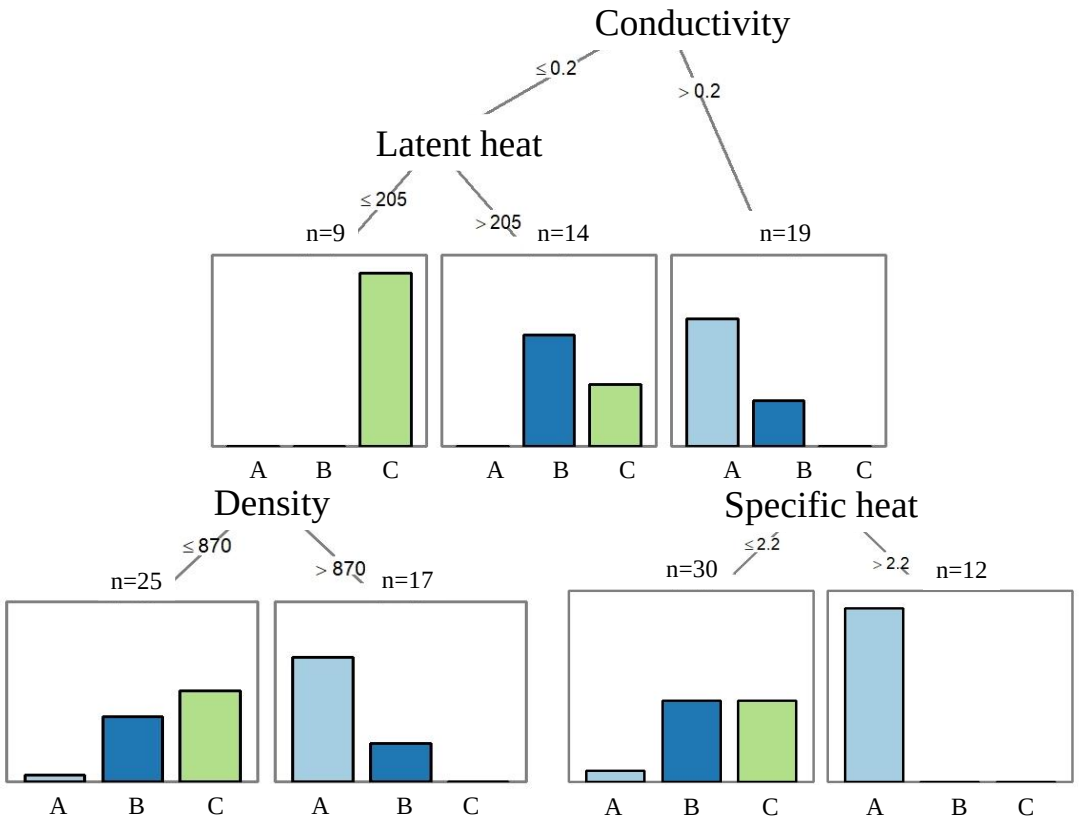

a) Cooling Storage

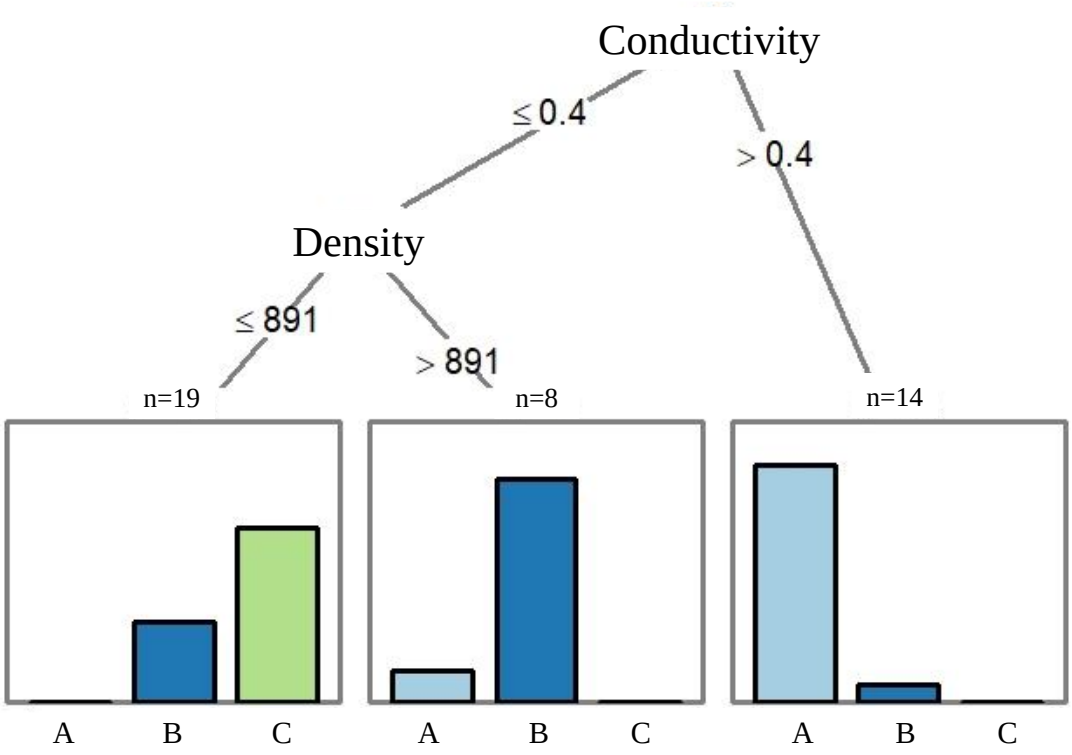

b) Building envelope application (Space cooling)

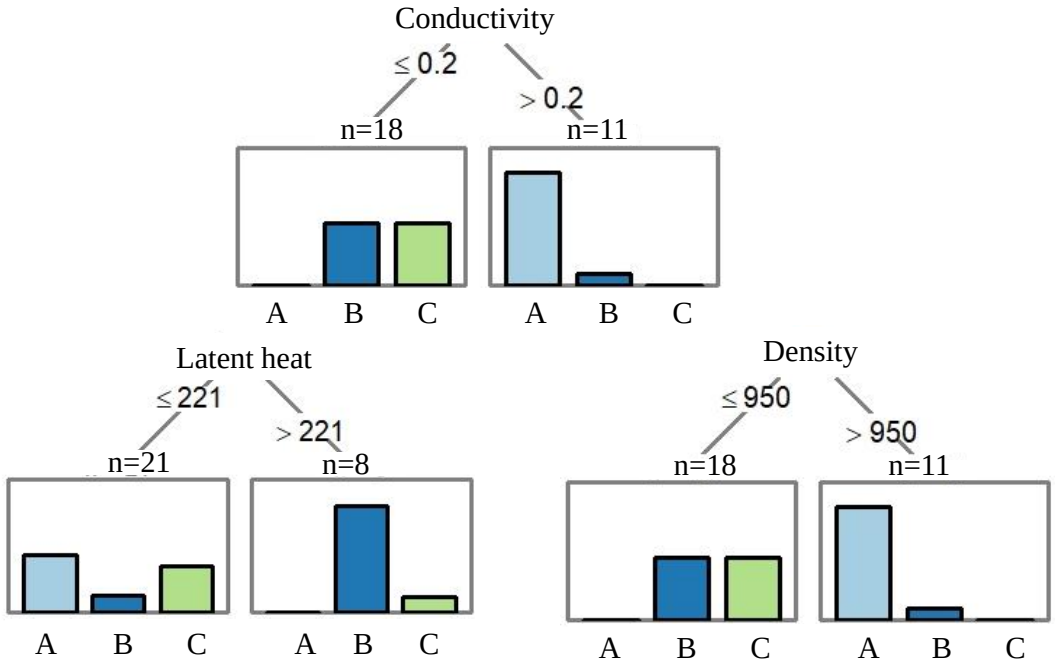

c) Heat Storage

Fig. 4.7 Application-specific CIT models for performance-based categorization of the PCMs, where A represented the best performance and C represented the relatively lower performance.

Collectively, the results presented in this section highlighted the feasibility of using the developed method to select a near-optimal PCM from a list of PCMs for a specific application. The results achieved from the data analytics can provide more details related to the PCM selection process. However, the weight assignment process is highly dependent on the decision-maker, which must be supported with strong domain knowledge.

4.2.3 Results verification using the simulation exercises

4.2.3.1 Description of the case study building

To verify the effectiveness of the results obtained from the above ranking, a simulation exercise using a Transient System Simulation Tool (TRNSYS) was carried out for a TES system integrated with an HVAC system implemented in a Solar Decathlon house (Fig. 4.8) with a total area of 92 m^2. Two PCMs from the cooling storage category of Table 4.6 were selected, and each PCM was separately used to provide energy flexibility to the HVAC system under the same working conditions. In this analysis, as the system was designed to supply chilled water at the temperature of 10 ^oC, the PCMs were hence selected based on this temperature requirement. Therefore, PCM C10 and A10, whose melting temperatures are 10 ^oC were selected and used in the simulation. The purpose of the simulation exercises was just to demonstrate whether the simulation results were consistent with the ranking results of the two PCMs selected. The top-ranked PCM in the cooling storage category was E0, whose melting temperature is 0 ^oC, which cannot be integrated into the heat pump system used in the simulation to provide chilled water. The HVAC system consists of an air source heat pump with a nominal cooling capacity of 6.35 kW to deal with the building sensible load, a dehumidification heat pump to deal with the building latent load, an enthalpy recovery ventilator to recover waste heat, fan coil units to handle air circulation, and two identical thermal energy storage tanks for handling building thermal load during desired period. TRNSYS simulation system developed to achieve the desired outcomes and generate data for verification of the strategy is shown in Fig. 4.9. A summary of the main HVAC system components is provided below:

- A commercial heat pump desiccant unit was used as the dehumidification device in this HVAC system. It consisted of two desiccant-coated heat

exchangers, one served as an evaporator, while the other as a condenser. It functioned as an evaporator during the air dehumidification process, allowing the adsorption heat to be removed. Because moisture can be trapped efficiently on the desiccant material at lower temperatures, moisture is hence more effectively trapped because of achieving low temperature at the evaporator, resulting in better performance. When the desiccant-coated heat exchanger serves as a condenser, the desiccant can then be regenerated using the released heat from the condenser. Integrating the dehumidification heat pump into the HVAC system allows temperature and humidity control to be decoupled. As the dehumidification heat pump covers latent thermal load, the main heat pump was only used to handle the sensible load of the building. Consequently, the chilled water supply temperature can be improved since the heat pump of the HVAC system only needs to handle the sensible cooling load. Hence, considerable improvement in the COP of the heat pump can be achieved.

- An enthalpy recovery ventilator (ERV) system tends to reduce the thermal load introduced by the fresh air in heating or cooling seasons. This system can recover both the sensible and latent heat from the exhaust air and exchange the recovered heat with fresh air to improve the overall performance of the HVAC system. ERV uses thin film elements for exchanging humidity and temperature. The use of thin film technology helps reduce the resistance of moisture exchange and thus improves the overall performance.

- A water-based TES system filled with PCM was coupled with the HVAC system. These systems tend to be more efficient than that of air-based storage systems. This system can effectively provide peak load-shifting in order to support power grid safety while reducing the operating costs of HVAC systems. Using the PCM-based thermal energy storage units, the coolness generated by the heat pump can be stored during the off-peak demand hours (usually night-time) with low energy prices. It can then be used for air-conditioning during the peak demand hours when the power prices are high. Furthermore, coolness charging during the night time can result in a higher Coefficient of performance (COP) for the chiller due to the lower ambient

temperatures at night time. Table 4.7 summarizes the details of the TES system used in this chapter. Fig. 4.10 illustrates the heat pump and PCM TES system implemented in this building. The PCM tanks were modeled as per the mathematical model developed by Lin et al (2020).

Fig. 4.8 Picture of the building.

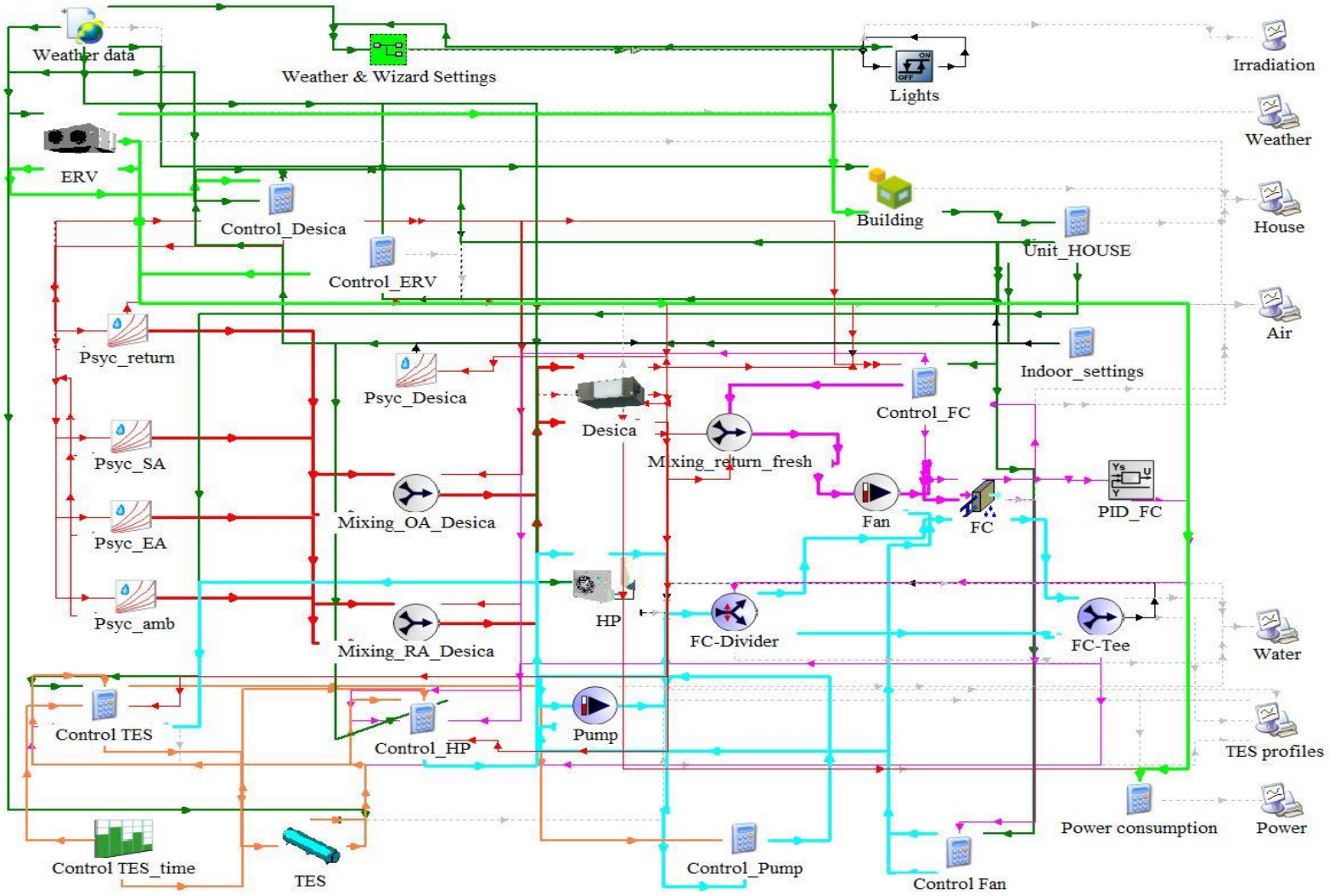

Fig. 4.9 TRNSYS simulation model.

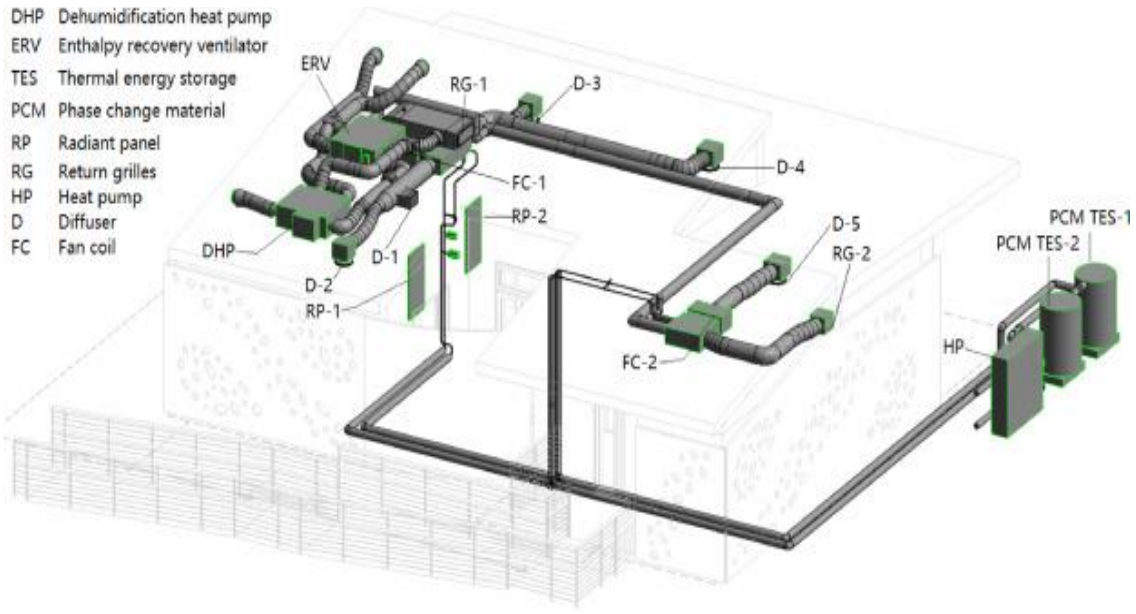

a) HVAC system implemented in the house

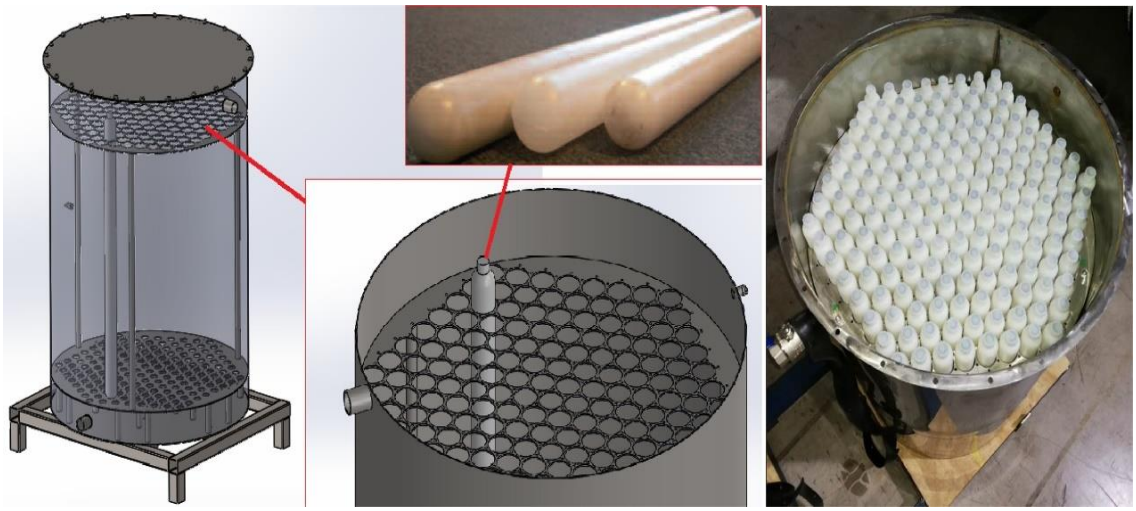

b) TES system with PCM-filled tubes

Fig. 4.10 Heat pump and TES system implemented in the building (Lin et al. 2020).

Table 4.7 Details of the parameters used in the simulation.

Parameter	Value
Nominal storage capacity (kWh)	33.5
Total number of PCM tubes	338
Height of single TES tank (m)	1.2
Diameter of single TES tank (m)	0.829
Height of each PCM tube (m)	1
Diameter of the PCM tube (m)	0.045
Ratio of the distance between PCM tubes and diameter of PCM tubes	1.167
Room temperature setpoint (^{0}C)	24
Relative humidity (%)	50
Occupancy	2 (all the time)

The main assumptions used in the simulation are as follows.

- The house was considered to be occupied all the time with two occupants, and the HVAC system was therefore operated all the time.
- As the dehumidification heat pump was used to remove the latent load of the building, the air-source heat pump was just used to cover the sensible load and charge the TES system during off-peak demand hours (7:30 PM to 9:30 AM of the next day).
- The TES system was used to cover the sensible load during the peak demand hours (9:30 AM to 7:30 PM), and it was designed with a capacity to meet the maximum sensible load during the peak demand hours.
- The unit cost of electricity during off-peak demand hours was 0.14 USD/kWh, whereas it was 2.5 times higher than that of off-peak demand hours during peak demand hours.
- The supply air temperature was set at 16 ^{o}C.
- The charging temperature of the TES was set at 5 ^{o}C, whereas during inflexible operation (i.e. without using the TES for comparison), the heat pump setpoint was set at 10 ^{o}C.

4.2.3.2 Simulation results

Three separate simulation exercises were performed, including two exercises with flexible operation using the two different PCMs to shift sensible load to the TES system during peak demand hours and one with inflexible operation without using

TES. The simulation was carried out for a typical summer day under the weather conditions of Dubai, as this house was designed for this climate in order to participate in the Middle East 2018 Solar Decathlon competition. The occupancy percentage in Fig. 4.11a presents the presence of each occupant in different rooms at different times. For instance, from 00:00 to 07:00, shaded regions with two different colors and each color covering 50% of the region for the bedroom-1 and bedroom-2 indicates that 50% of the occupants i.e. one occupant, was in bedroom-1 and the rest of the 50% occupants were in the bedroom-2. Similarly, a single color covering 100% of the region from 07:00 to 09:00 indicates that 100% of the occupants i.e. two occupants, were in the kitchen and dining area. Based on this occupancy schedule, sensible and latent thermal load added to the building by occupants and appliances were calculated, as shown in Fig. 4.11b and Fig. 4.11c, respectively. The kitchen and dining area added maximum thermal load to the building because of the operation of cooking appliances.

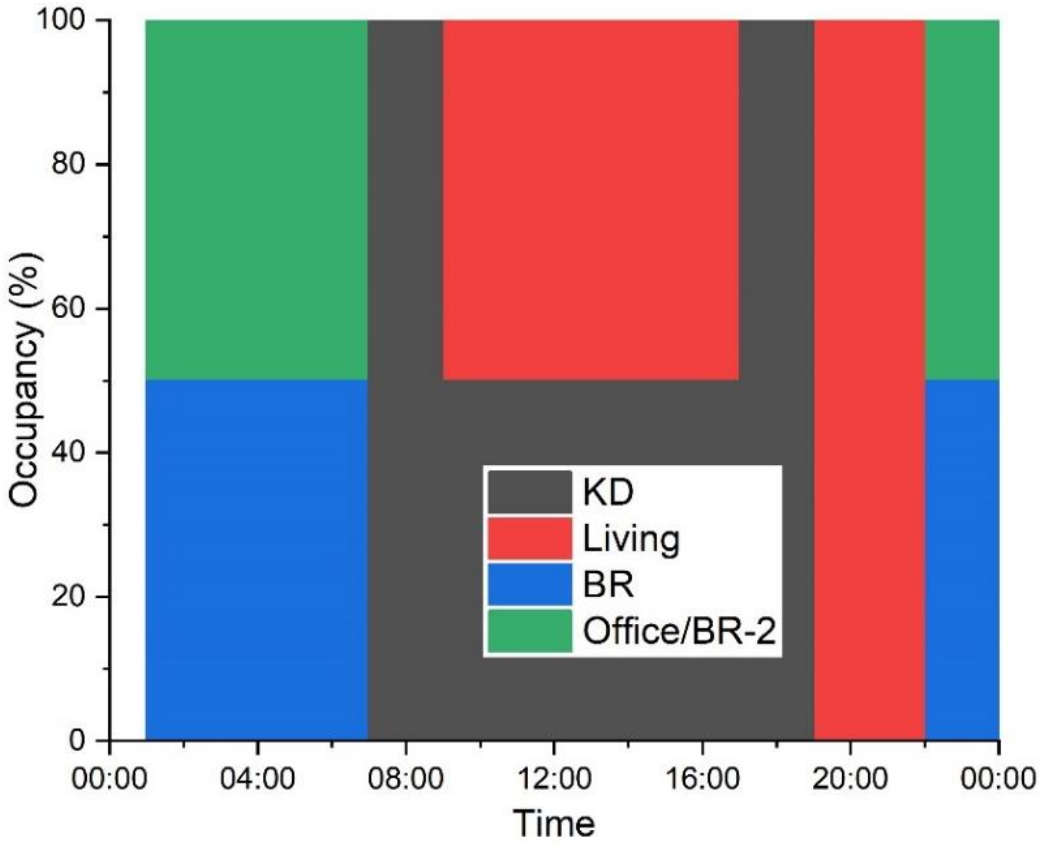

a) Occupancy schedule

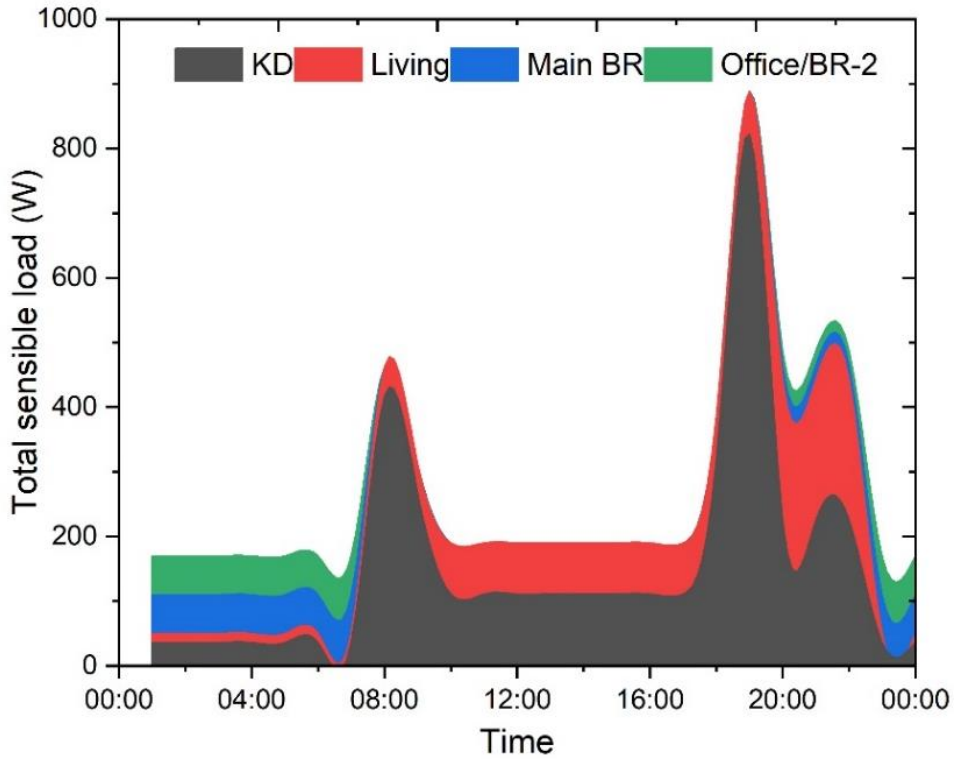

b) Sensible load

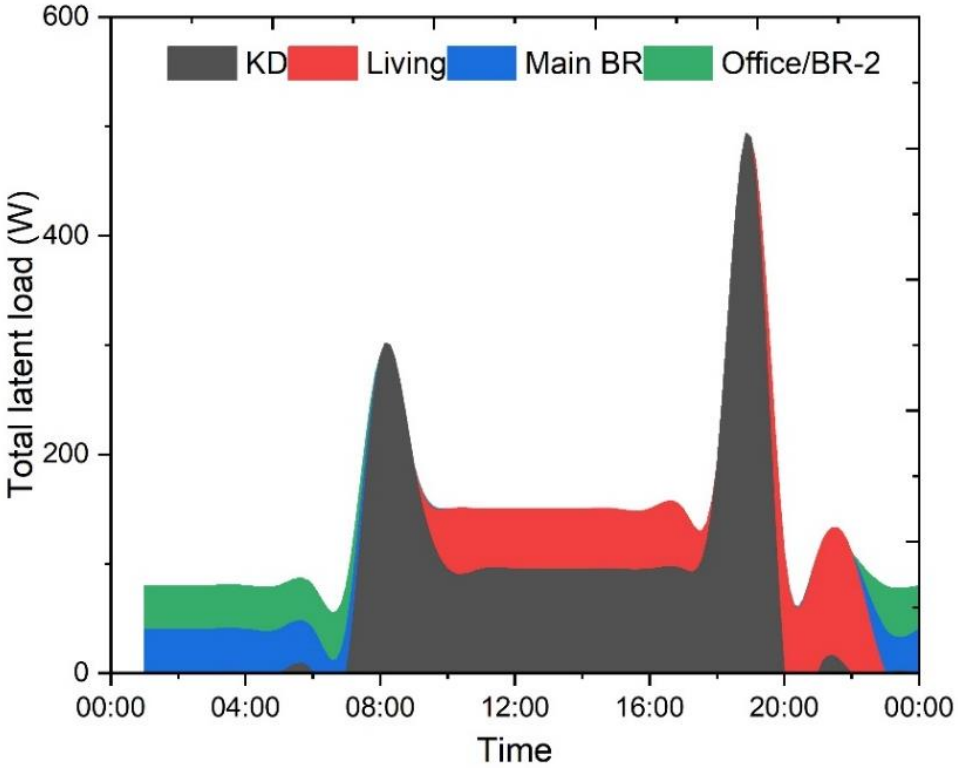

c) Latent load

Fig. 4.11 Loads added to the built environment as per occupant activities inside the building [KD: Kitchen and dining, BR: Bedroom].

The simulation for PCM A10 and PCM C10 was performed separately by considering the same volume of each PCM in the tubes. The energy consumption data of the HVAC system was used to calculate the flexibility potential of the HVAC system in terms of cost savings and peak-energy reduction/shifting using Eq. (4.11) and Eq. (4.12), respectively. A flexibility evaluation tool developed through the International Energy Agency Annex 67 project (Jensen et al. 2017) was used to generate Fig. 4.12 and Fig. 4.13. In this analysis, flexibility was considered as the ability of the HVAC system to shift its load to the off-peak demand period without disrupting the comfort of the occupants and thus reducing the peak demand hours energy consumption, and overall operating cost.

$$FP_C(\%) = \text{Max}\left[\left(1 - \left(\frac{\int_{t_{sop}}^{t_{eop}} (P_{flex} \times C)\, dt + \int_{t_{sp}}^{t_{ep}} (P_{flex} \times C)\, dt}{\int_{t_{sop}}^{t_{eop}} (P_{inflex} \times C)\, dt + \int_{t_{sp}}^{t_{ep}} (P_{inflex} \times C)\, dt}\right)\right), 0\right] \times 100 \quad (4.11)$$

$$FP_E(\%) = \text{Max}\left[\left(1 - \left(\frac{\int_{t_{sp}}^{t_{ep}} (P_{flex})\, dt}{\int_{t_{sp}}^{t_{ep}} (P_{inflex})\, dt}\right)\right), 0\right] \times 100 \quad (4.12)$$

where C, and P_{flex} and P_{inflex} represent the cost, and power consumption with and without the flexibility plan at time t, respectively, E represents energy, and the subscripts s and e respectively represent the start and end of the off-peak (op) and peak (p) demand periods.

The cost savings and the energy consumption of the HVAC system with and without integration of PCM A10-based TES system are illustrated in Fig. 4.12. The results showed that the use of PCM A10-based TES system can respectively provide 27.5% and 73% flexibility in terms of cost savings and peak-energy reduction to the HVAC system. The energy consumption of the HVAC system during peak demand hours was due to the operation of the dehumidification heat pump, pumps, fans, and ERV.

The results of using the PCM C10 are presented in Fig. 4.13. PCM C10 proved to be effective in providing 37.1% and 73% flexibility to the HVAC system in terms of cost savings and peak energy reduction, respectively. The performance of PCM C10 was around 35% better than that of PCM A10. This result also verified the effectiveness

of the ranking strategy, as PCM A10 was the lower-ranked (Rank 29) PCM as compared to PCM C10 (Rank 12) in Table 4.6.

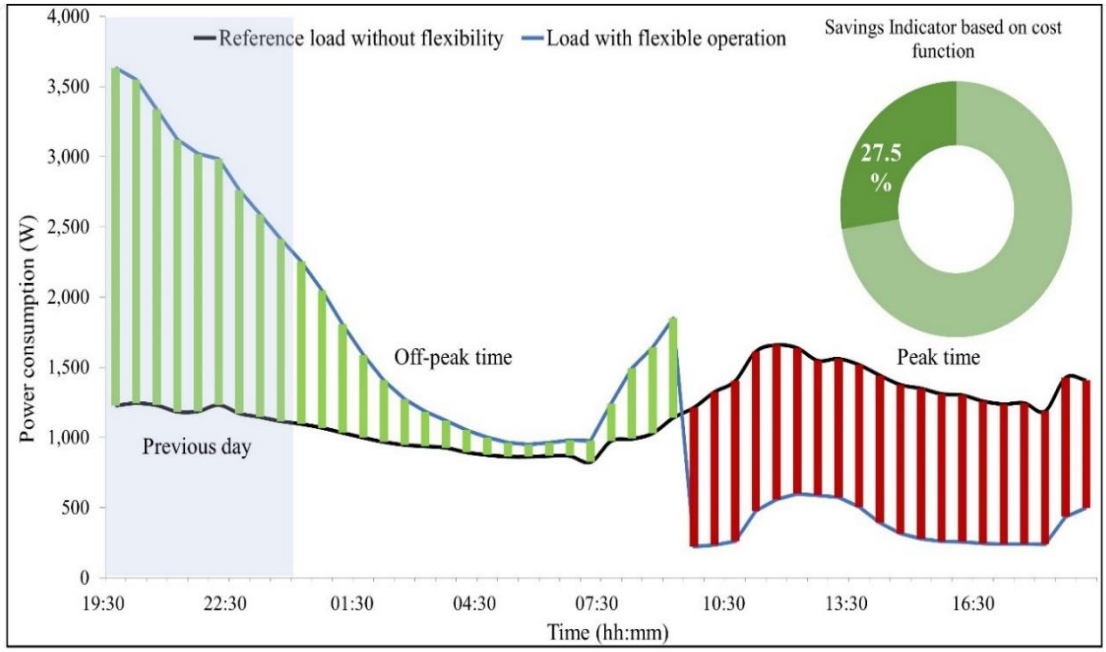

Fig. 4.12 Cost savings and power consumption profiles of the HVAC system with and without integration of PCM A10-based TES system.

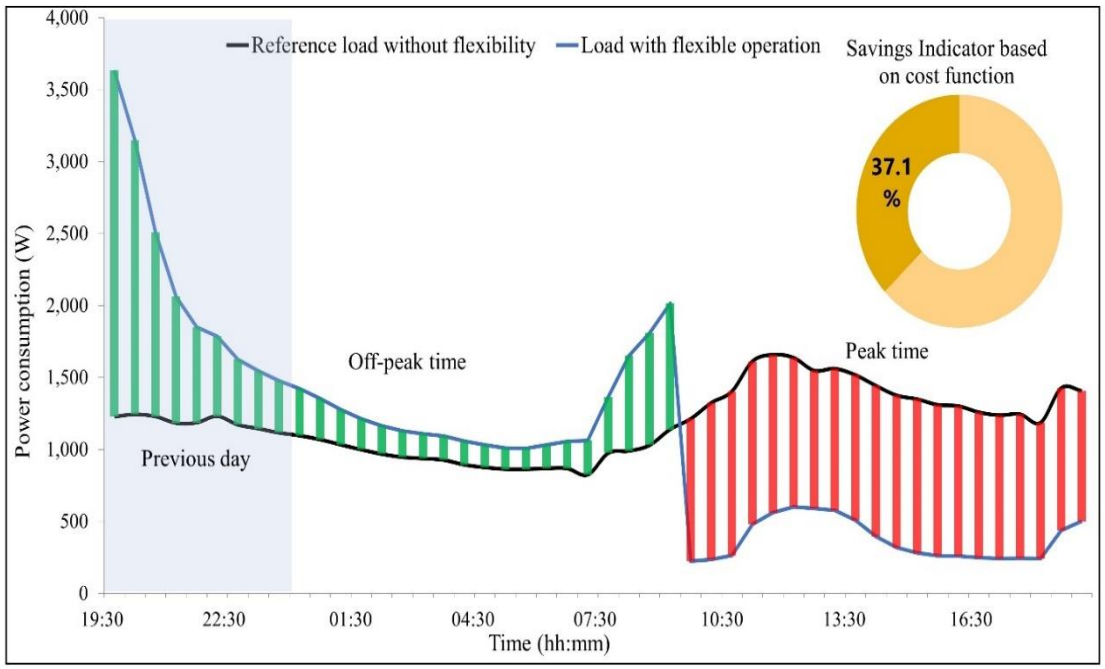

Fig. 4.13 Cost savings and power consumption profiles of the HVAC system with and without integration of PCM C10-based TES system.

Overall, the method developed proved to be effective to rank and select near-optimal PCMs for thermal energy storage in building applications. Further savings can also be achieved, and the rebound effect can be avoided, as observed in Fig. 4.12 and Fig. 4.13 from approximately 7:00 AM to 9:30 AM, and after 7:30 PM, if an optimum control strategy can be used to effectively distribute the charging of TES throughout the night. However, as per the scope of this study, the optimum control strategy was not considered in the analysis.

4.3 Case study II: Selection of a near-optimal PCM for a TES system coupled with a ground source heat pump system

The performance of the proposed method was further validated using another case study, in which the cost of the PCMs was considered along with several other qualitative and quantitative characteristics. Eight PCMs reported in a previous study (Yang et al. 2018) for a TES system integrated with a ground source heat pump system were used for ranking purposes. The quantitative and qualitative characteristics of the PCMs are illustrated in Table 4.8. The numeric values of the qualitative characteristics were assigned using the strategy described in Section 4.1.3 and by considering the same intensity of importance as described in (Yang et al. 2018). The weights were assigned using the method described in Section 4.1.4, and the results from the model were compared with that from (Yang et al. 2018). The CI value for the weight assignment was 0.048. The results showed that M6 was the top-performing PCM, and the ranking results were consistent with that reported in (Yang et al. 2018).

Table 4.8 List of the PCMs and their characteristics with relevant weights and ranks.

PCM	$T_{p.c}$ (°C)	Q_L (kJ/kg)	k (W/m.K)	ρ (kg/m^3)	c_p (kJ/kg.K)	C (RMB/m^3)	V	p	ƨ	ϕ	ϒ	ŧ	Ƒ	Rank
M1	67.9	242	0.2	808	2.5	4,307	0.6	0.8	0.8	0.8	0.8	0.9	0.3	7
M2	69.4	266	0.2	809	2.5	4,307	0.6	0.8	0.8	0.8	0.8	0.9	0.3	5
M3	71.4	256	0.2	810	2.5	4,307	0.6	0.8	0.8	0.8	0.8	0.9	0.3	6
M4	75.9	269	0.2	811	2.5	4,307	0.6	0.8	0.8	0.8	0.8	0.9	0.3	4
M5	70.9	210.8	0.172	848	1.9	3,302	0.6	0.7	0.8	0.8	0.8	0.9	0.3	8
M6	***78***	***280***	***1.26***	***2180***	***1.9***	***4,039***	***0.7***	***0.7***	***0.2***	***0.3***	***0.3***	***0.3***	***0.7***	***1***

PCM	$T_{p.c}$ (°C)	Q_L (kJ/kg)	k (W/m.K)	ρ (kg/m^3)	c_p (kJ/kg.K)	C (RMB/m^3)	V	p	ƨ	ϕ	ϒ	ŧ	Ƒ	Rank
M7	72	180	0.7	1713	2.6	6,872	0.7	0.7	0.3	0.3	0.3	0.3	0.7	3
M8	76	218	0.85	1438	1.9	8,145	0.7	0.7	0.5	0.5	0.5	0.5	0.6	2
Weights														
	0.087	0.203	0.203	0.203	0.087	0.087	0.015	0.024	0.015	0.024	0.015	0.015	0.024	

4.4 Summary

A strategy was introduced for performance-based ranking and selection of near-optimal PCMs for thermal energy storage in building applications, which included the development of a rational WPM-based ranking model for ranking of PCMs, conversion of qualitative characteristics into quantitative factors, and the introduction of a process for handling multiple PCM characteristics for weight assignment. For weight assignment, the AHP method was used, and three clusters were formed by considering the mutuality of PCM properties. Because of using the clustering technique, AHP pair-wise matrix was reduced from a 20 × 20 matrix to an 8 × 8 matrix. The performance of the method developed was tested and evaluated through two case studies. A sample of 134 commercial PCMs with melting temperatures ranging from −7 °C to 44 °C was selected in the first case study. The ranking results achieved using the developed model were further evaluated using data analytic techniques. It was shown that the top-ranked PCMs for cooling storage applications had a density > 870 (kg/m^3), thermal conductivity > 0.2 (W/m.K), and specific heat capacity > 2.2 (kJ/kg.K), while those for building envelope applications (space cooling) had thermal conductivity > 0.4 (W/m.K), and for heat storage applications had a thermal conductivity > 0.2 (W/m.K) and a density > 950 (kg/m^3). To verify the effectiveness of the developed method, a house integrated with an HVAC system, including a TES system, was simulated. Two different PCMs were selected from the cooling application list and used for HVAC load shifting during the peak demand hours. The simulation results were in line with the ranking results, and the better-ranked PCM provided 35 % more cost-based energy flexibility compared with that of the lower-ranked PCM. Overall, both PCMs proved to be effective in reducing energy

costs and peak-demand hours' electricity consumption of the HVAC system. 73% of the peak energy consumption was shifted to the off-peak demand hours using the TES system. In the second case study, a near-optimal PCM was selected from a list of eight PCMs based on several qualitative and quantitative characteristics, including the cost of PCMs, for a TES system integrated with a ground source heat pump system. The results were verified by comparing the results with a pre-published study with the same data set and the same system. It also proved the effectiveness of the method developed. However, one of the limitations relating to the implementation of this method is the subjectivity of the weight assignment process. Hence, a weight determined for a specific characteristic of the PCMs for one application may not be applicable to other applications. The method could be further tested using more PCMs and PCMs for other applications.

Chapter 5 A framework to formulate and aggregate performance indicators to quantify building energy flexibility

The literature review in Chapter 2 highlighted the importance of energy flexibility indicators (EFIs) and quantification methods in evaluating and improving the energy flexibility of buildings and building energy systems. It was emphasized that evaluation of energy flexibility offered by different building energy flexible sources is essential to determining and selecting cost-effective energy flexible sources for increased energy flexibility. Moreover, it was identified that the current literature lacks the development of a framework that can lead to the development of EFIs and an overall building-level aggregated quantification function that can consider the interactions between different stakeholders through the interlinking of different flexibility services and performance factors. Performance factors are important to estimate the footprint of flexible operation and provide information about systems' temporal performance. The lack of such a framework and the unavailability of an aggregated energy flexibility quantification function hinders a detailed understanding of the overall flexibility potential of buildings and building energy systems. This chapter addresses the current research gaps by introducing a systematic approach to developing EFIs by considering the penalties introduced by service providers, performance factors linked with flexibility services, and output and controlled variables of the participating systems. An Aggregated energy flexibility potential (AEFP) function was developed using the Multicriteria decision analysis (MCDA) method. AEFP can capture the interactions between buildings, power grids, occupants, and building energy systems, and hence, can provide valuable insights into building energy flexibility improvement opportunities.

5.1 Outline of the framework

Fig. 5.1 presents the outline of the framework used to develop and aggregate EFIs to quantify the flexibility potential of buildings and building energy systems. It consists of three main steps. Firstly, a systematic approach to developing EFIs was introduced, which consists of three main sub-steps. The first sub-step is the identification of energy flexible sources as part of building response to the grid needs. In the second sub-step, important characteristics of the energy flexible sources, including output and

controlled variables, performance factors linked with flexibility services such as occupant comfort and temporal performance, and penalty factors on which grid penalties are based, were identified and used to develop EFIs in the last sub-step. In the second step, an MCDA method was used to aggregate different EFIs. A hierarchy of EFIs was generated and used to represent the interactions between the building, building energy systems, and grid by considering the collaboration of different stakeholders, including government, consumers, and aggregators. A Fuzzy analytic hierarchy process (FAHP) was used to assign relative weights to the EFIs. The MCDA approach was then used to develop an inclusive building energy flexibility quantification function. Further details about how to aggregate EFIs are provided in Section 5.3. Lastly, a case study with two different scenarios was designed to respectively evaluate the flexibility potential of a heating, ventilation, and air-conditioning (HVAC) system with integrated thermal energy storage (TES), and a building with integrated photovoltaic (PV) system.

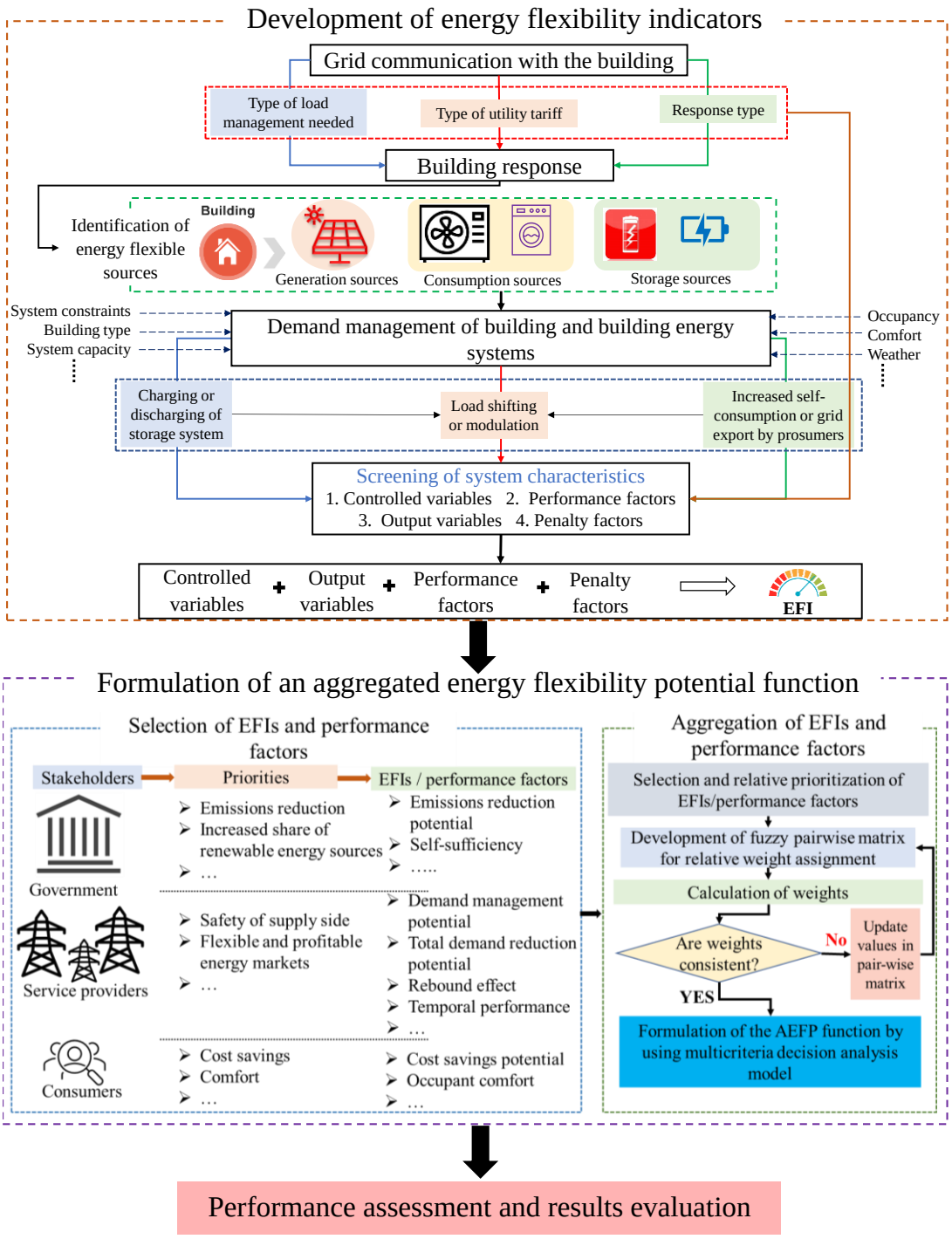

Fig. 5.1 Outline of the framework.

5.2 Selection/development of energy flexibility indicators

A series of EFIs were introduced and used to interlink the hierarchy of different flexibility services offered by building energy sources. The flexibility indicators are formulated based on the process illustrated in Fig. 5.1, in which the energy flexible systems were first identified, and relevant system characteristics were then selected to develop EFIs. Identification of energy flexible systems and their characteristics along with performance factors linked with flexibility services are important to gauge whether a building has enough sources to offer energy flexibility and which source should be called in case of a mismatch between generation and demand. As flexibility services are based on the interactions between the grid, buildings and building energy systems, factors related to these systems were hence identified and used for developing EFIs. For instance, grid penalty factors were selected to indicate the functions on which grid penalties are based. As most grid penalties are imposed in terms of cost that varies as a function of time (demand hours), time and cost were hence selected as the penalty factors. Controlled variables were selected to identify the factors that can be controlled to generate the desirable flexible service. For example, for curtailable loads, the power input to the system can be controlled, and similarly, for shiftable loads, the power input and time of use can be controlled during flexible operation. Performance factors were selected to measure the robustness of flexibility services, i.e. does a flexible source provide flexible services for the desired period without jeopardizing the occupants' comfort? Lastly, the main output variables with respect to the desired outcome of a flexible measure were selected, and one of the leading output variables for most of the building energy sources is power consumption.

5.2.1 Indicators for onsite generation sources

Using the identified variables, an indicator termed "building energy autonomy (γ)" was first introduced, as expressed in Eq. (5.1). This indicator can be used to represent the level of independence of a building from the grid with respect to the cumulative electricity demand of the building at each time step i.

$$\gamma_i = \frac{\mathrm{P}_{gen_i} \pm \mathrm{P}_{st_i}}{\mathrm{P}_{con_i}} \qquad where\ i = 1 \dots n \tag{5.1}$$

where P symbolizes the power, and the subscripts gen, st, and con, respectively represent self-generation, storage, and consumption. For onsite storage, the (-) sign represents that the power generated onsite is used to charge the storage system, whereas the (+) sign means the power is discharged from the storage system.

A value greater than 1 (i. e. $\gamma > 1$) indicates the availability of excess energy to be exported to the grid or supplied to the other buildings in the vicinity at each time step i, which can be calculated using Eq. (5.2) (Salom et al. 2011).

$$\mathrm{P}_{\mathrm{exp}_i} = \left(\mathrm{P}_{gen_{\mathrm{i}}} - \mathrm{P}_{st_i} - \mathrm{P}_{con_i}\right) \tag{5.2}$$

where $\mathrm{P}_{\mathrm{exp}}$ represents the amount of excess power available for export, in which the subscript exp represents export.

The duration of excessive self-power generation ($\mathrm{t}_{\gamma_{\mathrm{exp}}}$), when the energy produced by the onsite generation systems is more than the building demand and charging needs of the storage system, can be calculated using Eq. (5.3).

$$\mathrm{t}_{\gamma_{\mathrm{exp}}} = \sum_{i=1}^{n}(t_i \times f(\gamma)_i) \tag{5.3}$$

where $f(\gamma) = \begin{cases} 1 \; if & \gamma > 1 \\ 0 \; if & \gamma \leq 1 \end{cases}$ and t_i represent discrete time intervals.

The total amount of CO_2 reduced ($\mathrm{CO}_{2_{\downarrow \mathrm{kg}}}$) can be calculated using Eq. (5.4), which is based on the same concept reported by (Huang et al. 2017).

$$\mathrm{CO}_{2_{\downarrow \mathrm{kg}}} = \sum_{i=1}^{n}(\mathrm{P}_{con_i} - \mathrm{P}_{im_{\mathrm{i}}} + \mathrm{P}_{\mathrm{exp}_i}) \times \mathrm{CO}_{2_{\mathrm{grid}}} \tag{5.4}$$

where $\mathrm{CO}_{2_{\mathrm{grid}}}$represents the CO_2 emissions of the local energy network in kg/kWh, and P_{im} represents the amount of total power imported from the grid.

CO_2 reduction potential (%) can be considered a function of total power demand reduction potential (P_{S}), which can be calculated using Eq. (5.5).

$$\mathrm{CO}_{2_{\downarrow_{\%}}} = \mathrm{P}_{\mathrm{S}}(\%) = \left(\frac{\sum_{i=1}^{n}\left(\mathrm{P}_{con_i} - \mathrm{P}_{im_{\mathrm{i}}} + \mathrm{P}_{\mathrm{ex}_i}\right)}{\sum_{i=1}^{n}\mathrm{P}_{con_i}}\right) \times 100\% \tag{5.5}$$

where $\mathrm{CO}_{2_{\downarrow_{\%}}}$represents the CO_2 reduction potential (%), i.e. percent reduction in CO_2 emissions using the onsite generation compared with the electricity imported from the

local grid. For instance, a value of 75% indicates that importing all electricity from the local grid to meet the building load would cause 75% more emissions.

From the perspective of service providers, the most important characteristic of an energy-flexible building is its ability to modulate the required demand in the desired response time during a specific time period of concern. An indicator, as shown in Eq. (5.6), was developed to calculate the flexibility potential of an onsite generation system during peak demand hours, and the temporal performance of the system was also included in this formulation, which can be calculated using Eq. (5.7).

$$\mathrm{F_P}(\%) = \left(\frac{\sum_{i=1}^{n}\left(\mathrm{P}_{con_i} - \mathrm{P}_{im_i} + \mathrm{P}_{ex_i}\right)}{\sum_{i=1}^{n}\mathrm{P}_{con_i}}\right)_{peak} \times 100\% \times \mathrm{t_e} \tag{5.6}$$

$$\mathrm{t_e} = \frac{\text{Total activation time}}{\text{Activation time required}} \tag{5.7}$$

where $\mathrm{t_e}$ is a performance factor that considers the temporal performance of a flexibility provider.

The introduction of $\mathrm{t_e}$ was the originality of Eq. (5.6), as it is important to consider the effective flexible service time to measure how long a flexibility provider is active during the desired demand response period.

Energy cost savings are an important factor for the successful implementation of an energy flexibility plan. An energy flexibility plan is only attractive to consumers if it can result in a reduction in energy costs. Eq. (5.8) can be used to calculate the flexibility potential in terms of energy cost savings.

$$\mathrm{F_C}(\%) = \mathrm{Max}\left[\left(1 - \frac{\sum_{i=1}^{n}\left(\left(\mathrm{P}_{im_i} \times C_{im_i}\right) - \left(\mathrm{P}_{ex_i} \times C_{ex_i}\right)\right)}{\sum_{i=1}^{n}\mathrm{P}_{con_i} \times C_{im_i}}\right) \times 100\%, 0\right] \tag{5.8}$$

where C represents the cost of electricity that varies during different demand hours.

5.2.2 Indicators for building energy systems

EFIs were also formed to estimate the flexibility offered by building energy systems. Eq. (5.9) can be used to calculate the flexibility potential of building energy systems in terms of peak demand reduction/shifting.

$$\mathrm{F_P}(\%) = \left(\frac{\sum_{i=1}^{n}\left(\mathrm{P}_{con_{\mathrm{N}i}} - \mathrm{P}_{con_{\mathrm{F}i}}\right)}{\sum_{i=1}^{n}\mathrm{P}_{con_{\mathrm{N}i}}}\right)_{peak} \times 100\% \times \mathrm{t_e} \tag{5.9}$$

where the subscripts F and N respectively represent the parameters considering the system working under flexible and normal or business-as-usual (baseline) conditions.

In discrete time intervals, the flexibility potential in terms of peak demand reduction/shifting can be calculated using Eq. (5.10).

$$\mathrm{F}_{\mathrm{P}_i}(\%) = \left(\frac{\mathrm{P}_{con_{\mathrm{N}i}} - \mathrm{P}_{con_{\mathrm{F}i}}}{\mathrm{P}_{con_{\mathrm{N}i}}}\right)_{peak} \times 100\% \times \mathrm{t_e} \tag{5.10}$$

The flexibility potential in terms of energy cost savings can be calculated using Eq. (5.11) (Junker et al. 2018).

$$\mathrm{F_C}(\%) = \frac{\sum_{i=1}^{n}\left(\mathrm{P}_{con_{\mathrm{N}i}} - \mathrm{P}_{con_{\mathrm{F}i}}\right)\times C_{im_i}}{\sum_{i=1}^{n}\mathrm{P}_{con_{\mathrm{N}i}}\times C_{im_i}} \times 100\% \tag{5.11}$$

A negative value in Eq. (5.11) indicates an ineffective flexible measure in terms of energy cost savings.

The power demand reduction potential ($\mathrm{P_S}$) of a flexibility measure for consumption or storage sources can be calculated using Eq. (5.12) (Yin et al. 2016). The same expression can be used to calculate the CO_2 reduction potential for energy flexible sources.

$$\mathrm{P_S}(\%) = \mathrm{Max}\left[\left(\frac{\sum_{i=1}^{n}\left(\mathrm{P}_{con_{\mathrm{N}i}} - \mathrm{P}_{con_{\mathrm{F}i}}\right)}{\sum_{i=1}^{n}\mathrm{P}_{con_{\mathrm{N}i}}}\right) \times 100\% \, , 0\right] \tag{5.12}$$

A possible drawback of a flexible measure during peak demand hours can result in a rebound effect that can impact the grid stability. Rebound effect or rebound power is the excessive power demand during the non-flexible or non-penalty time period when power demand considering the flexible measures exceeds that in business as usual case. Eq. (5.13) can be used to calculate the rebound power ($\mathrm{P_{rb}}$) (Kathirgamanathan et al. 2020), whereas Eq. (5.14) can be used to calculate the rebound period ($\mathrm{t_{P_{rb}}}$). Eq. (5.15) can be used to gauge the intensity of rebound power. The calculation of the rebound period and intensity can offer opportunities to smooth the rebound power curve.

As the pre-bound effect is also considered an increase in power consumption because of the pre-emptive measures for a flexibility event, hence Eqs. (5.13)-(5.15) can also be used to calculate the pre-bound effect associated with the up-flexibility actions such as pre-cooling/heating by using HVAC systems.

$$\mathrm{P}_{\mathrm{rb}_i} = \left(\mathrm{Max}\left[\left(\mathrm{P}_{con_{\mathrm{F}_i}} - \mathrm{P}_{con_{\mathrm{N}_i}}\right), 0\right]\right)_{off-peak} \tag{5.13}$$

$$\mathrm{t}_{\mathrm{P}_{\mathrm{rb}}} = \left(\sum_{i=1}^{n}(t_i \times f(\mathrm{P}_{\mathrm{rb}})_i)\right)_{off-peak}, \tag{5.14}$$

where $f(\mathrm{P}_{\mathrm{rb}}) = \begin{cases} 1 \; if & \mathrm{P}_{\mathrm{rb}} > 0 \\ 0 \; if & \mathrm{P}_{\mathrm{rb}} \leq 0 \end{cases}$

$$\mathrm{I}_{\mathrm{rb}}(\%) = \left(\mathrm{Max}\left[\frac{\sum_{i=1}^{n}\left(\mathrm{P}_{con_{F_i}} - \mathrm{P}_{con_{\mathrm{N}_i}}\right)}{\sum_{i=1}^{n}\mathrm{P}_{con_{\mathrm{N}_i}}}, 0\right]\right)_{off-peak} \times 100\% \tag{5.15}$$

In discrete time intervals, the intensity of the rebound can be calculated using Eq. (5.16).

$$\mathrm{I}_{\mathrm{rb}_i}(\%) = \left(\frac{\mathrm{P}_{\mathrm{rb}_i}}{\mathrm{P}_{con_{\mathrm{N}_i}}}\right)_{off-peak} \times 100\% \tag{5.16}$$

5.3 Development of an Aggregated Energy Flexibility Potential function

The success of a building energy flexibility plan depends on the fulfillment of multiple objectives linked with different stakeholders, including government, aggregators, and consumers. Different stakeholders can have different preferences. For instance, energy cost savings can be the leading objective for consumers but not for the government, whose interest is in emissions reduction and increasing the share of renewable energy resources in the energy mix. Aggregators or service providers are primarily concerned about the safety of the supply side. EFIs can gauge the potential of any flexibility service individually but lack effectiveness in simultaneously representing the interactions between different stakeholders and flexibility services. Hence, an inclusive building energy flexibility function that can simultaneously represent the interactions between different stakeholders in terms of distinct flexibility services can better represent the performance of a flexibility plan.

As shown in Fig. 5.1, the main flexibility services and performance factors can be shortlisted based on the interactions between different stakeholders. Hence, several indicators and performance factors were selected, as summarized in Table 5.1. In this chapter, the peak demand management was selected to indicate the interaction of the building with the power grid, where a building can modulate its demand, i.e. increase or decrease as per grid needs. A decrease in demand can be achieved by a decrease in the power input for shiftable or curtailable loads. Similarly, an increase in power demand can be achieved by increasing the power consumption of curtailable loads, activating shiftable loads, or charging the onsite storage. The power demand reduction potential was also selected, which can also provide information about the reduction in carbon emissions. Other flexibility services/effects considered included energy cost savings (consumer priority), occupant comfort (consumer priority), emissions reduction (government priority), temporal performance (aggregator priority), and rebound effect (aggregator priority). Each flexibility indicator can be calculated using the respective EFIs, as formulated in Section 5.2. It is worthwhile to note that in this study several updated EFIs were used. However, the existing EFIs or new EFIs can also be used in this method for demand flexibility analysis.

To aggregate the selected flexibility services/effects, an MCDA model was used. Firstly, each selected energy flexibility service/effect was assigned a priority number, as an example presented in Table 5.1. In this example, the priority numbers were assigned based on grid and building interaction to prioritize the preferences of the aggregators and consumers, as both are considered to be important in successfully implementing a building energy flexibility plan. Peak demand management and energy cost savings were given the top priority. Energy savings, occupant comfort, and temporal performance were given the second priority, whereas emissions reduction and rebound effect were given the lowest priority, as both are the by-products of other flexibility services. Each priority number was assigned a numeric value on a relative scale of importance using the Saaty scale (Saaty 2002). It is noted that the priority can be different and is highly dependent on the objective of an energy flexibility plan.

Table 5.1 Priority number assigned to each attribute.

Sr. #	Flexibility service/effect	Priority #
1	Peak demand management	P1
2	Energy cost savings	P1
3	Total power demand reduction	P2
4	Temporal performance	P2
5	Occupant comfort	P2
6	Emissions reduction	P3
7	Rebound effect	P3

The relative weights were assigned to each EFI using the FAHP-based pair-wise matrix (Table 5.2). Fuzzification was achieved using the geometric mean technique, whereas defuzzification was achieved using the center of area method. The consistency of the matrix was also checked to validate the weight assignment process. The consistency ratio of the matrix was 0.06, which is below 0.1, proving the consistency of the weight assignment process. The weight (ω) of each flexibility indicator was multiplied by its corresponding flexibility indicator.

Table 5.2 Weight assignment using fuzzified AHP pairwise matrix [G.M: Geometric mean].

	P1	**P2**	**P3**	**Fuzzy G.M**	**Fuzzy weights**	**Defuzzification**	**Normalization**
	Membership functions						
P1	1,1,1	2,3,4	3,4,5	1.82, 2.30, 2.71	0.40, 0.62, 0.92	0.64	0.60
P2	1/4 , 1/3, 1/2	1,1,1	2,3,4	0.79, 1, 1.26	0.17, 0.28, 0.44	0.30	0.28
P3	1/5, 1/4, 1/3	1/4, 1/3, 1/2	1,1,1	0.37, 0.44, 0.55	0.08, 0.12, 0.19	0.13	0.12

Lastly, all weighted flexibility indicators were added together and then divided by the sum of all individual weights to formulate an overall building-level EFI, termed Aggregated energy flexibility potential (AEFP) function, as expressed in Eq. (5.17).

$$\mathrm{AEFP} = \left(\frac{\sum_{i=1}^{n} \alpha_{P_i} \times \omega_{P_i}}{W}\right) \tag{5.17}$$

where α is the sum of the EFIs in each priority (P), ω represents the weight obtained using Table 5.2, and W represents the cumulative weight that can be calculated using Eq. (5.18). It is worthwhile to note that in Eq. (5.17), only fraction values should be used, i.e. divide every percentage value by 100, and for normalization purposes, each

EFI/performance factor value should be limited to the maximum value of 1. Moreover, if a lower value of an EFI is desired, the obtained value must then be subtracted from 1, for instance, grid providers desire the lowest intensity of the rebound, hence, obtained value of the intensity of the rebound should be subtracted from 1 and then can be used in Eq. (5.17).

$$W = \sum_{i=1}^{n} \beta_{P_i} \times \omega_{P_i} \quad (5.18)$$

where β represents the number of EFIs/performance factors in each priority.

5.4 Performance test and assessment

The performance of the developed EFIs and quantification function was evaluated via a case study of a Solar Decathlon house under two distinct scenarios, that is, to evaluate the flexibility potential of an HVAC system with integrated TES, and a building with integrated PV system. For both scenarios, the same simulation model was considered, as summarized in Chapter 4. But for scenario II, the TES system was not considered, and a photovoltaic system was integrated with the house. Further details about scenario II are provided in Section 5.4.2.

5.4.1 Scenario I: Evaluating the flexibility potential of an HVAC system with integrated TES

In this scenario, an HVAC system, which consists of a PCM-based TES system, an air-source heat pump, an enthalpy recovery ventilator (ERV), a dehumidification heat pump, and a fan coil unit system was considered to condition the building. The TES system was used to provide cooling during the peak demand hours (9:30 am to 7:30 pm). The air-source heat pump was used to charge the TES system and provide cooling during the off-peak demand hours (7:30 pm to 9:30 am of the next day). The melting temperature of the PCM used was 10 ^{o}C with density, thermal conductivity, specific heat, and latent heat of 1400 kg/m^3, 0.7 W/m.K, 2.85 kJ/kg.K, and 116 kJ/kg, respectively. A detailed summary of the simulation model and components can be found in Section 4.2.3 of Chapter 4.

Firstly, two simulation exercises were performed in TRNSYS for the baseline operation and flexible operation, respectively, and the obtained datasets were used to calculate the performance of different flexibility services using the information presented in Sections 5.2 and 5.3. The simulation period was 24 hours, starting from

7:30 pm and ending at 7:30 pm of the next day, under the weather conditions of Dubai, United Arab Emirates, as this Solar Decathlon house participated in the Middle East Solar Decathlon Competition in 2018. The weather data for the selected test period are shown in Fig. 5.2. Whereas, Fig. 5.3a) and Fig. 5.3b) respectively show the total sensible and latent load in different zones of the buildings, which includes thermal load due to occupants, appliances, infiltration, heat transfer through the building envelope and working air. The HVAC system was used to handle these loads and maintain the indoor conditions at the desired level. An increase in outdoor temperature and radiation level caused a high thermal load inside the building.

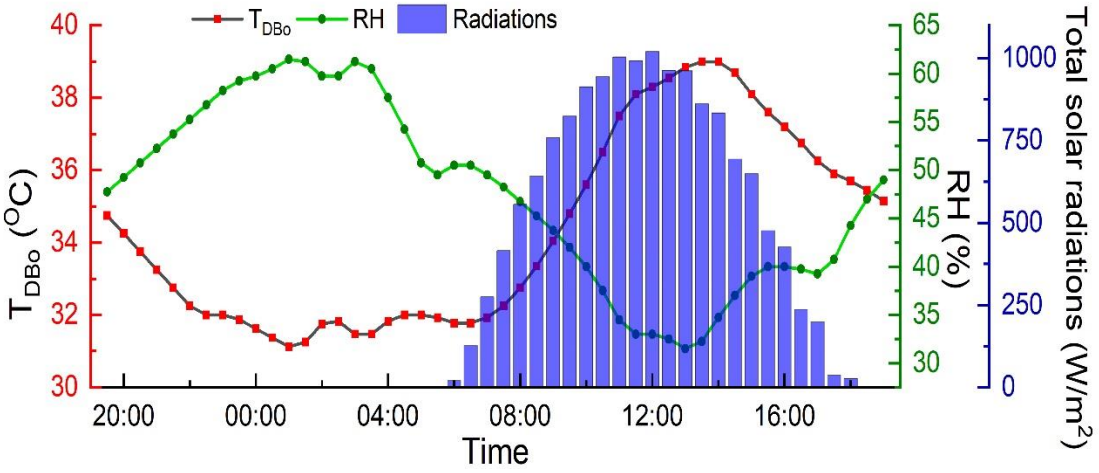

Fig. 5.2 Outdoor conditions [T_{DBo}: Outdoor dry-bulb temperature, RH: Relative humidity, TH_S: Total solar horizontal].

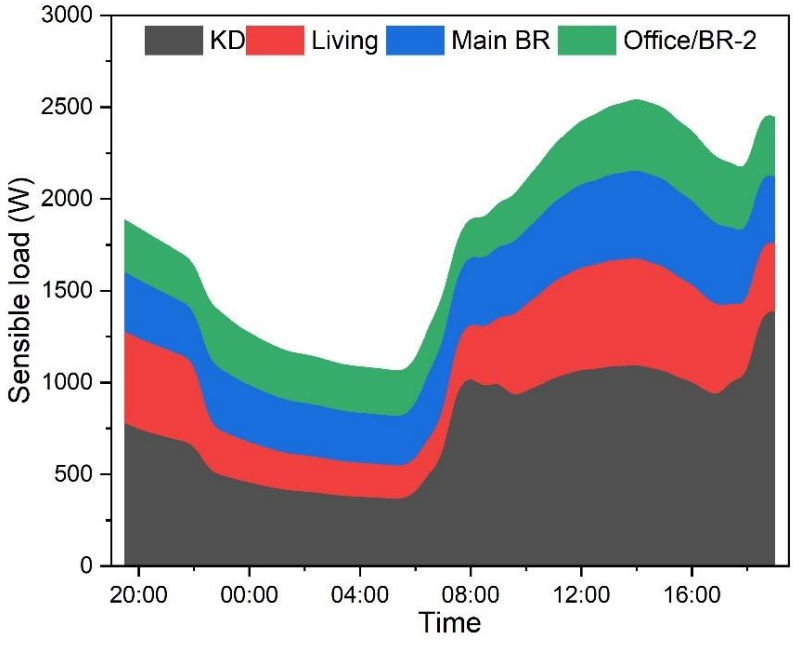

a) Sensible load

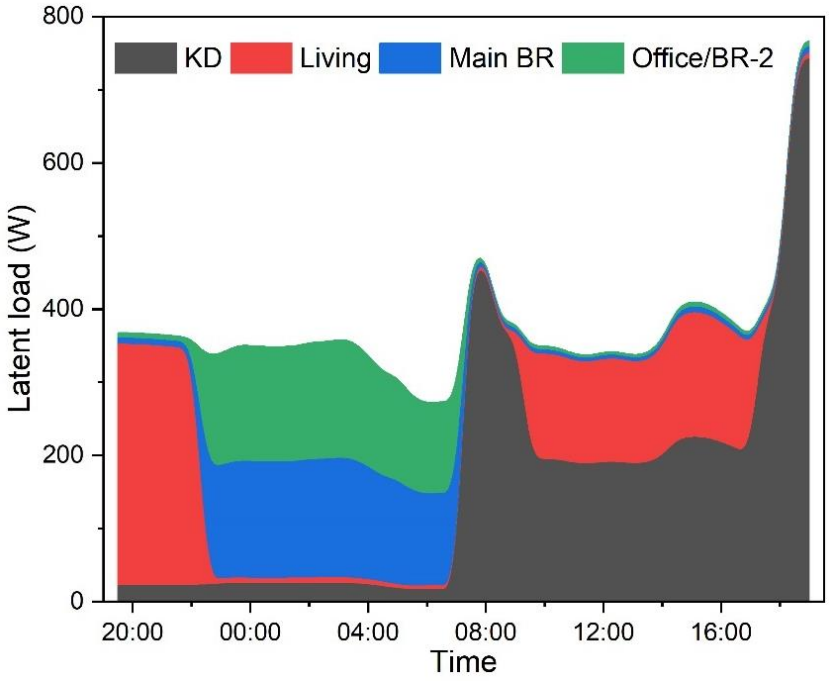

b) Latent load

Fig. 5.3 Indoor thermal load in different zones of the building.

Fig. 5.4 shows the performance of different flexibility indicators in evaluating the flexible performance of the HVAC system with integrated TES. It can be found that by shifting the load to the TES system during peak demand hours, around 56% of the HVAC peak power consumption/demand was reduced. A 32% reduction in the HVAC operational cost was also achieved. It is noted that the operation of the dehumidification heat pump, ERV, fan, and water pump was the main cause of energy consumption of the HVAC system during the peak demand hours. The TES system proved to be effective in providing energy flexibility in terms of peak demand reduction and cost savings. As the HVAC system was assumed completely grid-powered, the overall reduction in power consumption/demand (around 14.5%) resulted in the same percentage reduction in carbon emissions. The intensity of rebound was 24.2%, while 100% temporal performance was achieved, as the TES system was functional throughout the peak demand hours.

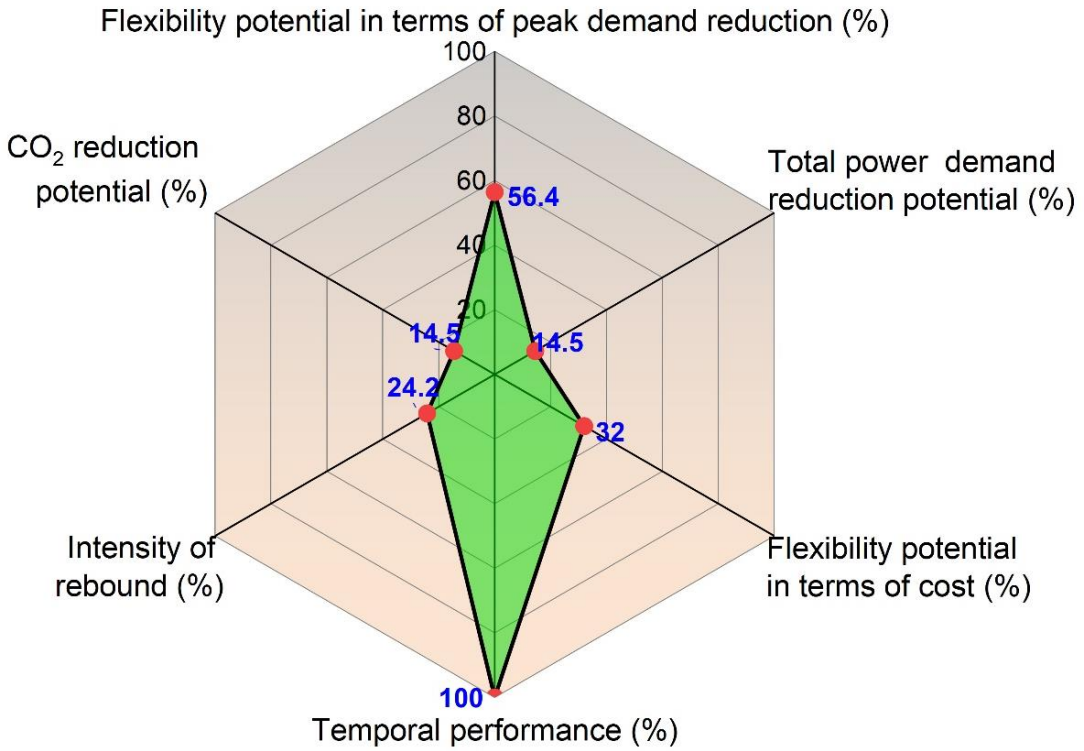

Fig. 5.4 System performance based on different EFIs.

The most important factor in the current study was peak load shifting, which serves two purposes i) to provide stability of the grid by reducing stress on the grid during peak demand hours, and ii) to provide energy cost reduction of the building. Fig. 5.5a) shows the temporal change in the flexibility potential of the HVAC system in terms of power reduction during peak-demand hours. The same values can be considered for calculating the flexibility potential in terms of percent cost reduction during peak-demand hours. The system showed high flexibility potential from 11:00-14:00, which was also the period of high sensible thermal load of the building. Furthermore, an increase in the latent load of the building resulted in a reduced flexibility potential. This trend resulted due to the operation of the dehumidification heat pump in peak-demand hours to handle the latent load of the building. Fig. 5.5b) was plotted to further analyze the impact of sensible and latent load on the energy flexibility of the HVAC system. It was found that an increase in the latent load tends to generate a significant impact on flexibility degradation. The system flexibility was reduced to its minimum value when the latent load reached its maximum value. In addition, energy consumption during normal and flexible periods can also be visualized in Fig. 5.5a),

in which a high rebound can be observed during off-peak demand hours, which was evaluated using Eqs. (5.13)-(5.16).

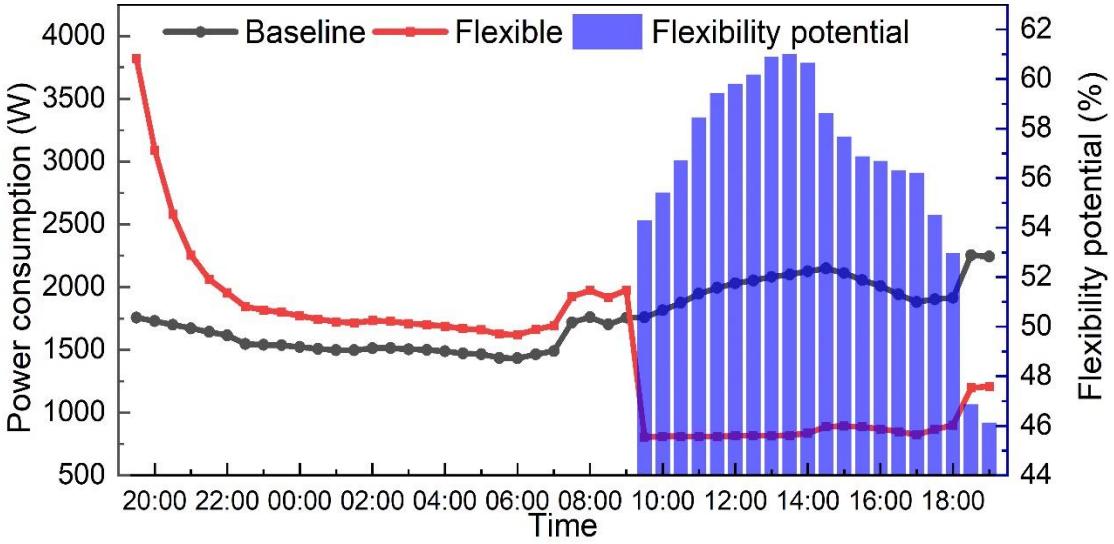

a) Flexibility potential of the system during peak demand hours

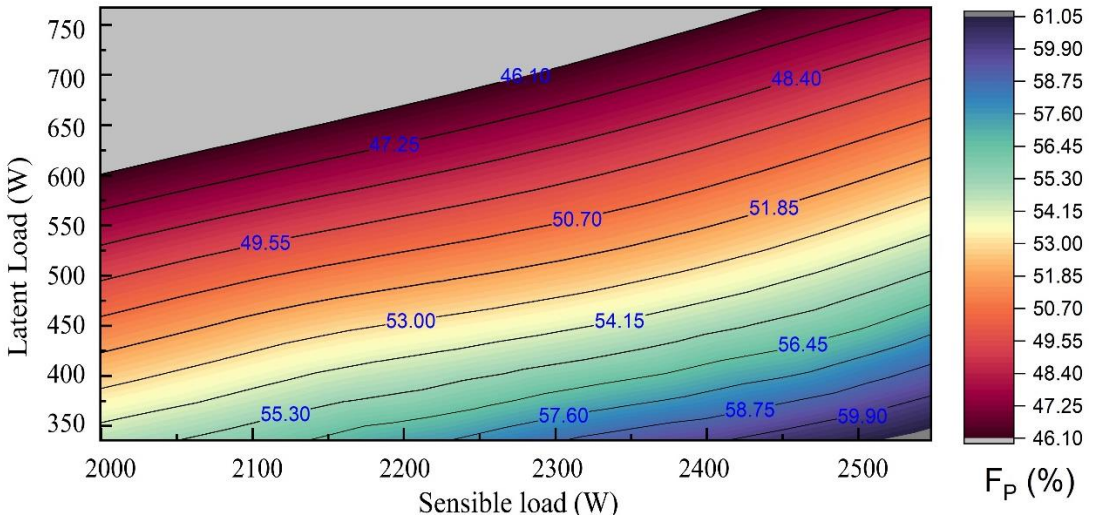

b) Impact of building thermal load on the flexibility of the HVAC system

Fig. 5.5 Flexibility potential and energy profiles of the HAVC system.

A major reason behind the emergence of rebound was the charging operation of the TES system during off-peak demand hours. In the absence of onsite generation, the rebound effect is inevitable but adjustable within the constraints of the system. A high rebound in the first two hours of the off-peak demand hours was recorded (Fig. 5.6) due to the higher discharging state of the TES system. The overall intensity of the rebound was around 24%. As the intensity of rebound is a function of power

consumed by the system, a value obtained for the intensity of rebound at any time shows the same percentage of increase in the cost for operating the system during the off-peak demand hours.

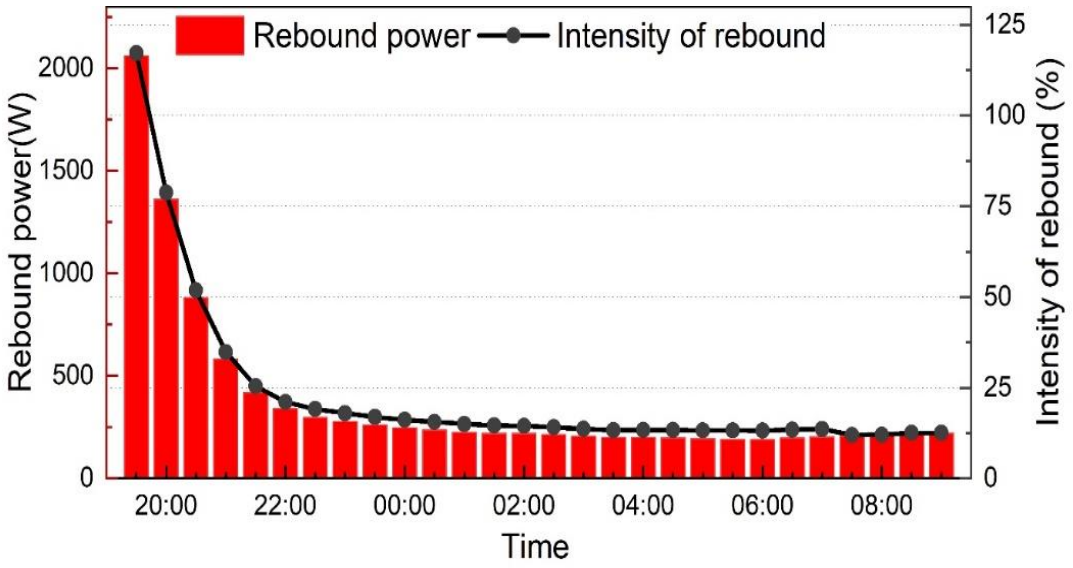

Fig. 5.6 Illustration of rebound power and intensity of rebound.

The Aggregated energy flexibility potential of the HVAC system using the TES system during the peak-demand hours and considering the interactions between stakeholders and different energy flexibility services was also calculated using the AEFP function as presented in Section 5.3. Based on the constraints of the analyzed system, different EFIs were selected, and their values were calculated, as shown in Fig. 5.7. Aggregation of the EFIs was achieved using Eq. (5.17), and the AEFP of the flexibility measure was calculated, which was found to be 0.54 (54%), as presented in Fig. 5.7, in which the 0.54 of the AEFP represents high temporal and comfort performance with a significant reduction in peak energy demand and cost of the HVAC system, but relatively low performance in reducing emissions and overall power demand by shifting the air-source heat pump load to the TES system during the peak demand hours. It is worthwhile to note that in this case study, occupant comfort was given preference to achieve the desired flexibility service without jeopardizing the comfort conditions, and it was maintained using a proportional–integral–derivative (PID) controller to keep the air temperature and relative humidity close to the desirable range.

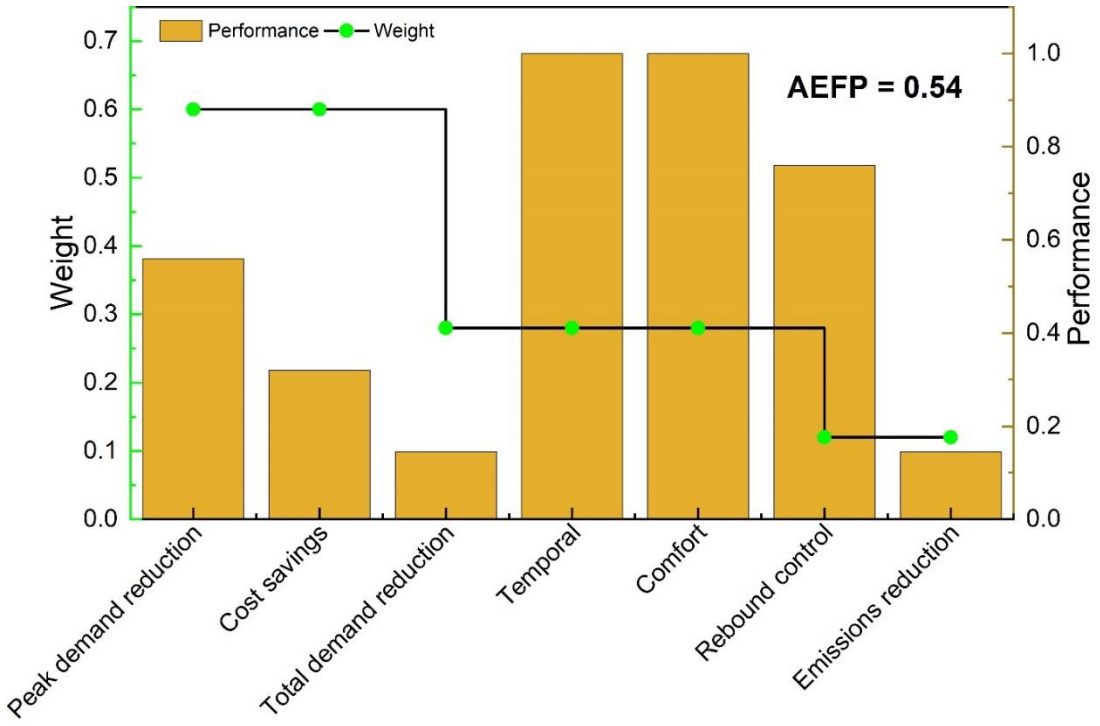

Fig. 5.7 Performance evaluation of different flexibility services and relevant effects on the AEFP.

5.4.2 Scenario II: Evaluating the flexibility of a building with an integrated PV system

In the second scenario, a 5 kW photovoltaic system was integrated with the same building as used in Scenario I. The efficiency of the PV panels was assumed to be constant at 15.3%, and a constant efficiency inverter was used to convert direct current to alternating current with an efficiency of 92%. The effect of onsite generation on enhancing building energy flexibility was analyzed under the same thermal load and working conditions as Scenario I. The operation of the HVAC system was also the same as the baseline operation in Scenario I without considering the TES system. Moreover, the flexibility potential of the whole building was evaluated by considering a single flexibility source only, i.e. onsite generation system.

For this scenario, two simulation exercises were performed, i.e. one for normal conditions without considering the onsite generation system, and the other for the flexible conditions with the consideration of the photovoltaic system. Fig. 5.8a) shows self-generated power and grid power import as well as the power exported to the grid. The PV system reduced the peak demand load significantly, and extra power

generation was exported to the grid. The cost of the exported electricity was assumed to be 0.05 USD/kWh. The negative values in the right-side y-axis of Fig. 5.8a) indicate the power exported to the grid. Power consumption of the building during the period of power export can be calculated by adding these negative values of the exported power to the left-side y-axis values of power production. Eq. (5.1) was used to calculate building energy autonomy (ϒ) that varied throughout the daytime and peaked from 8:00 to around 15:00. A value of ϒ above 1 indicated that onsite generation exceeded the power demand of the building and can potentially export the excessive power to the grid that can be calculated using Eq. (5.2). The building energy autonomy along with the duration of excessive self-power generation can be visualized in Fig. 5.8b), which also shows a high export potential of the building during the peak demand hours.

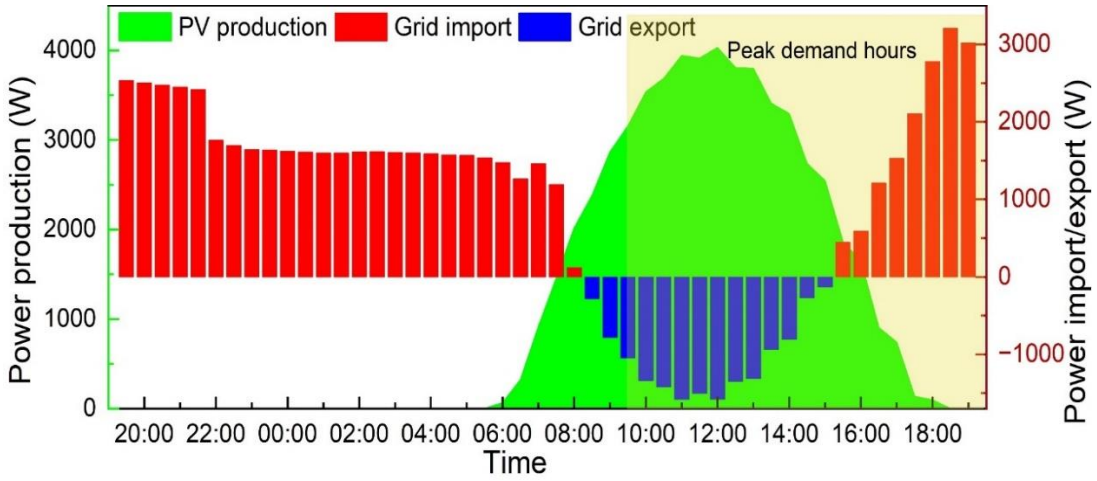

a) Building self-generation potential and grid power import/export

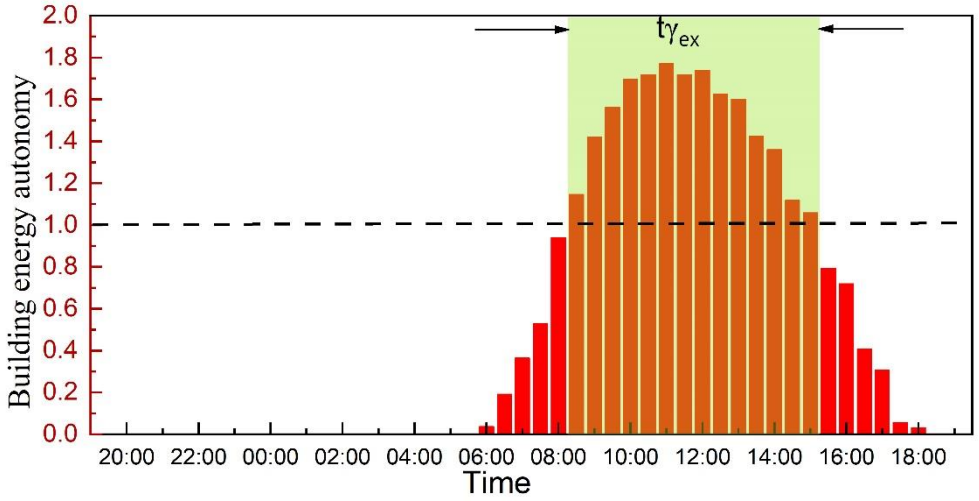

b) Temporal changes in building energy autonomy

Fig. 5.8 Performance of onsite generation system as the energy flexibility source.

The overall performance of this flexible measure was calculated using different EFIs, as shown in Fig. 5.9. The PV system provided a 46% reduction in the overall building carbon emissions, and the same reduction in the overall energy demand of the building was also recorded. Building energy costs were reduced by 54%. Building flexibility potential in terms of the peak demand reduction and the energy cost was 75% and 54%, respectively, proving on-site generation highly effective in enhancing the flexibility potential of the building. PV system also proved to be robust in eliminating rebound effects but lacked little in terms of temporal performance based on the selected demand hours conditions, where they were able to provide flexible services for 80% of the peak demand hours for the given peak demand hours.

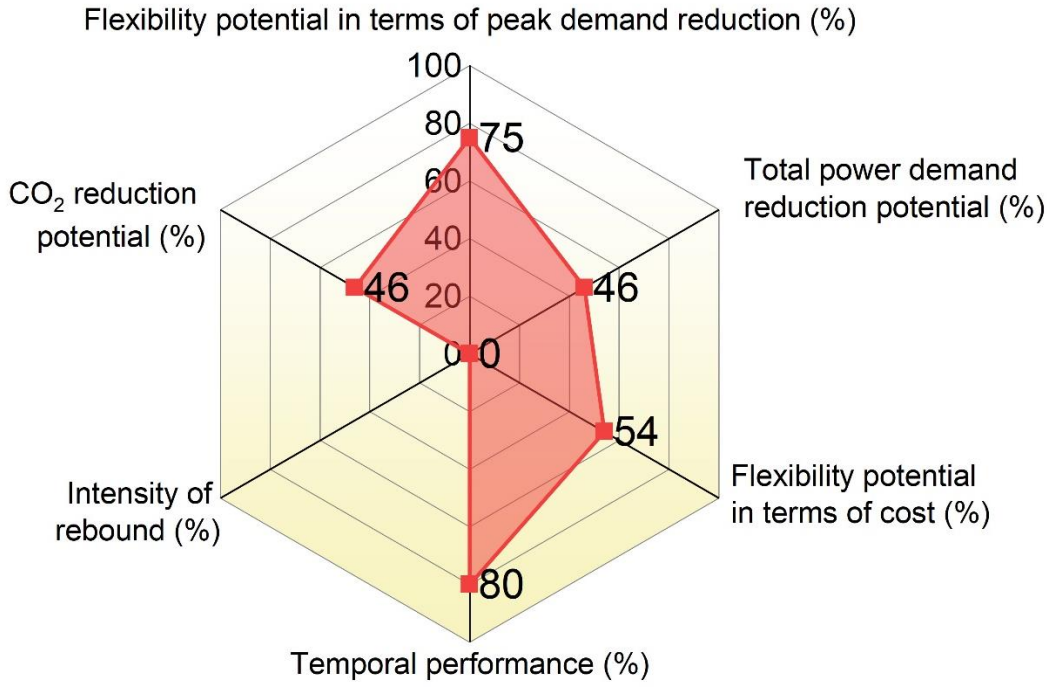

Fig. 5.9 Overview of system performance based on different EFIs.

The Aggregated energy flexibility potential was calculated, as shown in Fig. 5.10, by considering different flexibility services and using the same process as illustrated in Scenario I. The AEFP value was 0.74 (74%). The best performance was observed in terms of peak demand reduction (94%) and rebound effect reduction (100%).

Overall, the impact of the onsite energy generation system was more significant on the flexibility potential of the building in terms of all selected flexible measures. It is worthwhile to note that performance optimization was not achieved in either of these scenarios considered and hence further improvement can be achieved through

appropriate optimization. It is noted that the main purpose of this case study was to illustrate the performance of the developed EFIs and AEFP, and how these indicators can lead to improved performance of the buildings and building energy systems.

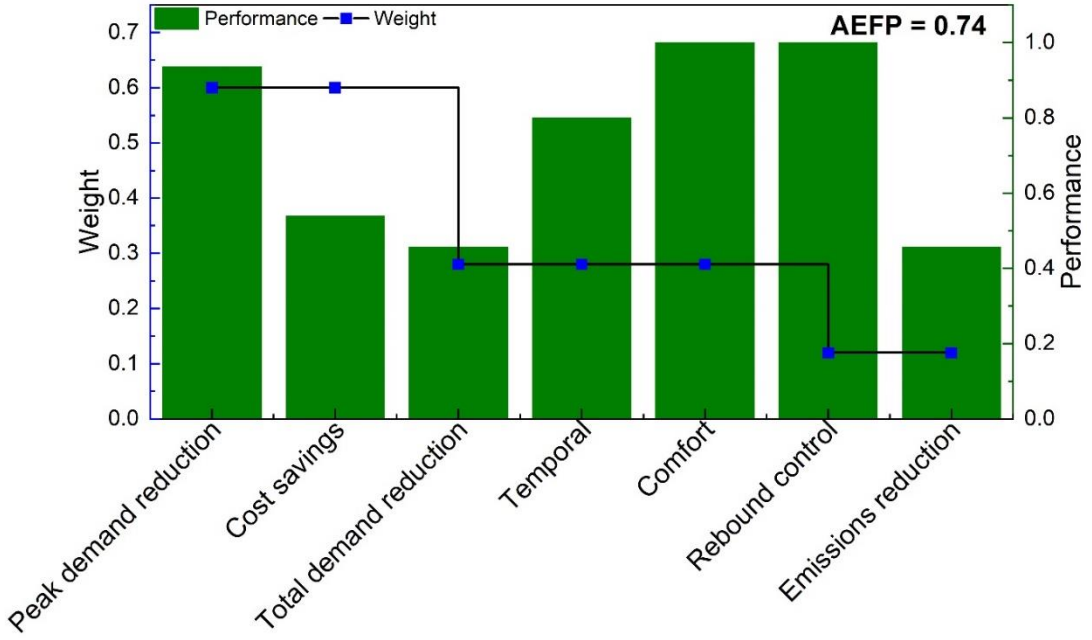

Fig. 5.10 Performance evaluation of different flexibility services and relevant effects.

Both scenarios verified the effectiveness of the developed indicators in evaluating the flexibility potential of buildings and building energy systems. The AEFP function developed proved to be highly effective in evaluating different aspects of energy flexibility by considering the distinct priorities of the stakeholders. The framework introduced to develop the AEFP is generic and flexible, which can be used to include or exclude additional flexibility services and sources. Moreover, it can also be used to compare the performance of different flexibility sources and trace further performance improvement opportunities.

5.5 Summary

A framework to develop and aggregate building EFIs was presented in this chapter, which can be used to quantify the aggregated energy flexibility potential of buildings and building energy systems. An MCDA method was used to develop an inclusive building EFI, which was termed Aggregated energy flexibility potential function. AEFP was developed by aggregating different energy-flexible services and

performance factors based on the interactions between different stakeholders. The developed indicators and AEFP were evaluated by performing a case study with two distinct scenarios, i.e. evaluating the energy flexibility of an HVAC system with integrated thermal energy storage, and a building with an integrated onsite generation system. The HVAC peak energy demand was reduced by 56%, overall energy demand and emissions by 14.5%, and energy cost by 32% using the thermal energy storage system during peak demand hours. The AEFP was found to be 0.54 (54%). The AEFP value for the building with an integrated onsite generation system was 0.74 (74%), and the onsite generation system helped achieve around 94% demand reduction during peak demand hours, a 54% reduction in building energy cost, and a 46% reduction each in carbon emissions and overall power demand of the building. The indicators developed demonstrated a high value in evaluating the flexibility of buildings and building energy systems and offered insights into different performance factors, which can aid in making informed decisions for optimizing energy usage and improving overall system performance. The framework introduced can be used to further develop EFIs, and the method used to develop AEFP has the potential to include more flexible services and factors based on the specific requirements of a particular application.

Chapter 6 Predicting energy flexibility potential and energy consumption of heating, ventilation, and air-conditioning systems with integrated thermal energy storage using an Extreme Gradient Boosting (XGBoost) model

The literature review in Chapter 2 demonstrated the critical role of predicting building energy flexibility and energy consumption to maximize the benefits of demand management programs and improve the resilience of both the demand and supply sides. It was also noted that additional prediction models are needed to accurately forecast the energy flexibility potential of buildings and building energy systems. Furthermore, Chapter 5 highlighted the role of heating, ventilation, and air-conditioning (HVAC) systems with integrated thermal energy storage (TES) in reducing building energy costs, peak loads, and carbon emissions while maintaining occupant comfort. The importance of peak demand reduction for increased grid safety was also emphasized. Additionally, it was found that building thermal load can greatly impact the energy flexibility potential of HVAC systems. This chapter presents the development of a methodology for predicting the energy flexibility potential and energy consumption of building HVAC systems with integrated TES using an Extreme gradient boosting (XGBoost) model-based prediction model. The performance of this strategy was evaluated using four months of simulation data of an HVAC system with an integrated TES system.

6.1 Methodology

6.1.1 Outline of the methodology

Fig. 6.1 shows the methodology developed to predict the energy flexibility and energy consumption of an HVAC system with integrated TES. Building thermal load can also be predicted under varying environmental conditions using the same model. The methodology consists of three main steps, including data acquisition and preparation, prediction model development, and model testing. In the first step, the data of the target (i.e. dependent variables) and independent variables should be measured or collected. Data is then separated into training and testing data sets. Independent variables are used to predict the target variable(s). For instance, flexibility potential

can be characterized as the target variable, and outdoor air temperature and relative humidity, and building thermal load can be used as the independent variables. In the second step, a prediction model is developed, in which the first step is the selection of a forecasting/prediction model and an evaluation metric. Regression is used for forecasting, whereas root mean square error (RMSE) is selected as an evaluation metric. Initially, a higher value of 1000 can be selected as the maximum iteration number in each prediction task, and the model is run based on the XGBoost algorithm. The model should be tested for over- and under-fitting, and an optimized value of the iteration number should be selected with a minimum value of the root mean square error (RMSE) to optimize the computational performance of the model. The model is then re-run based on the optimized value of the iteration number, and the value of each target variable can be predicted separately. In the last step, the performance of the model can be evaluated by performing a case study to predict the energy flexibility and energy consumption of an HVAC system with integrated TES. The predicted and actual data of the target variables can be compared to test the accuracy of the prediction model.

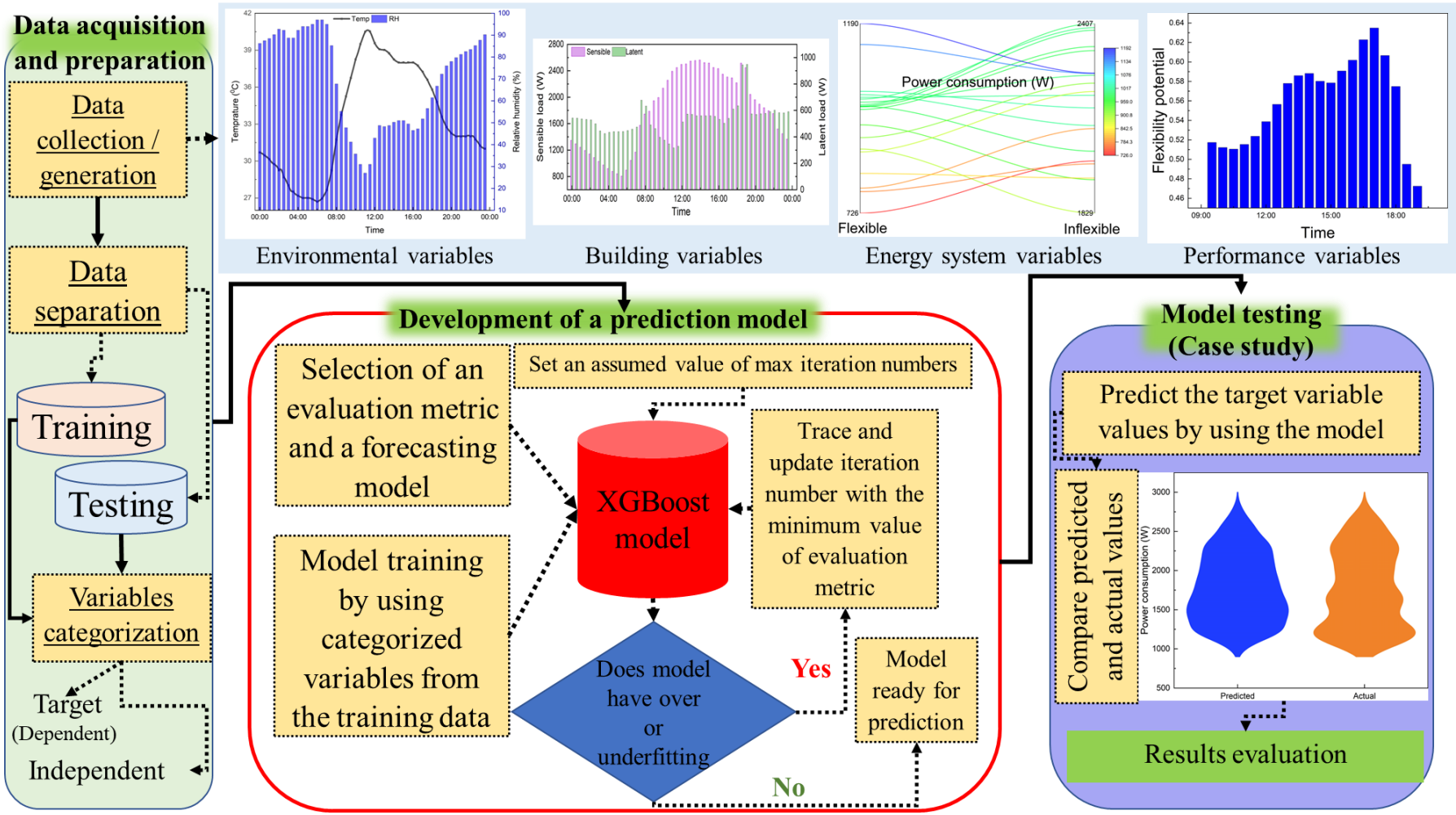

Fig. 6.1 Outline of the developed methodology.

6.1.2 Extreme Gradient Boosting model

XGBoost is a robust data analytics model for classification and regression tasks. It implements gradient-boosted decision trees, which are a kind of ensemble model that combines the predictions of several decision trees to create a more accurate and balanced model. The individual trees are trained in sequence, and each tree learns from the mistake of the previous tree. This sequential training process allows the model to improve its accuracy further. Each decision tree in the XGBoost algorithm is a weak learner, but combining several weak learners creates a strong learner with improved accuracy. The XGBoost algorithm uses a specific loss function and a second-order approximation of the loss function to train each decision tree in a way that maximizes the overall performance of the model. It uses the Taylor expansion of the loss function up to the second order and combines the estimates of simpler and weaker models by adding the regularization term to the Taylor expansion to find the optimal solution. It avoids overfitting by balancing the model complexity and objective function minimization. In addition to training decision trees, XGBoost also includes a number of regularization parameters that can help prevent overfitting. This makes XGBoost a highly effective and robust algorithm. During the training process, the XGBoost model iteratively calculates the node loss and picks the leaf node with the largest gain loss to add new trees that predict residuals of antecedent trees and combine them with the former trees. Residuals are the losses incurred after each model prediction and calculated based on the observed and predicted values (Chen & Guestrin 2016; Guo et al. 2020). It can be effectively used for regression, prediction, classification, and ranking problems. Eq. (6.1) illustrates the XGBoost mathematical model.

$$\hat{y}_i = \sum_{k=1}^{N} f_k(x_i) \ , f_k \in F \tag{6.1}$$

where $\hat{y}_i$ represents the predicted value, N, $f_k(x_i)$ and F, respectively, represent the number of decision trees, the function of input in the k_{th} decision tree, and the set of all possible classification and regression trees. In this chapter, the XGBoost model was used to predict the flexibility potential of an HVAC system with an integrated TES system. Energy consumption of the HVAC system was also predicted. The mathematics behind the development of the XGBoost model can be found in Guo et al. (2020). Fig. 6.2 illustrates the flow chart of the XGBoost algorithm.

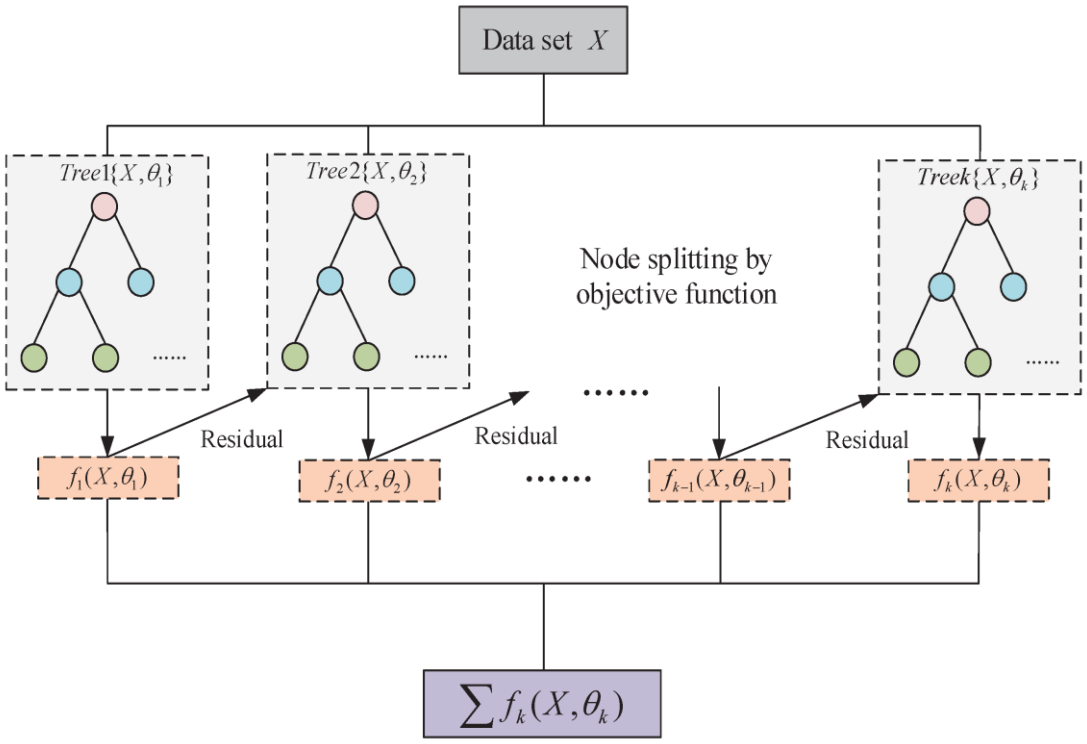

Fig. 6.2 Flow chart of the XGBoost model (Guo et al. 2020).

6.2 Performance evaluation and testing

6.2.1 Description of the Case Study

To test the performance of the developed method, a case study building conditioned by an HVAC system with integrated TES, as introduced in Chapter 4, was considered. Firstly, a simulated dataset of the four summer months of May, June, July, and August was generated for the HVAC system with integrated TES using the TRNSYS simulation, under the weather conditions of Dubai, United Arab Emirates, as this house participated in the Middle East Solar Decathlon Competition in 2018. Details about the house and the energy system have been presented in Chapter 4. The dataset was then divided into training and testing datasets, with 75% of the data (May, June, and July) used for training and 25% (August) for testing purposes. For the operation of the HVAC system, the assumptions were used that the TES system was charged during off-peak demand hours using the air-source heat pump, and during peak demand hours, the air-source heat pump was switched-off, and building sensible load

was handled by the TES system. A dehumidification heat pump handled the latent load of the buildings during peak and off-peak demand hours.

The training dataset was used to train the XGBoost model, and the desired target variables (i.e. flexibility potential and energy consumption of the HVAC system, and building sensible load) were predicted separately, as summarized in the following sections, using the selected independent variables. The model was trained for each prediction task using both the independent variables and target variables. Whereas in the testing process, only independent variables were used as the input of the model, and target variables were predicted. The model was also tested for over- and under-fitting. An optimized value of the evaluation metric was selected to reduce the computational time, as an example shown in Fig. 6.3, in which the model was first run based on 1000 iterations, and by tracing the minimum value of the evaluation metric, 75th iteration was traced as the optimum iteration with the minimum value of RMSE.

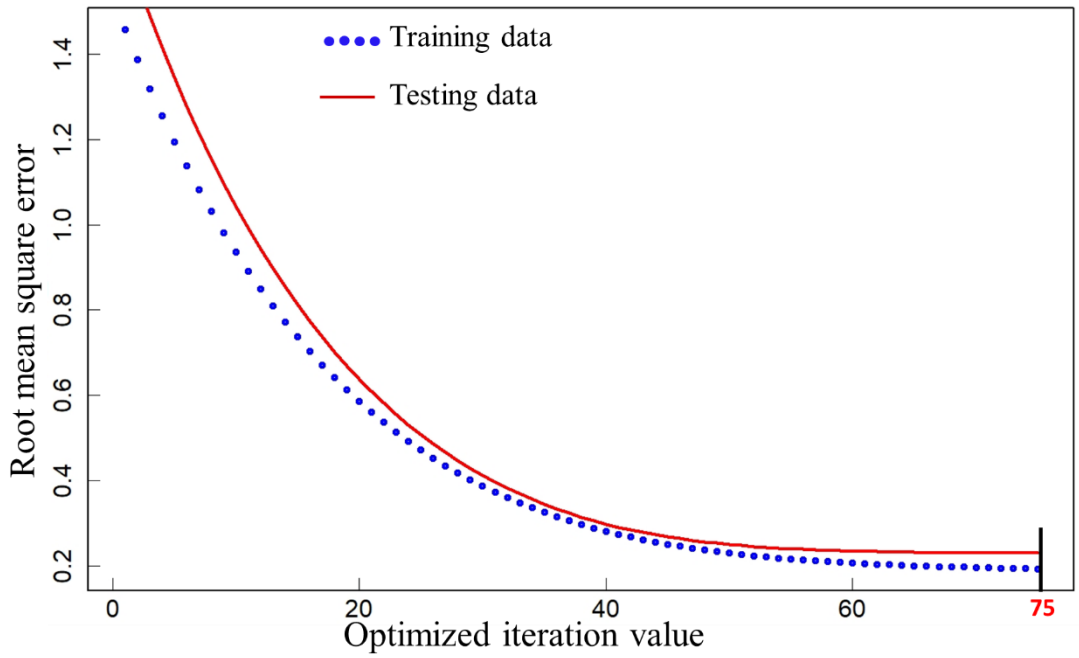

Fig. 6.3 Selection of an iteration number with the minimum root mean square error.

6.2.2 Prediction of the energy flexibility potential of the HVAC system with integrated TES system

Firstly, outdoor air temperature and relative humidity, and building sensible and latent thermal load were used to predict the flexibility potential (F_P) of the HVAC system. The flexibility potential of the system was selected as the performance factor, which was considered as the ability of a system to shift the load during peak demand hours to the off-peak demand hours, and was calculated using Eq. (6.2). Because in this case, the flexible operation was achieved during the peak demand hours only, hence the data during the peak demand hours was selected for the prediction of energy flexibility. A TES system was used to handle the building's sensible load during peak demand hours and was the only flexibility provider in this case. Only the air-source heat pump was switched off during the peak demand hours, and the other components of the HVAC system functioned the same as in the normal case. A sample representation of the selected data for a single day is shown in Fig. 6.4 and Fig. 6.5. Fig. 6.4 represents the independent variables used for predicting the flexibility potential of the HVAC system, and Fig. 6.5 is the representation of the target variables. Flexible and inflexible operations in Fig. 6.5a, respectively represent the HVAC system operation with and without considering the TES system.

$$\mathrm{F_{P}}_i = \frac{P_{N_i} - P_{F_i}}{P_{N_i}} \qquad \text{where i=1…n} \qquad (6.2)$$

where P represents power consumption, and subscripts F and N are the representation of flexible and normal (baseline) operations, respectively.

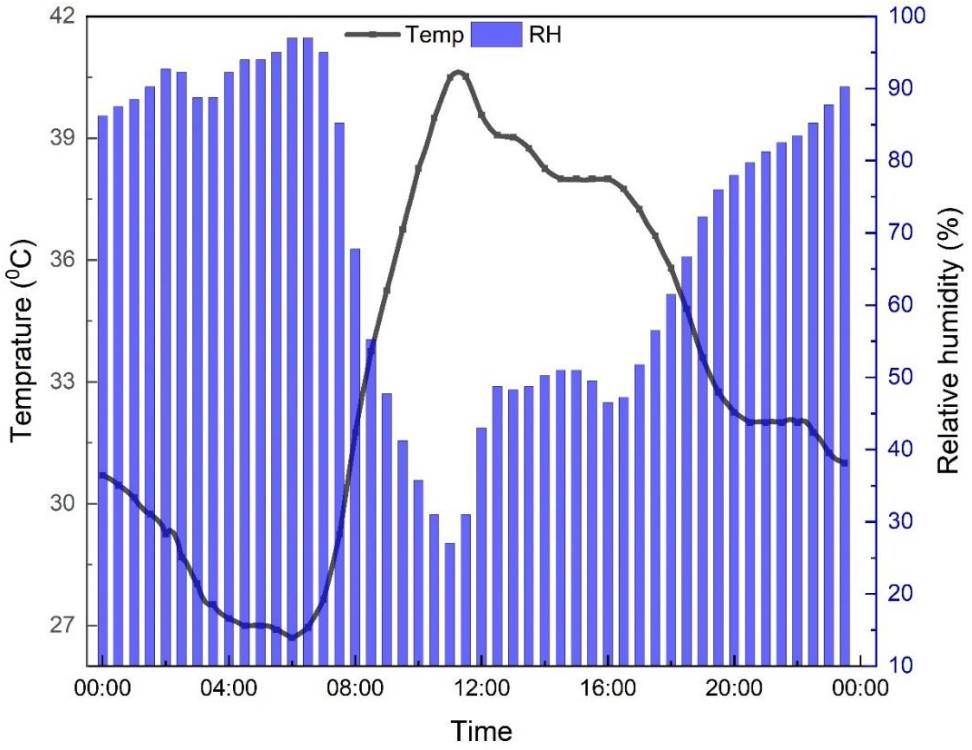

a) Outdoor air temperature and relative humidity

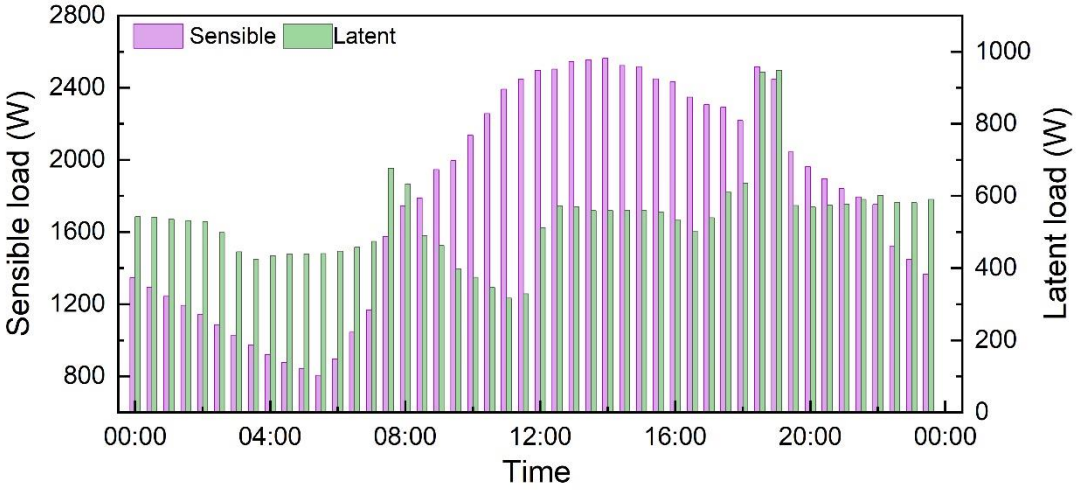

b) Internal thermal loads

Fig. 6.4 Representation of the independent variables.

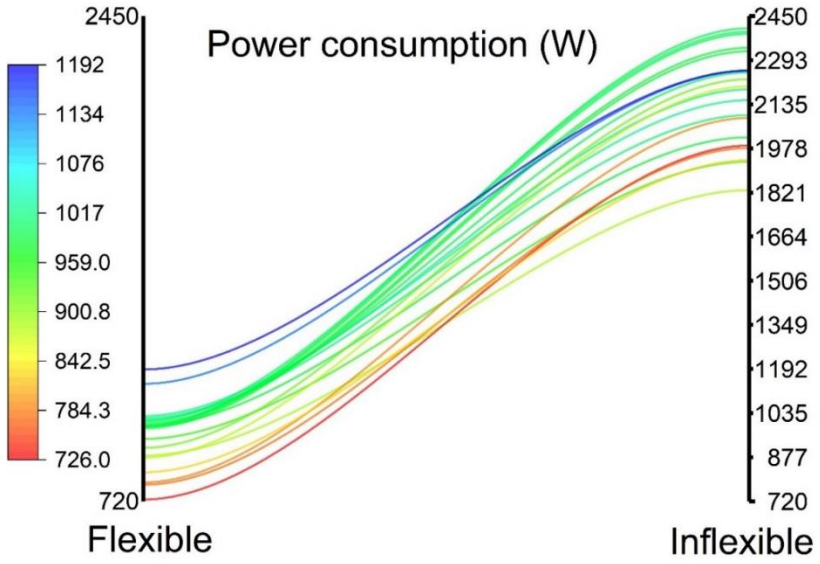

a) Power consumption of the HVAC system during flexible and inflexible operations

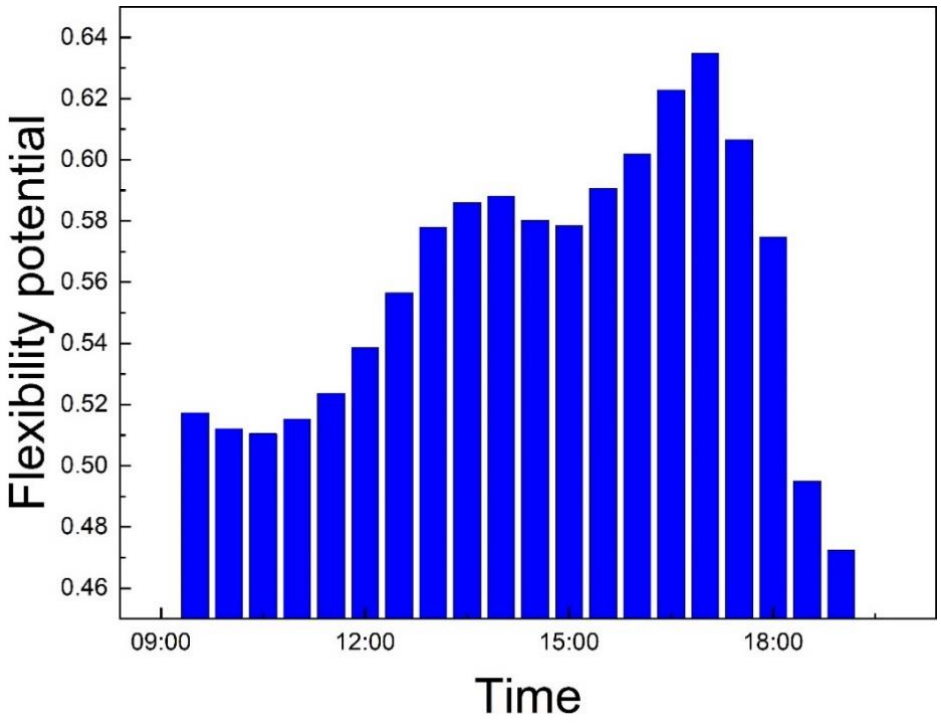

b) Flexibility potential representation

Fig. 6.5 Representation of the target variables.

Using the XGBoost-based prediction model, the flexibility potential of the HVAC system with an integrated TES system was predicted. The predicted values were compared with the actual values, as shown in Fig. 6.6. Flexibility potential values were calculated using Eq. (6.2). As the model was trained based on the data of three

consecutive months of May, June, and July, hence prediction was only made for the month of August, as shown in Fig 6.6a. Fig. 6.6b compares the predicted and actual values for a single representative day. For flexibility potential prediction, only the data of the peak demand hours was used, as in this case, the HVAC system only provided flexibility during the peak demand hours. A high average prediction accuracy of 99% was achieved, proving the model's effectiveness in accurately predicting the energy flexibility of building energy systems. The model also proved successful in predicting the energy flexibility under varying weather conditions and the thermal load of the building, as these were used as the input variables for prediction.

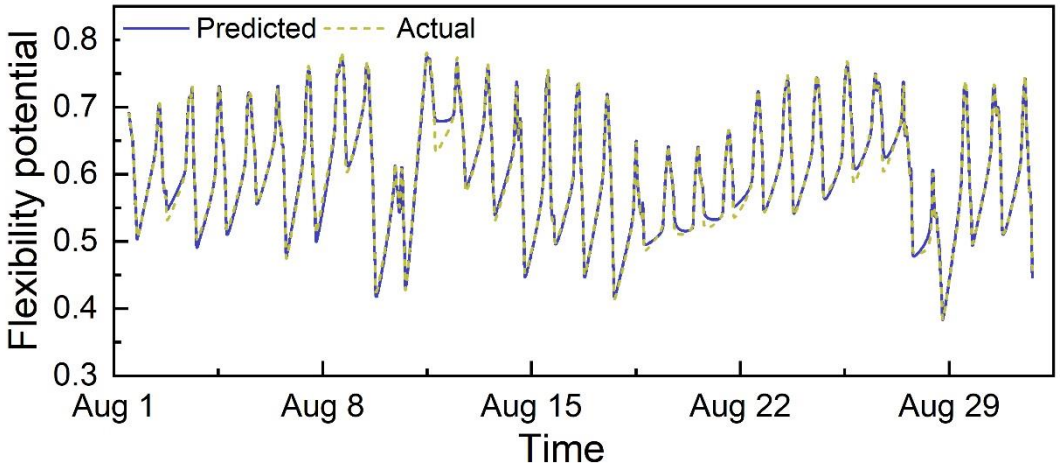

a) Prediction results of the energy flexibility potential

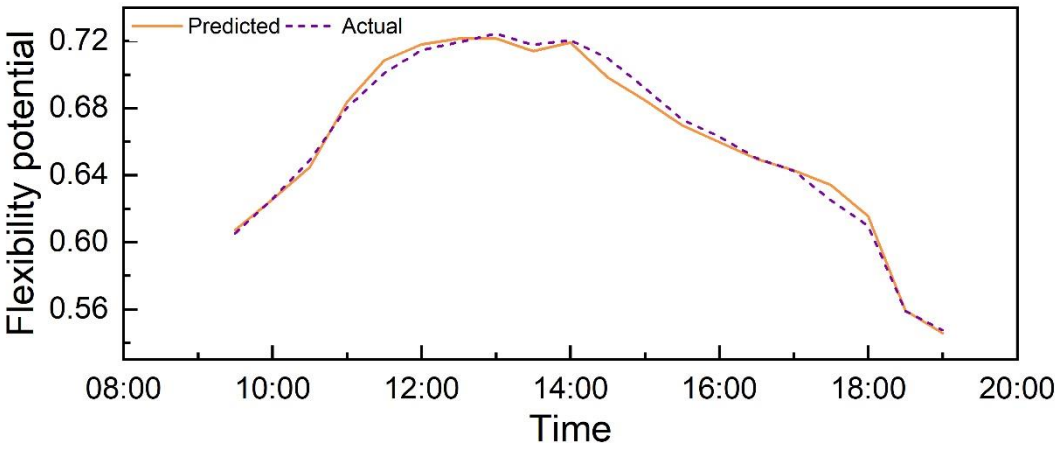

b) Prediction results during peak demand hours of a day

Fig. 6.6 Comparison between the predicted and actual values of the HVAC flexibility potential.

Furthermore, to test the performance of the prediction model, the distribution of the predicted and actual values and the binomial distribution of the prediction error was

analyzed, as shown in Fig. 6.7. Fig. 6.7a is the Violin plot of the predicted and actual values. It can be used to visualize the distribution of the numerical values. The wider parts of the violins represent the areas where the data was denser, while the narrower parts represent the areas where the data was less dense. The flexibility potential of the HVAC system was between 0.6 (60%) and 0.75 (75%) for most of the observations, which indicated the high effectiveness of the HVAC system with integrated TES in enhancing building energy flexibility. Because of the higher prediction accuracy, both the Violin plots were nearly identical.

In Fig. 6.7b, it can be seen that most of the datasets showed a prediction error varying from 2 to -2 %. Thus, this model can be used to estimate the capacity of a system to participate in demand response programs under variable environmental and thermal loading conditions. Moreover, a combination of system energy consumption and energy flexibility prediction can support the grid services and help aggregators to cost-effectively manage the bidding process in the energy markets because of having prior knowledge about energy consumption and demand patterns.

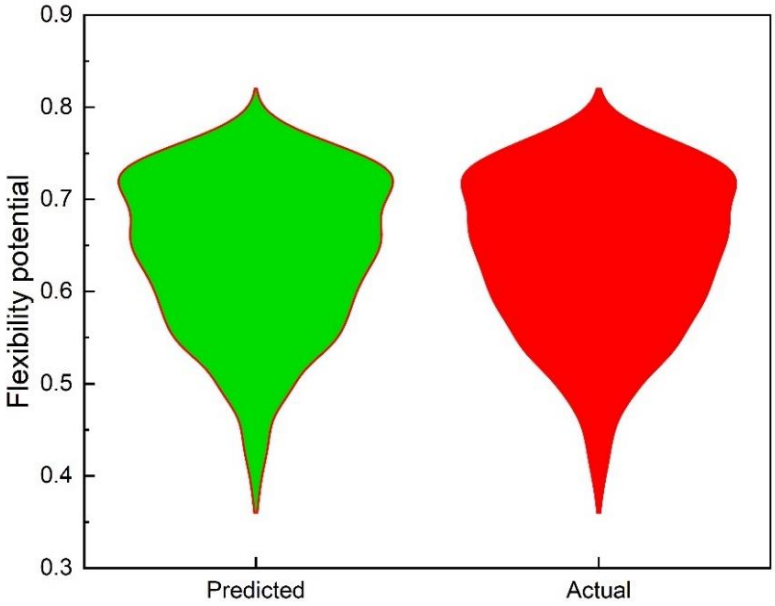

a) Variation in predicted and actual values

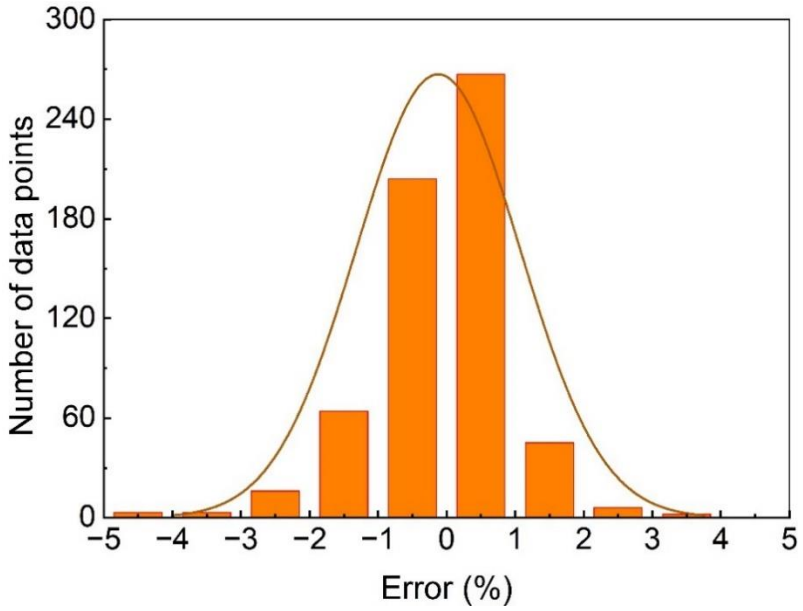

b) Distribution of the prediction error

Fig. 6.7 Performance testing of the prediction of the HVAC flexibility potential.

6.2.3 Predicting the power consumption of the HVAC system

The flexibility potential of buildings or building energy systems is a function of power consumption. Hence, the effect of weather conditions on the power consumption of the HVAC system was also analyzed. Using the same prediction process, as illustrated above, and tracing the optimized iteration number for improving the computational performance of the XGBoost model, the power consumption of the HVAC system was predicted and compared with the simulated values. The predicted results for the month of August and a single representative day are shown in Fig. 6.8.

An average accuracy of 93% was achieved using the developed model. A major prediction error was caused by a sudden change in the power consumption, especially from 18:00 to around 20:00. This sudden change in power consumption was because of the increase in the building's sensible load. The period from 18:00 to around 20:00 was assumed to be the cooking period in this case, and hence an increase in the building's sensible load was observed. It is noted that power consumption was predicted without considering the flexible operation.

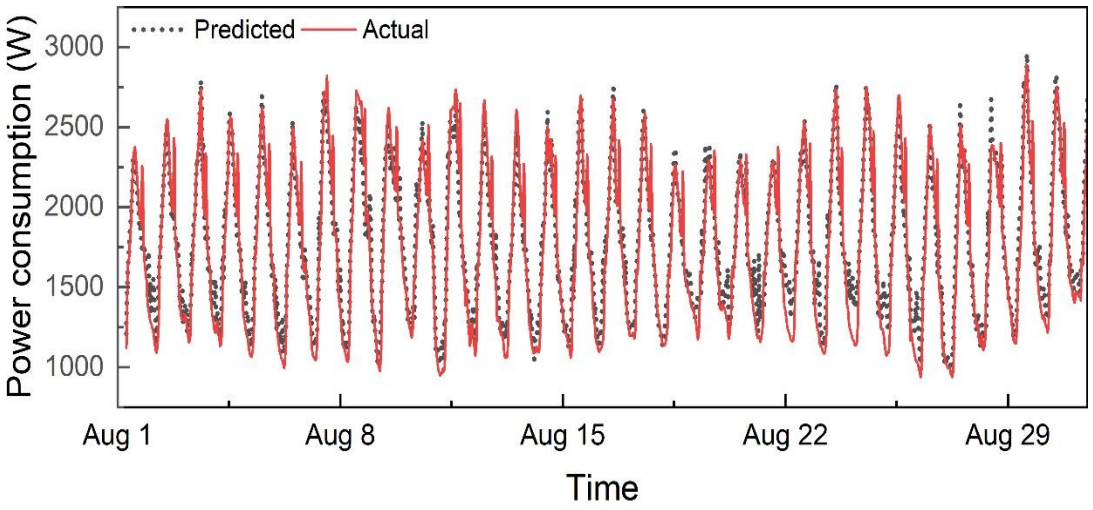

a) Prediction results for one month

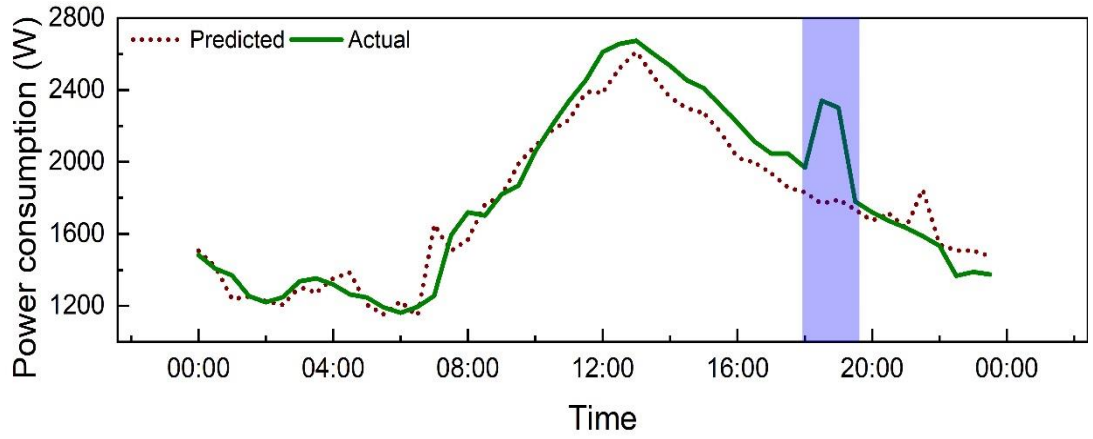

b) Prediction results for one day

Fig. 6.8 Comparison between the predicted and actual values of the HVAC power consumption.

The distribution of the prediction error is visualized in Fig. 6.9. It indicated that the prediction was mostly negatively skewed, and the prediction error was mainly between 5 and -10%. A higher prediction error in the negative range illustrated that the model under-predicted in some cases. It is also evident from Fig. 6.8a that the model was unable to capture the sudden increase in the building's sensible load because of the occupant activity.

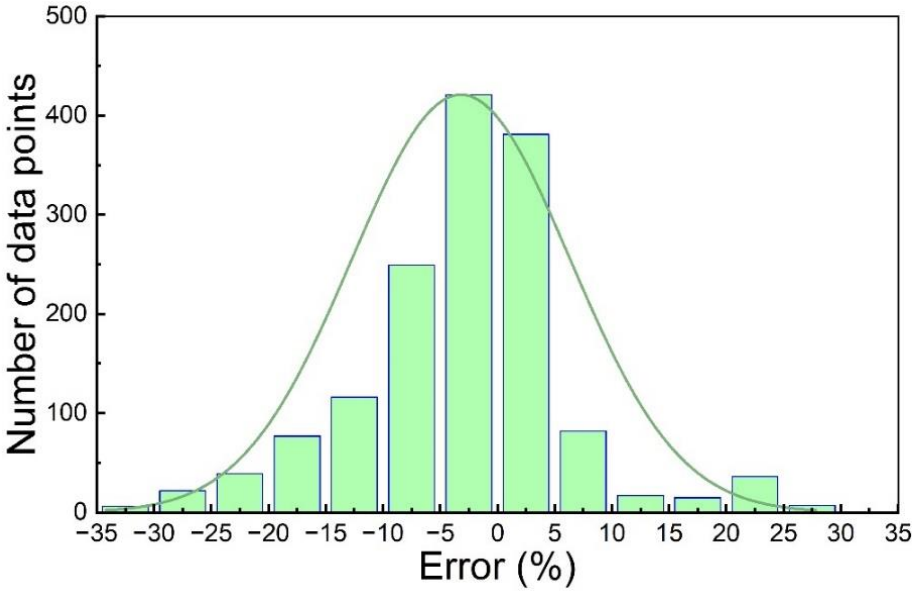

Fig. 6.9 Distribution of the error in predicting HVAC energy consumption.

6.2.4 Prediction of the building sensible load

The main purpose of an HVAC system is to handle the thermal load of the building to provide thermal comfort to occupants. Building thermal load is mainly a function of occupants' activity, building geometry and construction, appliance operation, and outdoor conditions. In this chapter, appliances, and occupant activity schedules were assumed to be similar for each day, and thermal energy storage was only used to handle the sensible load of the building. Hence, only building sensible load was predicted using the outdoor conditions. Prediction of building thermal load can provide opportunities to optimize the flexibility potential of the building HVAC systems. A combination of prior knowledge about building thermal load and renewable power-based generation can be collectively used to develop strategies like pre-cooling/pre-heating or delayed operation to concurrently optimize energy costs and improve the flexibility potential of building HVAC systems. An average accuracy of 90% was achieved in predicting the sensible load of the building by just using the outdoor air temperature and relative humidity data as the input. The comparison between the predicted and actual values of the building sensible load is depicted in Fig. 6.10. Fig. 6.10b shows that the decrease in the prediction accuracy occurred during the same period as illustrated in Fig. 6.8b. It was because of the sudden increase in the sensible load due to the occupant activity. However, the overall prediction was quite closer to the actual values.

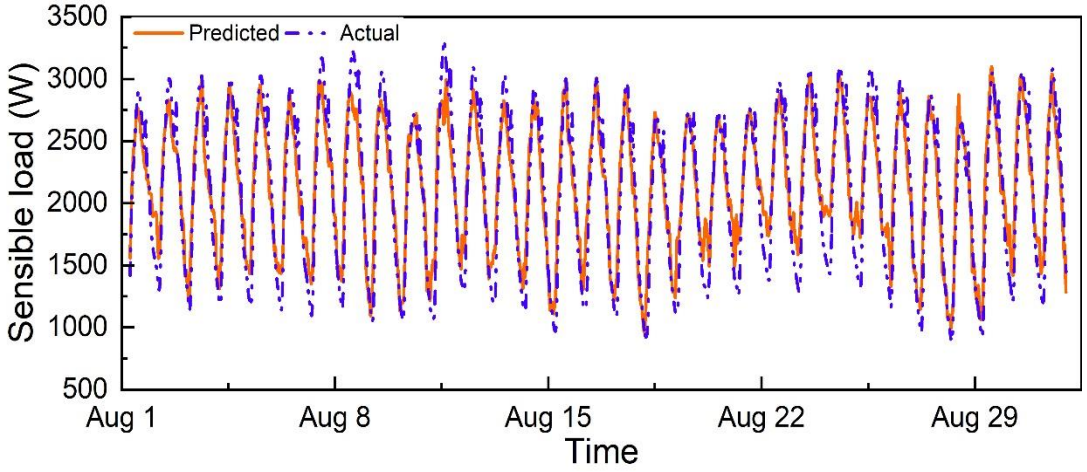

a) Prediction results for one month

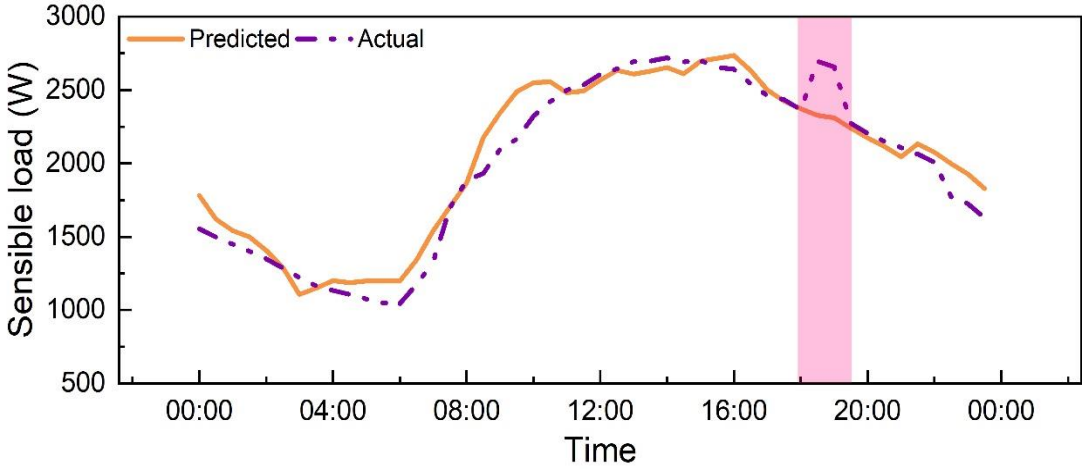

b) Prediction results for one day

Fig. 6.10 Comparison between the predicted and actual values of the building sensible load.

The distribution of the prediction error was also evaluated (Fig. 6.11) using the same process as reported above. The prediction of the building sensible load was mainly negatively skewed, and the majority of the error was between 10 and -15%. The thermal load of the building can vary abruptly because of occupant activities. Hence, the prediction of the building sensible load with an overall accuracy of 90% by just using outdoor air temperature and relative humidity showed the high effectiveness of the developed model for building thermal load prediction purposes.

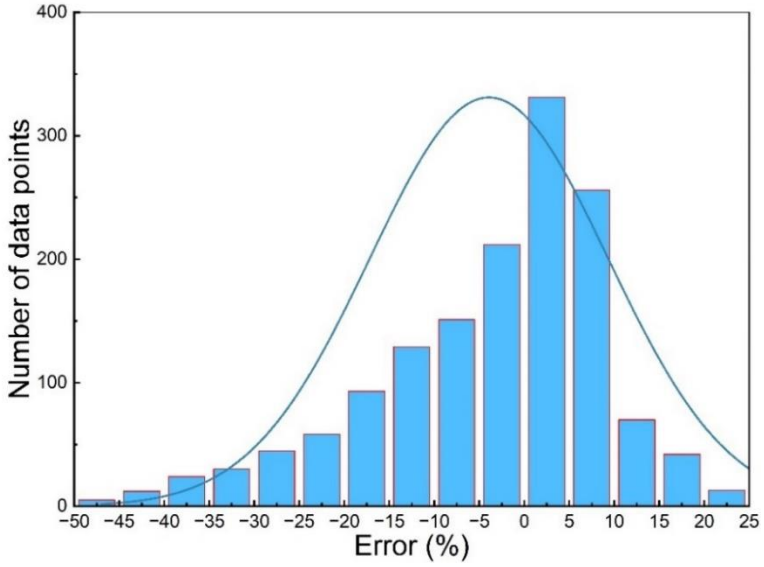

Fig. 6.11 Distribution of the error in predicting building sensible load.

Overall, the results proved that the XGBoost model-based prediction model effectively predicted the energy flexibility and energy consumption of the building HVAC system. The model also proved to be efficient in predicting the sensible load of the building. Predictions performed in the current study can help improve the flexibility potential of building energy systems. They can also support the grid services and aggregators in cost-effective decision-making in evolving energy markets.

6.3 Summary

An Extreme gradient boosting-based prediction model was used to predict the energy flexibility potential and energy consumption of an HVAC system with an integrated TES system. The building's sensible load was also predicted using the same model. The XGBoost model was optimized to enhance the computational performance of the model. The simulation data of the four summer months, including May, June, July, and August, under the weather conditions of Dubai, United Arab Emirates, was used to test the model, in which 75% of the data (i.e. May, June, July) was used to train the XGBoost model, whereas 25% of the data (i.e. August) was used for testing purposes. Hence, the prediction was only made for the month of August. Firstly, the energy flexibility potential of the HVAC system with an integrated TES system was predicted using the outdoor air temperature and relative humidity, and indoor sensible and latent thermal load of the building as independent variables. The model proved to

be highly effective in predicting the energy flexibility potential of the HVAC system with an overall accuracy of 99%. Secondly, the energy consumption of the HVAC system was predicted with an accuracy of 93%. Lastly, the building's sensible load was predicted with an accuracy of 90%. For each prediction, model testing was accomplished by analyzing the distribution of the prediction errors. Testing procedures verified the effectiveness of the model. Overall, the prediction of energy flexibility and energy consumption can further support grid stability by providing prior information about the building energy consumption patterns and flexibility potential of the building. This information can be used by aggregators to optimize the bidding process in energy markets and save a considerable amount of capital costs. Furthermore, the prediction of building thermal load can be used to optimize the energy consumption of building energy systems using strategies, such as pre-cooling or pre-heating.

Chapter 7 Conclusions and recommendations

7.1 Conclusions

The pursuit of a sustainable energy future demands a paradigm shift towards renewable energy resources to preserve the ecosystem from extreme and uncertain climatic events. While renewable energy resources are the cardinal part of sustainable transformation, their intermittency presents significant challenges to the electricity grids, hence demanding innovative solutions and advanced technologies to enable effective integration and management of these resources. One of the key approaches to tackling such challenges is to make the demand side flexible. Building energy flexibility has evolved as an effective measure to enable buildings to adjust their demand as per the fluctuations on the supply side. A key source on the building side in this context is the building heating, ventilation, and air-conditioning (HVAC) systems, which are considered one of the main energy consumers in buildings and offer substantial flexibility because of their capability to modulate and shift loads.

This thesis provided methodologies to evaluate and improve energy flexibility and performance of building HVAC systems to overcome some existing research gaps and further support the evolving field of building energy flexibility and demand management.

Overall, strategies introduced in this thesis can be used to develop and implement energy-efficient measures for enhanced building energy flexibility. Moreover, an HVAC system with integrated thermal energy storage (TES) can reduce energy consumption during peak periods by adjusting the building's energy use in response to changes in energy prices or grid conditions. Energy storage systems can store excess energy during periods of low demand and release it during peak periods, reducing the need for energy from the grid. Integrating renewable energy sources, such as photovoltaic (PV) panels, can further enhance building energy flexibility and reduce building dependence on the grid. These strategies can be used to improve building energy efficiency and reduce energy costs and carbon emissions. Additionally, energy flexibility prediction can be used to further increase the value proposition of demand management strategies.

The key findings of this research and future recommendations are summarized in the following sections.

7.1.1 Performance assessment strategy for building chiller systems

A data-driven strategy for performance assessment of building chiller systems was introduced using data mining and advanced visualization techniques, including Agglomerative hierarchical clustering (AHC), Conditional inference tree (CIT), and Association rule mining (ARM) in combination with domain knowledge. One year data collected from a chiller system of a commercial building was used to investigate the collective effects of the operating variables on the chiller system performance. Outliers in the collected data were detected and removed using the Density-based spatial clustering of applications with noise (DBSCAN) algorithm. Heat maps were then generated to visualize the chiller power ratio (CPR) for each day of the year. Temporal variations in the CPR were further visualized and analyzed using the CIT. CIT and AHC helped to analyze the effect of the operating variables on the performance of the system. A new performance indicator, termed COP Destruction, was introduced to analyze the quality of the achieved COP. Lastly, a qualitative analysis was performed using the ARM model, which generated a set of 57 rules among COP, part load ratio (PLR), water temperature differences across the evaporator and condenser, CPR, and COP Destruction. The main findings are as follows:

- A combination of black-box models and domain knowledge can trace unique opportunities for performance improvement of building energy systems.
- COP Destruction can further enhance the reliability of the analysis.
- The CIT model can be used to trace performance improvement opportunities during different hours of the day, and days of the week. Such detailed performance assessment is key for enhancing the flexibility of building energy systems.
- AHC can generate different combinations through clustering and provide several opportunities for performance improvement.
- ARM can be used as a tool for knowledge discovery by interlinking system performance and operating variables.

- Chiller performance was most strongly influenced by the temperature differences across the evaporator and decreased when the PLR and water temperature differences across the condenser and evaporator were concurrently below their median values for the analyzed system. The qualitative results generated using the ARM model showed a range of combinations of the operating conditions that can be selected for energy-efficient operation.
- The developed method can aid in developing energy-efficient control strategies that can support energy-flexible decision-making.

7.1.2 Ranking and near-optimal selection of phase change materials (PCMs) for thermal energy storage in building applications

A Weighted product method (WPM) based ranking model was developed for performance-based ranking and selection of near-optimal PCMs for thermal energy storage in building applications. A strategy to convert qualitative characteristics into quantitative factors and a process for handling multiple PCM characteristics for weight assignment were also introduced. The developed strategy was tested through two different case studies by selecting near-optimal PCMs for thermal energy storage system (TES) systems coupled with the HVAC systems. The main findings are as follows:

- PCMs-based TES systems can aid HVAC systems in load shifting during peak demand hours. In the analyzed case, PCM-based thermal energy storage helped to shift 73% of the peak HVAC energy consumption to the off-peak demand hours.
- Selection of near-optimal PCMs is important to increase the flexibility potential of building HVAC systems, which resulted in 35% extra cost savings in the analyzed case by selecting the better-ranked PCM using the developed ranking model.
- The developed strategy proved to be computationally fast and did not require extensive experimentation to select near-optimal PCMs for the desired application.

- Criteria introduced to convert qualitative characteristics into quantitative factors enhanced the effectiveness of the multi-criteria decision analysis-based ranking strategy.
- The formation of clusters in the Analytic hierarchy process (AHP) matrix for weight assignment to the PCM characteristics improved the performance of this method.
- One of the limitations relating to the implementation of this method is the subjectivity of the weight assignment process. Hence, a weight determined for a specific characteristic of the PCMs for one application may not apply to other applications.

7.1.3 A framework to formulate and aggregate performance indicators to quantify building energy flexibility

A framework to develop and aggregate building energy flexibility indicators (EFIs) was introduced, which can be used to quantify the aggregated energy flexibility potential of buildings and building energy systems. EFIs were developed by considering the energy system characteristics, penalty functions based on the penalties introduced by the grids, and performance factors of flexibility measures. An all-inclusive building energy flexibility quantification function was developed by aggregating EFIs and performance factors, and it was termed Aggregated energy flexibility potential (AEFP) function. The developed indicators and quantification function were used to evaluate the flexibility potential of an HVAC system with integrated TES, and a building with integrated PV system. The main findings are as follows:

- It is important to consider the temporal and comfort performance in the development of AEFP, as such information is important to gauge the performance of a flexible source or flexibility measure.
- The developed AEFP function can be used to compare the performance of different flexibility sources, and it can help to trace flexibility improvement opportunities.
- The aggregation of EFIs is subjective and depends on the scope of the desired objective.

- The photovoltaic system offered more flexibility than the TES system. Overall, both systems can offer considerable benefits to building owners and service providers.
- TES systems can cause a rebound effect that is usually undesirable.
- The photovoltaic systems' ability to export electricity to grids further enhanced the flexibility potential of these systems.
- The indicators developed can offer insights into different performance factors, aiding in making informed decisions for optimizing energy usage and improving building energy flexibility.
- The framework introduced can be used to develop additional EFIs, and the method used to develop AEFP has the potential to include more flexible services and factors based on the specific requirement of a particular application.

7.1.4 Predicting the energy flexibility potential and energy consumption of building HVAC systems

An Extreme gradient boosting (XGBoost) model was used to develop a method for predicting the flexibility potential and energy consumption of HVAC systems with integrated thermal energy storage. XGBoost model was also computationally optimized. Root mean square error (RMSE) was selected as an evaluation metric, and regression was selected for the prediction tasks. The method was tested using the four-month data of the summer months under the weather conditions of Dubai, and prediction error was also analyzed. The results proved the accuracy of the method in predicting the energy flexibility potential of the HVAC system, as a prediction accuracy of 99% was achieved. The method also showed high accuracy in predicting the energy consumption of the HVAC system and building sensible load that were respectively predicted with an accuracy of 93% and 90%. The main findings are as follows:

- Prediction of energy flexibility and energy consumption of HVAC systems can increase the resilience of both the demand and supply sides. The current practice of just predicting the energy consumption of systems limits the effectiveness of building energy flexibility strategies.

- Prediction of building thermal load can be used to develop strategies like pre-cooling or pre-heating to further enhance the flexibility of HVAC systems and support grid operation.
- The developed method can also be used to predict the flexibility of other building energy flexible sources.

7.2 Recommendations for future work

This thesis focused on two key elements: i) building energy flexibility, and ii) building HVAC systems. The overall aim of the thesis was to evaluate and improve the energy flexibility and performance of building HVAC systems. Although the results proved the effectiveness of the developed strategies in analyzing and enhancing the performance and energy flexibility of building HVAC systems, additional research can be continued to further enhance the usefulness of the strategies developed. For instance, this thesis mainly focused on PCM-based TES integration with the building HVAC systems to improve building energy flexibility. However, it is crucial to recognize that commercial or industrial buildings deploy high-capacity HVAC systems and offer only limited opportunities for the integration of large PCM-based TES systems. Consequently, the optimization of HVAC system operation becomes crucial in such cases, which can be achieved by combining technical solutions and data mining strategies. Hence, research in the future can be conducted to evaluate the value proposition of PCM-based TES systems for commercial HVAC systems. Some other future recommendations are as follows:

- The chiller power ratio patterns generated using heat maps and CIT in Chapter 3 can be used to develop energy-flexible strategies such as pre-cooling. Moreover, the effect of these patterns on the enhancement of the chiller energy flexibility and energy efficiency can be further investigated.
- The method introduced in Chapter 5 can be further tested by selecting different flexible sources and/or a combination of these sources. The performance of these sources and combinations can be compared to trace the best source and the combination of sources under the given conditions for enhanced building energy flexibility. Furthermore, the developed method can be used to indicate the energy flexibility level of different buildings in a vicinity based on the

available energy sources. However, it is worthwhile to note that the weight assignment process in the development of the aggregated energy flexibility potential function is subjective, and must be supported by strong domain knowledge.

- The model introduced in Chapter 6 can be used for prediction tasks in other applications. Prediction of energy consumption can help aggregators save capital by optimizing the bidding process in the energy markets because of having prior knowledge about demand patterns. A combination of different data analytic-based prediction models can be tested for the prediction tasks, and a trade-off can be found among these models by selecting the prediction error as the key performance indicator.

Bibliography

Abhat, A. 1983, ‘Low temperature latent heat thermal energy storage: Heat storage materials’, Solar Energy, vol. 30, no. 4, pp. 313–32.

Agyenim, F., Hewitt, N., Eames, P. & Smyth, M. 2010, ‘A review of materials, heat transfer and phase change problem formulation for latent heat thermal energy storage systems (LHTESS)’, Renewable and Sustainable Energy Reviews, pp. 615–28.

Airò Farulla, G., Tumminia, G., Sergi, F., Aloisio, D., Cellura, M., Antonucci, V. & Ferraro, M. 2021, ‘A review of key performance indicators for building flexibility quantification to support the clean energy transition’, Energies.

Akeiber, H., Nejat, P., Majid, M.Z.A., Wahid, M.A., Jomehzadeh, F., Zeynali Famileh, I., Calautit, J.K., Hughes, B.R. & Zaki, S.A. 2016, ‘A review on phase change material (PCM) for sustainable passive cooling in building envelopes’, Renewable and Sustainable Energy Reviews, pp. 1470–97.

Almansory, A. 2018, ‘Applying Association Rules and Decision Tree Algorithms with Tumor Diagnosis Data’, SSRN Electronic Journal.

Amasyali, K. & El-Gohary, N.M. 2018, ‘A review of data-driven building energy consumption prediction studies’, Renewable and Sustainable Energy Reviews, pp. 1192–205.

Anand, G. & Kodali, R. 2008, ‘Benchmarking the benchmarking models’, Benchmarking, vol. 15, no. 3, pp. 257–91.

Anilkumar, B.C., Maniyeri, R. & Anish, S. 2021, ‘Optimum selection of phase change material for solar box cooker integrated with thermal energy storage unit using multi-criteria decision-making technique’, Journal of Energy Storage, vol. 40, p. 102807.

Awan, M.B., Li, K., Li, Z. & Ma, Z. 2021, ‘A data driven performance assessment strategy for centralized chiller systems using data mining techniques and domain knowledge’, Journal of Building Engineering, vol. 41.

Axiotherm 2022, https://www.axiotherm.de/en/produkte/axiotherm-pcm/, last

accessed 15 sep 2022.

Baeten, B., Rogiers, F. & Helsen, L. 2017, 'Reduction of heat pump induced peak electricity use and required generation capacity through thermal energy storage and demand response', Applied Energy, vol. 195, pp. 184–95.

Balint, A. & Kazmi, H. 2019, 'Determinants of energy flexibility in residential hot water systems', Energy and Buildings, vol. 188–189, pp. 286–96.

Bampoulas, A., Saffari, M., Pallonetto, F., Mangina, E. & Finn, D.P. 2021, 'A fundamental unified framework to quantify and characterise energy flexibility of residential buildings with multiple electrical and thermal energy systems', Applied Energy, vol. 282.

Bastiaansen, R., Doelman, A., Eppinga, M.B. & Rietkerk, M. 2020, 'The effect of climate change on the resilience of ecosystems with adaptive spatial pattern formation', Ecology Letters, vol. 23, no. 3, pp. 414–29.

Beltrán, R.D. & Martínez-Gómez, J. 2019, 'Analysis of phase change materials (PCM) for building wallboards based on the effect of environment', Journal of Building Engineering, vol. 24.

Bhawan, S. & Puram, R.K. 2006, 'Energy Performance Assessment for Equipment and Utility systems: Chapter 10 - Energy Performance, Assessment of Lighting Systems', Bureau of Energy Efficiency, no. ii, pp. 107–14.

Buchholz, M., Schmidt, M., Buchholz, R., Geyer, P. & Steffan, C. 2009, 'Heating And Cooling With Sun And Salt – A Thermo-Chemical Seasonal Storage System In Combination With Latent Heat Accumulation', RIO 9 - World Climate & Energy Event, Rio de Janeiro, Brazil.

Chen, T. & Guestrin, C. 2016, 'XGBoost: A scalable tree boosting system', Proceedings of the ACM SIGKDD International Conference on Knowledge Discovery and Data Mining, vol. 13-17- August-2016, pp. 785–94.

Chen, Y., Chen, Z., Xu, P., Li, W., Sha, H., Yang, Z., Li, G. & Hu, C. 2019, 'Quantification of electricity flexibility in demand response: Office building case study', Energy, vol. 188.

Clauß, J., Finck, C., Vogler-Finck, P. & Beagon, P. 2017, Control strategies for building energy systems to unlock demand side flexibility – A review, Building Simulation Conference Proceedings.

Climator 2022, https://www.climator.com/en/pcm-climsel/product-data-sheets, last accessed 15 sep 2022.

De Coninck, R. & Helsen, L. 2016, 'Quantification of flexibility in buildings by cost curves - Methodology and application', Applied Energy, vol. 162, pp. 653–65.

Das, D., Sharma, R.K., Saikia, P. & Rakshit, D. 2021, 'An integrated entropy-based multi-attribute decision-making model for phase change material selection and passive thermal management', Decision Analytics Journal, vol. 1, p. 100011.

'Default market offer prices 2022–23 - Fact sheet' 2022, Australian Energy Regulator, last accessed 15 June 2022, <https://www.aer.gov.au/retail-markets/guidelines-reviews/default-market-offer-prices-2022–23/final-decision>.

Le Dréau, J. & Heiselberg, P. 2016, 'Energy flexibility of residential buildings using short term heat storage in the thermal mass', Energy, vol. 111, pp. 991–1002.

Du, Z. & Jin, X. 2007, 'Detection and diagnosis for sensor fault in HVAC systems', Energy Conversion and Management, vol. 48, no. 3, pp. 693–702.

Ester, M., Kriegel, H.-P., Sander, J. & Xu, X. 1996, 'A Density-Based Algorithm for Discovering Clusters in Large Spatial Databases with Noise', Proceedings of the 2nd International Conference on Knowledge Discovery and Data Mining, pp. 226–31.

European Smart Grids Task Force Expert Group 3 2019, Demand Side Flexibility: Perceived barriers and proposed recommendations, European Smart Grids Task Force Expert Group 3, <https://ec.europa.eu/energy/sites/ener/files/documents/eg3_final_report_demand_side_flexiblity_2019.04.15.pdf>.

Fan, C., Xiao, F., Madsen, H. & Wang, D. 2015, 'Temporal knowledge discovery in big BAS data for building energy management', Energy and Buildings, vol. 109, pp. 75–89.

Fernandez, A.I., Martnez, M., Segarra, M., Martorell, I. & Cabeza, L.F. 2010, 'Selection of materials with potential in sensible thermal energy storage', Solar Energy Materials and Solar Cells, vol. 94, no. 10, pp. 1723–9.

Fernández Álvarez, C. & Gergely, M. 2021, 'What is behind soaring energy prices and what happens next?', IEA, Paris, viewed <https://www.iea.org/commentaries/what-is-behind-soaring-energy-prices-and-what-happens-next>.

Firoozi, H., Khajeh, H. & Laaksonen, H. 2021, 'Flexibility Forecast at Local Energy Community Level', Proceedings of 2021 IEEE PES Innovative Smart Grid Technologies Europe: Smart Grids: Toward a Carbon-Free Future, ISGT Europe 2021.

Foteinaki, K., Li, R., Péan, T., Rode, C. & Salom, J. 2020, 'Evaluation of energy flexibility of low-energy residential buildings connected to district heating', Energy and Buildings, vol. 213.

Guo, J., Zheng, W., Tian, Z., Wang, Yaolong, Wang, Ye & Jiang, Y. 2022, 'The short-term demand response potential and thermal characteristics of a ventilated floor heating system in a nearly zero energy building', Journal of Energy Storage, vol. 45, no. December 2021, p. 103643.

Guo, R., Zhao, Z., Wang, T., Liu, G., Zhao, J. & Gao, D. 2020, 'Degradation State Recognition of Piston Pump Based on ICEEMDAN and XGBoost', Applied Sciences 2020, Vol. 10, Page 6593, vol. 10, no. 18, p. 6593.

H. Parveen & N. Showlat 2017, 'Data collection Data collection', SAGE Research Methods, vol. 2014, pp. 1–5.

Hall, M. & Geissler, A. 2015, 'Einfluss der Wärmespeicherfähigkeit auf die energetische Flexibilität von Gebäuden', Bauphysik, vol. 37, no. 2, pp. 115–23.

Han, Z., Zheng, M., Kong, F., Wang, F., Li, Z. & Bai, T. 2008, 'Numerical simulation of solar assisted ground-source heat pump heating system with latent heat energy storage in severely cold area', Applied Thermal Engineering, vol. 28, no. 11–12, pp. 1427–36.

Hirmiz, R., Teamah, H.M., Lightstone, M.F. & Cotton, J.S. 2019, 'Performance of heat pump integrated phase change material thermal storage for electric load shifting in building demand side management', Energy and Buildings, vol. 190, pp. 103–18.

Homaei, S. & Hamdy, M. 2021, 'Quantification of energy flexibility and survivability of all-electric buildings with cost-effective battery size: Methodology and indexes', Energies, vol. 14, no. 10.

Horowitz, C.A. 2016, 'Paris Agreement', International Legal Materials, vol. 55, no. 4, pp. 740–55.

Hothorn, T., Hornik, K. & Zeileis, A. 2006, 'Unbiased recursive partitioning: A conditional inference framework', Journal of Computational and Graphical Statistics, vol. 15, no. 3, pp. 651–74.

Hu, J., Zhou, H., Zhou, Y., Zhang, H., Nordströmd, L. & Yang, G. 2021, 'Flexibility Prediction of Aggregated Electric Vehicles and Domestic Hot Water Systems in Smart Grids', Engineering, vol. 7, no. 8, pp. 1101–14.

Huang, W., Li, F., Cui, S.H., Huang, L. & Lin, J.Y. 2017, 'Carbon Footprint and Carbon Emission Reduction of Urban Buildings: A Case in Xiamen City, China', Procedia Engineering, vol. 198, pp. 1007–17.

Hutty, T.D., Patel, N., Dong, S. & Brown, S. 2020, 'Can thermal storage assist with the electrification of heat through peak shaving?', Energy Reports, vol. 6, pp. 124–31.

International Energy Agency & Timothy, G. 2021, 'Global Energy Review 2021', last accessed 28 June 2022, <https://iea.blob.core.windows.net/assets/d0031107-401d-4a2f-a48b-9eed19457335/GlobalEnergyReview2021.pdf>.

International Renewable Energy Agency 2020, 'Innovation Outlook: Thermal Energy Storage', International Renewable Energy Agency, Abu Dhabi, p. 144, viewed 16 November 2022, <https://www.irena.org/publications/2020/Nov/Innovation-outlook-Thermal-energy-storage>.

Jabir, H.J., Teh, J., Ishak, D. & Abunima, H. 2018, 'Impacts of demand-side

management on electrical power systems: A review', Energies.

Jacobsen, H.K. 2009, 'Energy intensities and the impact of high energy prices on producing and consuming sectors in Malaysia: An input-output assessment of the Malaysian economy and the vulnerability to energy price changes', Environment, Development and Sustainability, vol. 11, no. 1, pp. 137–60.

Jensen, S.Ø., Marszal-Pomianowska, A., Lollini, R., Pasut, W., Knotzer, A., Engelmann, P., Stafford, A. & Reynders, G. 2017, 'IEA EBC Annex 67 Energy Flexible Buildings', Energy and Buildings, vol. 155, pp. 25–34.

Ji, Y., Xu, P. & Xie, J. 2017, 'A Performance Assessment Method for Main HVAC Equipment with Electricity Submetering Data', Procedia Engineering, vol. 205, pp. 3104–11.

Johra, H., Heiselberg, P. & Dréau, J. Le 2019, 'Influence of envelope, structural thermal mass and indoor content on the building heating energy flexibility', Energy and Buildings, vol. 183, pp. 325–39.

Jolliffe, I.T. 2002, 'Principal Component Analysis, Second Edition', Encyclopedia of Statistics in Behavioral Science, vol. 30, no. 3, p. 487.

Junker, R.G., Azar, A.G., Lopes, R.A., Lindberg, K.B., Reynders, G., Relan, R. & Madsen, H. 2018, 'Characterizing the energy flexibility of buildings and districts', Applied Energy, vol. 225, pp. 175–82.

Karger, C.R. & Hennings, W. 2009, 'Sustainability evaluation of decentralized electricity generation', Renewable and Sustainable Energy Reviews, pp. 583–93.

Kathirgamanathan, A., Péan, T., Zhang, K., De Rosa, M., Salom, J., Kummert, M. & Finn, D.P. 2020, 'Towards standardising market-independent indicators for quantifying energy flexibility in buildings', Energy and Buildings, vol. 220.

Kaur, M. & Kang, S. 2016, 'Market Basket Analysis: Identify the Changing Trends of Market Data Using Association Rule Mining', Procedia Computer Science, vol. 85, pp. 78–85.

Kelly, N.J., Tuohy, P.G. & Hawkes, A.D. 2014, 'Performance assessment of tariff-based air source heat pump load shifting in a UK detached dwelling featuring

phase change-enhanced buffering', Applied Thermal Engineering, vol. 71, no. 2, pp. 809–20.

Klein, K., Herkel, S., Henning, H.M. & Felsmann, C. 2017, 'Load shifting using the heating and cooling system of an office building: Quantitative potential evaluation for different flexibility and storage options', Applied Energy, vol. 203, pp. 917–37.

Kolios, A., Mytilinou, V., Lozano-Minguez, E. & Salonitis, K. 2016, 'A comparative study of multiple-criteria decision-making methods under stochastic inputs', Energies, vol. 9, no. 7.

Kuboth, S., Heberle, F., Weith, T., Welzl, M., König-Haagen, A. & Brüggemann, D. 2019, 'Experimental short-term investigation of model predictive heat pump control in residential buildings', Energy and Buildings, vol. 204.

Laski, J. & Burrows, V. 2017, 'From Thousands to billions. Coordinated Action towards 100% Net Zero Carbon Buildings By 2050', World Green Building Council, p. 52.

Lei, L., Chen, W., Wu, B., Chen, C. & Liu, W. 2021, 'A building energy consumption prediction model based on rough set theory and deep learning algorithms', Energy and Buildings, vol. 240, p. 110886.

Leung, K.S., Wong, K.C., Chan, T.M., Wong, M.H., Lee, K.H., Lau, C.K. & Tsui, S.K.W. 2010, 'Discovering protein-DNA binding sequence patterns using association rule mining', Nucleic Acids Research, vol. 38, no. 19, pp. 6324–37.

Li, H., Wang, Z., Hong, T. & Piette, M.A. 2021, 'Energy flexibility of residential buildings: A systematic review of characterization and quantification methods and applications', Advances in Applied Energy, vol. 3.

Li, K. 2020, 'Thesis: Energy performance assessment of campus buildings using data mining technologies ', University of Wollongong, Wollongong..

Li, K., Ma, Z., Robinson, D. & Ma, J. 2018, 'Identification of typical building daily electricity usage profiles using Gaussian mixture model-based clustering and hierarchical clustering', Applied Energy, vol. 231, pp. 331–42.

Li, K., Sun, Y., Robinson, D., Ma, J. & Ma, Z. 2020, 'A new strategy to benchmark and evaluate building electricity usage using multiple data mining technologies', Sustainable Energy Technologies and Assessments, vol. 40.

Li, K., Yang, R.J., Robinson, D., Ma, J. & Ma, Z. 2019, 'An agglomerative hierarchical clustering-based strategy using Shared Nearest Neighbours and multiple dissimilarity measures to identify typical daily electricity usage profiles of university library buildings', Energy, vol. 174, pp. 735–48.

Li, M. & Ju, Y. 2017, 'The analysis of the operating performance of a chiller system based on hierarchal cluster method', Energy and Buildings, vol. 138, pp. 695–703.

Li, Y., Mojiri, A., Rosengarten, G. & Stanley, C. 2021, 'Residential demand-side management using integrated solar-powered heat pump and thermal storage', Energy and Buildings, vol. 250.

Lin, W., Ma, Z., McDowell, C., Baghi, Y. & Banfield, B. 2020, 'Optimal design of a thermal energy storage system using phase change materials for a net-zero energy Solar Decathlon house', Energy and Buildings, vol. 208.

Liu, Y., Chen, H., Zhang, L. & Feng, Z. 2021, 'Enhancing building energy efficiency using a random forest model: A hybrid prediction approach', Energy Reports, vol. 7, pp. 5003–12.

Lizana, J., Chacartegui, R., Barrios-Padura, A. & Valverde, J.M. 2017, 'Advances in thermal energy storage materials and their applications towards zero energy buildings: A critical review', Applied Energy, pp. 219–39.

Lizana, J., Friedrich, D., Renaldi, R. & Chacartegui, R. 2018, 'Energy flexible building through smart demand-side management and latent heat storage', Applied Energy, vol. 230, pp. 471–85.

Luc, K.M., Li, R., Xu, L., Nielsen, T.R. & Hensen, J.L.M. 2020, 'Energy flexibility potential of a small district connected to a district heating system', Energy and Buildings, vol. 225.

Lundh, M. & Dalenbäck, J.O. 2008, 'Swedish solar heated residential area with

seasonal storage in rock: Initial evaluation', Renewable Energy, vol. 33, no. 4, pp. 703–11.

Luthander, R., Widén, J., Nilsson, D. & Palm, J. 2015, 'Photovoltaic self-consumption in buildings: A review', Applied Energy, pp. 80–94.

Ma, J., Silva, V., Belhomme, R., Kirschen, D.S. & Ochoa, L.F. 2013, 'Evaluating and planning flexibility in sustainable power systems', IEEE Transactions on Sustainable Energy, vol. 4, no. 1, pp. 200–9.

Ma, Z., Yan, R., Li, K. & Nord, N. 2018, 'Building energy performance assessment using volatility change based symbolic transformation and hierarchical clustering', Energy and Buildings, vol. 166, pp. 284–95.

Ma, Z., Yan, R. & Nord, N. 2017, 'A variation focused cluster analysis strategy to identify typical daily heating load profiles of higher education buildings', Energy, vol. 134, pp. 90–102.

Marszal-Pomianowska, A., Johra, H., Weis, T., Knotzer, A., Jensen, S.Ø., Kazmi, H., Vigna, I., Pernet, R., Le Dréau, J. & Zhang, K. 2019, 'International Energy Agency-Characterization of Energy Flexibility in Buildings: Energy in Buildings and Communities Programme Annex 67 Energy Flexible Buildings'.

Mateo, J.R.S.C. 2012, 'Weighted sum method and weighted product method', Green Energy and Technology, vol. 83, pp. 19–22.

Matevosyan, J., Giannakidis, G., Joyeau, A., Gómez Simon, C., Lallemand, M., Martin, A., Anisie, A., Marquant, J., Gutiérrez, L., Sani, L., Janeiro, L., Komor, P., Miranda, R. & Collins, S. 2019, demand-side flexibility for power sector transformation analytical brief demand-side flexibility for power sector transformation.

Mouzakitis, A. 2013, 'Classification of fault diagnosis methods for control systems', Measurement and Control (United Kingdom), vol. 46, no. 10, pp. 303–8.

Muhsen, D.H., Haider, H.T., Al-Nidawi, Y. & Khatib, T. 2019, 'Optimal home energy demand management based multi-criteria decision making methods', Electronics (Switzerland), vol. 8, no. 5.

Olson, D.L. 1990, ‘The analytic hierarchy process’, Decision Aids for Selection Problems, vol. 45, p. 378.

Operations, P.E. 2010, Guide To Ancillary Services in the National Electricity Market, Power, Australian energy market operator.

Oró, E., de Gracia, A., Castell, A., Farid, M.M. & Cabeza, L.F. 2012, ‘Review on phase change materials (PCMs) for cold thermal energy storage applications’, Applied Energy, pp. 513–33.

Öztürk, H.H. 2005, ‘Experimental evaluation of energy and exergy efficiency of a seasonal latent heat storage system for greenhouse heating’, Energy Conversion and Management, vol. 46, no. 9–10, pp. 1523–42.

Paksoy, H.O., Andersson, O., Abaci, S., Evliya, H. & Turgut, B. 2000, ‘Heating and cooling of a hospital using solar energy coupled with seasonal thermal energy storage in an aquifer’, Renewable Energy, vol. 19, no. 1–2, pp. 117–22.

Panapakidis, I.P., Papadopoulos, T.A., Christoforidis, G.C. & Papagiannis, G.K. 2014, ‘Pattern recognition algorithms for electricity load curve analysis of buildings’, Energy and Buildings, vol. 73, pp. 137–45.

PCP 2022, https://pcpaustralia.com.au/pcm-range-products/, last accessed 15 sep 2022.

Pean, T., Costa-Castello, R., Fuentes, E. & Salom, J. 2019, ‘Experimental Testing of Variable Speed Heat Pump Control Strategies for Enhancing Energy Flexibility in Buildings’, IEEE Access, vol. 7, pp. 37071–87.

Perera, A.T.D., Nik, V.M., Wickramasinghe, P.U. & Scartezzini, J.L. 2019, ‘Redefining energy system flexibility for distributed energy system design’, Applied Energy, vol. 253.

Pitchforth, D.J., Rogers, T.J., Tygesen, U.T. & Cross, E.J. 2021, ‘Grey-box models for wave loading prediction’, Mechanical Systems and Signal Processing, vol. 159.

Pluss 2022, https://www.pluss.co.in/product-range-PCM.php, last accessed 15 sep 2022.

Rathod, M.K. & Kanzaria, H. V. 2011, 'A methodological concept for phase change material selection based on multiple criteria decision analysis with and without fuzzy environment', Materials and Design, vol. 32, no. 6, pp. 3578–85.

Reka, S.S. & Ramesh, V. 2016, 'Demand response scheme with electricity market prices for residential sector using stochastic dynamic optimization', 2016 - Biennial International Conference on Power and Energy Systems: Towards Sustainable Energy, PESTSE 2016.

Ren, H., Sun, Y., Albdoor, A.K., Tyagi, V. V., Pandey, A.K. & Ma, Z. 2021, 'Improving energy flexibility of a net-zero energy house using a solar-assisted air conditioning system with thermal energy storage and demand-side management', Applied Energy, vol. 285.

Rgees 2022, https://rgees.com/products/, last accessed 15 sep 2022.

Rubitherm 2022, https://www.rubitherm.eu/en/productCategories.html, last accessed 15 sep 2022.

Saaty, T.L. 2002, 'Decision making with the Analytic Hierarchy Process', Scientia Iranica, vol. 9, no. 3, pp. 215–29.

Saffari, M., de Gracia, A., Fernández, C., Belusko, M., Boer, D. & Cabeza, L.F. 2018, 'Optimized demand side management (DSM) of peak electricity demand by coupling low temperature thermal energy storage (TES) and solar PV', Applied Energy, vol. 211, pp. 604–16.

Sajjad, I.A., Chicco, G. & Napoli, R. 2016, 'Definitions of Demand Flexibility for Aggregate Residential Loads', IEEE Transactions on Smart Grid, vol. 7, no. 6, pp. 2633–43.

Salom, J., Marszal, A.J., Widén, J., Candanedo, J. & Lindberg, K.B. 2014, 'Analysis of load match and grid interaction indicators in net zero energy buildings with simulated and monitored data', Applied Energy, vol. 136, pp. 119–31.

Salom, J., Widén, J., Candanedo, J., Sartori, I., Voss, K. & Marszal, A. 2011, 'Understanding net zero energy buildings: Evaluation of load matching and grid interaction indicators', Proceedings of Building Simulation 2011: 12th

Conference of International Building Performance Simulation Association, pp. 2514–21.

De Schepper, G., Paulus, C., Bolly, P.Y., Hermans, T., Lesparre, N. & Robert, T. 2019, 'Assessment of short-term aquifer thermal energy storage for demand-side management perspectives: Experimental and numerical developments', Applied Energy, vol. 242, no. March, pp. 534–46.

Sharma, S.D., Kitano, H. & Sagara, K. 2004, 'Phase Change Materials for Low Temperature Solar Thermal Applications', Res. Rep. Fac. Eng. Mie Univ., vol. 29, pp. 31–64.

Socaciu, L., Giurgiu, O., Banyai, D. & Simion, M. 2016, 'PCM Selection Using AHP Method to Maintain Thermal Comfort of the Vehicle Occupants', Energy Procedia, vol. 85, pp. 489–97.

Stinner, S., Huchtemann, K. & Müller, D. 2016, 'Quantifying the operational flexibility of building energy systems with thermal energy storages', Applied Energy, vol. 181, pp. 140–54.

Stojčić, M., Zavadskas, E.K., Pamučar, D., Stević, Ž. & Mardani, A. 2019, 'Application of MCDM methods in sustainability engineering: A literature review 2008-2018', Symmetry.

Swiss Re 2021, 'World economy set to lose up to 18% GDP from climate change if no action taken, reveals Swiss Re Institute's stress-test analysis', Swiss Re Group.

Tang, H. & Wang, S. 2021, 'Energy flexibility quantification of grid-responsive buildings: Energy flexibility index and assessment of their effectiveness for applications', Energy, vol. 221.

Trinkl, C. & Zörner, W. 2008, 'A domestic solar/heat pump heating system incorporating latent and stratified thermal storage', Proceedings of ES2008, Jacksonville, Florida USA.

Tulabing, R., Yin, R., DeForest, N., Li, Y., Wang, K., Yong, T. & Stadler, M. 2016, 'Modeling study on flexible load's demand response potentials for providing

ancillary services at the substation level', Electric Power Systems Research, vol. 140, pp. 240–52.

Tyagi, V.V. & Buddhi, D. 2007, 'PCM thermal storage in buildings: A state of art', Renewable and Sustainable Energy Reviews, pp. 1146–66.

Uddin, M., Romlie, M.F., Abdullah, M.F., Abd Halim, S., Abu Bakar, A.H. & Chia Kwang, T. 2018, 'A review on peak load shaving strategies', Renewable and Sustainable Energy Reviews, pp. 3323–32.

Verbruggen, B. & Driesen, J. 2015, 'Grid impact indicators for active building simulations', IEEE Transactions on Sustainable Energy, vol. 6, no. 1, pp. 43–50.

Vesa, A.V., Cioara, T., Anghel, I., Antal, M., Pop, C., Iancu, B., Salomie, I. & Dadarlat, V.T. 2020, 'Energy flexibility prediction for data center engagement in demand response programs', Sustainability (Switzerland), vol. 12, no. 4.

Vigna, I., De Jaeger, I., Saelens, D., Lovati, M., Lollini, R. & Pernetti, R. 2019, 'Evaluating energy and flexibility performance of building clusters', Building Simulation Conference Proceedings, vol. 5, pp. 3326–33.

Wei, Y., Zhang, X., Shi, Y., Xia, L., Pan, S., Wu, J., Han, M. & Zhao, X. 2018, 'A review of data-driven approaches for prediction and classification of building energy consumption', Renewable and Sustainable Energy Reviews, pp. 1027–47.

Whiffen, T.R. & Riffat, S.B. 2013, 'A review of PCM technology for thermal energy storage in the built environment: Part I', International Journal of Low-Carbon Technologies, vol. 8, no. 3, pp. 147–58.

Xu, H., Sze, J.Y., Romagnoli, A. & Py, X. 2017, 'Selection of Phase Change Material for Thermal Energy Storage in Solar Air Conditioning Systems', Energy Procedia, vol. 105, pp. 4281–8.

Xu, T., Humire, E.N., Chiu, J.N. & Sawalha, S. 2021, 'Latent heat storage integration into heat pump based heating systems for energy-efficient load shifting', Energy Conversion and Management, vol. 236.

Yang, K., Zhu, N., Chang, C., Wang, D., Yang, S. & Ma, S. 2018, 'A methodological

concept for phase change material selection based on multi-criteria decision making (MCDM): A case study', Energy, vol. 165, pp. 1085–96.

Yin, R., Kara, E.C., Li, Y., DeForest, N., Wang, K., Yong, T. & Stadler, M. 2016, 'Quantifying flexibility of commercial and residential loads for demand response using setpoint changes', Applied Energy, vol. 177, pp. 149–64.

Yu, F.W. & Chan, K.T. 2009, 'Environmental performance and economic analysis of all-variable speed chiller systems with load-based speed control', Applied Thermal Engineering, vol. 29, no. 8–9, pp. 1721–9.

Yu, F.W. & Chan, K.T. 2012a, 'Assessment of operating performance of chiller systems using cluster analysis', International Journal of Thermal Sciences, vol. 53, pp. 148–55.

Yu, F.W. & Chan, K.T. 2012b, 'Chiller system performance benchmark by data envelopment analysis', International Journal of Refrigeration, vol. 35, no. 7, pp. 1815–23.

Yu, F.W. & Chan, K.T. 2012c, 'Improved energy management of chiller systems by multivariate and data envelopment analyses', Applied Energy, vol. 92, pp. 168–74.

Yu, F.W. & Chan, K.T. 2012d, 'Using cluster and multivariate analyses to appraise the operating performance of a chiller system serving an institutional building', Energy and Buildings, vol. 44, no. 1, pp. 104–13.

Yu, F.W. & Chan, K.T. 2013, 'Improved energy management of chiller systems with data envelopment analysis', Applied Thermal Engineering, vol. 50, pp. 309–17.

Yu, F.W., Chan, K.T., Sit, R.K.Y. & Yang, J. 2014, 'Review of standards for energy performance of chiller systems serving commercial buildings', Energy Procedia, vol. 61, pp. 2778–82.

Yu, J., Chang, W.S. & Dong, Y. 2022, 'Building Energy Prediction Models and Related Uncertainties: A Review', Buildings 2022, Vol. 12, Page 1284, vol. 12, no. 8, p. 1284.

Zhang, L., Jin, G., Liu, T. & Zhang, R. 2022, 'Generalized hierarchical expected

improvement method based on black-box functions of adaptive search strategy', Applied Mathematical Modelling, vol. 106, pp. 30–44.

Zhang, P., Lu, X. & Li, K. 2021, 'Achievable Energy Flexibility Forecasting of Buildings Equipped with Integrated Energy Management System', IEEE Access, vol. 9, pp. 122589–99.

Zhou, R., Pan, Y., Huang, Z. & Wang, Q. 2013, 'Building energy use prediction using time series analysis', Proceedings - IEEE 6th International Conference on Service-Oriented Computing and Applications, SOCA 2013, pp. 309–13.

Zhou, Y. & Cao, S. 2020, 'Quantification of energy flexibility of residential net-zero-energy buildings involved with dynamic operations of hybrid energy storages and diversified energy conversion strategies', Sustainable Energy, Grids and Networks, vol. 21.

Zhou, Y., Wang, J., Dong, F., Qin, Y., Ma, Z., Ma, Y. & Li, J. 2021, 'Novel flexibility evaluation of hybrid combined cooling, heating and power system with an improved operation strategy', Applied Energy, vol. 300.